National Library
of Canada

Bibliothèque nationale
du Canada

Canadian Theses Service

Services des thèses canadiennes

Ottawa, Canada
K1A 0N4

CANADIAN THESES

THÈSES CANADIENNES

NOTICE

The quality of this microfiche is heavily dependent upon the quality of the original thesis submitted for microfilming. Every effort has been made to ensure the highest quality of reproduction possible.

If pages are missing, contact the university which granted the degree.

Some pages may have indistinct print especially if the original pages were typed with a poor typewriter ribbon or if the university sent us an inferior photocopy.

Previously copyrighted materials (journal articles, published tests, etc.) are not filmed.

Reproduction in full or in part of this film is governed by the Canadian Copyright Act, R.S.C. 1970, c. C-30.

AVIS

La qualité de cette microfiche dépend grandement de la qualité de la thèse soumise au microfilmage. Nous avons tout fait pour assurer une qualité supérieure de reproduction.

S'il manque des pages, veuillez communiquer avec l'université qui a conféré le grade.

La qualité d'impression de certaines pages peut laisser à désirer, surtout si les pages originales ont été dactylographiées à l'aide d'un ruban usé ou si l'université nous a fait parvenir une photocopie de qualité inférieure.

Les documents qui font déjà l'objet d'un droit d'auteur (articles de revue, examens publiés, etc.) ne sont pas microfilmés.

La reproduction, même partielle, de ce microfilm est soumise à la Loi canadienne sur le droit d'auteur, SRC 1970, c. C-30.

THIS DISSERTATION
HAS BEEN MICROFILMED
EXACTLY AS RECEIVED

LA THÈSE A ÉTÉ
MICROFILMÉE TELLE QUE
NOUS L'AVONS REÇUE

NL-339 (r.86/06)

Canada

THE UNIVERSITY OF ALBERTA

EVALUATION OF A TECHNOLOGICALLY APPROPRIATE MICRO HYDROELECTRIC SYSTEM

by

© DARRELL LARRY MARTINDALE

A THESIS
SUBMITTED TO THE FACULTY OF GRADUATE STUDIES AND RESEARCH
IN PARTIAL FULFILMENT OF THE REQUIREMENTS FOR THE DEGREE
OF MASTER OF SCIENCE

DEPARTMENT OF AGRICULTURAL ENGINEERING

EDMONTON, ALBERTA
FALL 1986

Permission has been granted to the National Library of Canada to microfilm this thesis and to lend or sell copies of the film.

The author (copyright owner) has reserved other publication rights, and neither the thesis nor extensive extracts from it may be printed or otherwise reproduced without his/her written permission.

L'autorisation a été accordée à la Bibliothèque nationale du Canada de microfilmer cette thèse et de prêter ou de vendre des exemplaires du film.

L'auteur (titulaire du droit d'auteur) se réserve les autres droits de publication; ni la thèse ni de longs extraits de celle-ci ne doivent être imprimés ou autrement reproduits sans son autorisation écrite.

ISBN 0-315-32388-4

THE UNIVERSITY OF ALBERTA

RELEASE FORM

NAME OF AUTHOR DARRELL LARRY MARTINDALE

TITLE OF THESIS EVALUATION OF A TECHNOLOGICALLY APPROPRIATE MICRO HYDROELECTRIC SYSTEM

DEGREE FOR WHICH THESIS WAS PRESENTED MASTER OF SCIENCE

YEAR THIS DEGREE GRANTED FALL 1986

Permission is hereby granted to THE UNIVERSITY OF ALBERTA LIBRARY to reproduce single copies of this thesis and to lend or sell such copies for private, scholarly or scientific research purposes only.

The author reserves other publication rights, and neither the thesis nor extensive extracts from it may be printed or otherwise reproduced without the author's written permission.

(SIGNED) Darrell Martindale

PERMANENT ADDRESS:

Box 36 Site 3 RR1
St. Albert Alberta
T8N 1M8

DATED July 7 1986

THE UNIVERSITY OF ALBERTA
FACULTY OF GRADUATE STUDIES AND RESEARCH

The undersigned certify that they have read, and recommend to the Faculty of Graduate Studies and Research, for acceptance, a thesis entitled EVALUATION OF A TECHNOLOGICALLY APPROPRIATE MICRO HYDROELECTRIC SYSTEM submitted by DARRELL LARRY MARTINDALE in partial fulfilment of the requirements for the degree of MASTER OF SCIENCE in AGRICULTURAL ENGINEERING.

A.W. Anderson
Supervisor

V.G. Gowrishankar

Date.....7...July...1986.....

DEDICATION

This study is dedicated to rural peoples throughout the world.

ABSTRACT

Additional energy is required by subsistance farmers in developing countries to improve farm productivity. Most farmers in developing countries are unable to make use of micro hydroelectric systems due to the high cost of Pelton turbines and electronic load controllers, two important components of the system. This is not a problem, however, in the El Dormilon valley of Colombia, where multiple jet micro hydroelectric systems have been built and are operated by subsistance farmers to increase farm income.

The primary objectives of this study were to evaluate the effect of multiple jet configurations for speed control and to compare the performance of the handcast Pelton turbine built and used in Colombia with a Pelton turbine designed for laboratory use. These two variables were tested to determine their impact on reduction and control of rotational speed. Other objectives were to develop a better understanding of the mechanisms of water jet interference and the development of a computer model capable of predicting power output and runaway speed for Pelton turbines.

To this end the author built a 3.6 kW micro hydroelectric system at the University of Alberta. The system was monitored to determine hydraulic efficiency and runaway speed for different combinations of hydraulic head,

flow rate, waterjet configuration and turbine design.

This study concluded that multiple jet configurations were effective at reducing runaway speed. The four-jet configuration could reduce runaway speeds by 27 percent with very little loss of hydraulic efficiency. The handcast turbine was able to reduce runaway speed nearly as well as the manufactured turbine when flowrates exceeded five litres per second.

The computer model developed to simulate the performance of the multiple jet micro hydroelectric system was able to predict the runaway speed for the manufactured turbine with the one and two-jet no interference configurations. More research is needed to understand the mechanisms of water jet interference before accurate predictions for runaway speed for multiple jet configurations can be made.

ACKNOWLEDGEMENTS

The author would like to recognize and express his gratitude to some of the people who contributed to this thesis and gave him their support.

The financial assistance provided in the developmental stages of this project by the University of Alberta's Fund for Support of International Development and by the Department of Agricultural Engineering is gratefully acknowledged. The author appreciated the kind and warm hospitality of Alvaro Villa who hosted him during his stay in Colombia and whose commitment to rural development and practical demonstration of a micro hydroelectric system in El Dormilon inspired this project. The author wishes to thank Professor Wayne Anderson and Doctor Peter Apedaile for their advice and encouragement.

The author is especially grateful to his wife, Georgina, for her encouragement and assistance throughout the project.

TABLE OF CONTENTS

Page

1. Introduction....................................1
    1.1 Objectives....................................1
    1.2 Appropriate Technology....................................2
    1.3 Farming Systems Analysis....................................5
    1.4 Energy and Agriculture in Developing Nations....................................7
        1.4.1 Rural Enery Use....................................8
            1.4.1.1 Farming Activities....................................9
            1.4.1.2 Post-Harvest Production activities....................................13
            1.4.1.3 Domestic Energy Use....................................15
    1.5 Technical Appropriateness of Micro Hydroelectric Power....................................17
    1.6 Micro Hydroelectric Power as an Appropriate Technology....................................18
2. Literature Review....................................21
    2.1 Hydraulic Turbines....................................21
    2.2 Pelton Turbines....................................22
    2.3 Electric Power Generation....................................27
        2.3.1 Electric Generating Equipment....................................28
        2.3.2 Speed Regulation....................................30
            2.3.2.1 Mechanical Governors....................................30
            2.3.2.2 Load Controllers....................................32
            2.3.2.3 Runaway Speed....................................35

2.3.2.4 Runaway Speed Reduction..........37

3. Theoretical Framework.................................45

3.1 Introduction.......................................45

3.2 Experimental Method..............................46

3.3 Theoretical Model Development...................52

3.3.1 Determination of Wastewater Volume........53

3.3.2 Power Calculations..........................58

3.3.3 Runaway Speed Determination..............61

3.4 CSMP Model Description..........................66

3.5 CSMP Model Verification.........................67

3.6 CSMP Model Results..............................70

4. Experimental Program.................................77

4.1 Introduction.......................................77

4.2 Apparatus Utilized...............................77

4.2.1 Overview......................................77

4.2.2 Power Input Components....................79

4.2.3 Power Output Components...................97

4.2.4 Infrastructure...............................99

4.2.5 Data Acquisition............................114

5. Results and Discussion..............................119

5.1 CSMP Model Prediction and Evaluation...........119

5.2 Effect of Jet Arrangement on Runaway Speed......130

5.2.1 Analysis of Variance of Runaway Speed..................................134

5.2.2 Multiple Classification Analysis.........140

5.3 Turbine Efficiency...............................148

5.4 Voltage at Runaway Speed........................155

6. Conclusions...157

7. References..160

8. Appendices..167

List of Tables

Table Page

3.1 TURBINE CHARACTERISTICS.....47

3.2 CHARACTERISTICS OF WATERJET AT 30 AND 50 METERS OF HYDRAULIC HEAD.....49

3.3 ORIFICE SIZE DEVIATION.....51

3.4 MOTOR DRAW TEST RESULTS.....66

3.5 WASTEWATER SLUG VOLUME CALCULATION.....70

3.6 PARAMETERS FOR THEORETICAL POWER CURVES.....71

3.7 THEORETICAL POWER CURVE SPEED REDUCTION SUMMARY.....71

4.1 JET DIAMETER REDUCTION MEASUREMENT SUMMARY.....105

5.1 STUDENTS t-TEST COMPARISON OF RUNAWAY SPEED DATA ORIFICE SIZE DEVIATION.....124

5.2 ORIFICE SIZE DEVIATION.....135

5.3 ANOVA SUMMARY.....138

A.4.1 SUMMARY DATA FOR MANUFACTURED TURBINE AND SERIES 1 ORIFICES.....196

A.4.2 SUMMARY DATA FOR MANUFACTURED TURBINE AND SERIES 2 ORIFICES.....197

A.4.3 DATA SUMMARY FOR MANUFACTURED TURBINE AND SERIES 3 ORIFICES.....198

A.4.4 SUMMARY DATA FOR MANUFACTURED TURBINE AND SERIES4 ORIFICES.....199

A.4.5 SUMMARY DATA FOR MANUFACTURED TURBINE AND SERIES 5 ORIFICES.....200

A.4.6 SUMMARY DATA FOR HANDCAST TURBINE AND SERIES 1 ORIFICES.....201

A.4.7 SUMMARY DATA FOR HANDCAST TURBINE AND SERIES 2 ORIFICES.....202

A.4.8 SUMMARY DATA FOR HANDCAST TURBINE AND SERIES 3 ORIFICES.....203

A.4.9 SUMMARY DATA FOR HANDCAST TURBINE AND SERIES 4 ORIFICES....................................204

A.4.10 SUMMARY DATA FOR HANDCAST TURBINE AND SERIES 5 ORIFICES....................................205

A.6.1 MULTIPLE CLASSIFICATION ANALYSIS FOR TURBINES.....211

A.6.2 MULTIPLE CLASSIFICATION ANALYSIS OF JET CONFIGURATION ON RUNAWAY SPEED................................212

A.6.3 MULTIPLE CLASSIFICATION ANALYSIS OF HEAD ON RUNAWAY SPEED...213

List of Figures

Figure Page

1.1 Farming System within environment....................6

2.1 Small Pelton turbine 23

2.2 Power triangle showing effect of inductive loads on power factor..34

2.3 Velocity relations at discharge....................41

3.1 Five water jet configurations evaluated in this research...48

3.2 Waste water determination..........................55

3.3 Velocity acting on a single Pelton turbine bucket....60

3.4 Components of velocity at Pelton turbine bucket......62

3.5 High friction and low friction curves..............65

3.6 End view of waste water segment for verification of wastewater volume calculations.......................69

3.7 Theoretical power curves for handcast Colombian turbine..72

3.8 Theoretical power curves for manufactured English turbine..73

3.9 Comparison of handcast and manufactured Pelton turbine power curves for the single-jet and four-jet configurations....................................75

4.1 Effect of efficiency on runaway speed reduction......78

4.2 Major components of experimental apparatus...........80

4.3 Components of total head.............................84

4.4 Static pressure assembly.............................85

4.5 Plywood screen used to creat laminar flow............90

4.6 Weir...95

4.7 Nozzle mount..102

4.8 Orifice-water jet diameter relationship.............104

4.9 Water jet diameter measurement apparatus............103

4.10 Water seal..113

5.1 Theoretical power curves for a two-jet-no-interference configuration..120

5.2 Theoretical power curves for a four-jet configuration..121

5.3 High friction curve adjustment......................128

5.4 Power curves for handcast turbine....................132

5.5 Power curves for manufactured turbine...............133

5.6 Effect of turbine selection on runaway speed as a percent of total speed variation.....................142

5.7 Effect of jet configuration on runaway speed as a percent of total runaway speed variation............144

5.8 Effect of jet configuration on runaway speed as a percent reduction of runaway speed for the low friction system..146

5.9 Hill curves of manufactured turbine under influence of two-jet-no-interference configuration...............150

5.10 Hill curves of manufactured turbine under influence of four-jet configuration...............................151

5.11 Hill curves of handcast turbine under influence of a two-jet-no-interference configuration...............153

5.12 Hill curves of handcast turbine under influence of a four-jet configuration...............................154

List of Photographs

Photograph Page

2.1 Pelton turbine operating at maximum load with four water jets....................................39

2.2 Pelton turbine operating at runaway speed conditions.40

4.1 Gasoline powered irrigation pump used to simulate hydraulic head..................................81

4.2 Water divider to evenly distribute water to all four nozzles...82

4.3 Pressure transducer mounted on header................86

4.4 Calibration of pressure transducer using hydrostatic apparatus.......................................88

4.5 Water level measurement apparatus...................92

4.6 Water flow measurement system, from turbulent flow to suction hose....................................93

4.7 Hall effect sensor in wooden support and magnet mounted to shaft.......................................96

4.8 Voltmeter and wattmeter.............................98

4.9 Resistor Bank.......................................100

4.10 Measuring the diameter of the orifice of an endcap nozzle...109

4.11 Preparation of handcast Pelton turbine.............110

4.12 Manufactured turbine mounted on shaft positioned with a two-jet configuration................................111

4.13 Alternator connection to shaft with v-belt and pulleys...115

4.14 MINC terminal demonstrating power curve............118

Nomenclature

A_j	cross sectional area of waterjet
A_o	cross sectional area of orifice
C_d	discharge coefficient
E	voltage at generator
F	calculated F value
F_s	striking force of water on turbine, Newtons
H_e	elevation head, m
H_p	pressure head, m
H_o	null hypothesis
H_t	total head at nozzle, m
H_v	velocity head, m
H_w	elevation of water surface above weir notch, cm
I	amperage
K	number of waterjets
L	number of interference points
N	number of buckets
N_s	normal speed
P	power, watts
P_L	power loss in alternator windings
P_{HF}	power absorbed by friction with generator connected
P_{LF}	power absorbed by friction without the generator
Q_j	flow rate of wastewater generated per water jet, m^3/s
Q_N	flow rate at nozzle, ℓ/s
Q_s	flow rate of water striking turbine, ℓ/s

Q_t	total flow rate, ℓ/s
Q_w	total wastewater flow rate, m^3/s
R	resistance, ohms
R_o	turbine radius, m
R_w	winding resistance, ohm
S_l	length of wastewater slug, m
S_w	width of wastewater slug, m
V	volume of wastewater slug, m^3
V_b	tangential velocity of buckets, m/s
V_j	water jet velocity measured at nozzle, m/s
V_p	velocity of water in pipe before nozzle, m/s
V_r	relative velocity of water jet to buckets, m/s
X	reactance
Z	impedence
ac	alternating current
dc	direct current
d	diameter of orifice, m
d_j	water jet diameter, m
g	acceleration due to gravity, m/s^3
n	size of sample population
kW	kilowatts
r	pitch radius, m
rpm	revolutions per minute
t	tabulated t value from Student's t-table
t_b	time required by buckets to move angular distance
t_s	calculated t value for Student's t-test
t_w	time required by water jet to move fixed distance

x	perpendicular distance to d_x section in water jet, m
x_o	pitch radius, m
α	level of satistical significance
β	angle between water jet and tangential velocity of bucket
γ	half the angle AOC
δ	angle of water leaving buckets with respect to observer
λ	angle between adjacent buckets
μ	sample mean
θ	angle between current and voltage vectors
θ_{max}	runaway speed in terms of speed ratio
θ_n	speed ratio
π	circumference of unit circle
ρ	density of water, kg/m^3
ϕ	angle between vertical line and the radius of waste water segment
ψ	angle of return within bucket
ω	angular velocity, radians/s

1. INTRODUCTION

1.1 Objectives

The objectives of this research were four fold. The main objective was to evaluate the effect of multiple nozzle configurations on the rotational speed of micro* hydroelectric power plants when these are used without the use of traditional governors to control rotational speed. The generation of electrical power often requires that the generator operate at a constant rotational speed. Electrical generating plants accomplish this using sophisticated and relatively expensive governors. Removal of the governor reduces the capital cost and technical complexity of micro hydroelectric power plants making them more appropriate for use in rural areas of developing nations.

The second objective was to determine to what extent water jet interference reduces runaway speed. Multiple jet configurations reduce runaway speed in two ways. The first mechanism of speed control occurs when water passes through the turbine without impinging its energy on the buckets. This phenomena is well documented and is discussed in chapter 3. The second mechanism is caused by the removal of water that would have impinged on the turbine had it not been removed as a result of a collision with the adjacent water jet.

---

* Micro hydroelectric systems, as defined by Fritz (1984, pp.1.5), refers to any hydropower system that generates 100 kW or less.

The third objective was to evaluate the performance of a handcast aluminium Pelton turbine produced in Columbia by a small engineering firm. The performance of the handcast turbine was compared to the performance of a laboratory Pelton turbine manufactured by the Gilbert Gilkes and Gordon Ltd. of England. The two Pelton turbines were tested to determine hydraulic efficiencies and how water volume and water jet configuration affect rotational speed and power output of each turbine. If the two turbines proved to have similar hydraulic efficiencies and performance characteristics, then the low cost of the handcast turbine would make it more appropriate than the manufactured turbine for use in third world countries.

The final objective was to develop a computer model capable of predicting power output and runaway speed for Pelton turbines. The model facilitates the optimization of the design of multiple jet systems by allowing one to alter the values used for particular design variables and quickly recalculate an estimate of turbine performance.

1.2 Appropriate Technology

The term "appropriate technology" defines the usefulness of a particular technology in terms of its social and economic measures and not in terms of its complexity or sophistication. Stevens (1977) argues that, given their resources, subsistence farmers (ie. farmers where the majority of the life sustaining needs of the farmer and his family are produced on the farmers land) are economically efficient as they have attained the best possible allocation of their resources of land, labor and capital. Appropriate technologies represent an improvement in capital resources which improves labor productivity and increases the net income of the subsistence farmer.

Schumacher (1974) argues that self-reliance and increased economic benefits for the poorer segments of society are not always the goals of government of developing nations. This, he suggests, is why little support is given to organizations promoting appropriate technologies and why appropriate technologies which threaten the status quo will not be used. Government leaders who see industrialization as the only path to development claim that appropriate technologies are "second best" technologies and that, if developing nations are to compete in the international market, only the most advanced of technologies must be used. He goes on to state that these viewpoints represent "the voice of those who are not in need, who can help themselves and want to be assisted in reaching a higher standard of living (Schumacher, 1974)."

Today, most research and development on "appropriate technologies" is done in the industrialized nations. Burch (1982) suggests that this situation creates for developing nations a deeper dependence on foreign capital which will "undermine the autonomy and self-reliance which is an explicit goal of appropriate technology." Technologies developed in industrialized nations are often inappropriate for developing nations because of the large differences in their economic and social environments.

Todaro (1977) characterized developing nations as having:

a. chronic high underemployment and unemployment,
b. scarce, (hence expensive), capital and cheap labor,
c. large income disparities,
d. an extremely poor rural sector, and
e. rural-urban migration.

An appropriate technology must address these problems.

The use of local human resources to maintain and improve the technology is one of the factors which ensures the success of an appropriate technology. It is important that jobs be meaningful to the worker and develop in him/her a sense of self esteem, responsibility and commitment to his/her community. The new technology must involve the participation of those benefiting from the technology. Wherever possible, the new technology should be financed with local capital, must be economically viable and must benefit those it was designed to benefit (Canadian Hunger Foundation, 1976). These conditions must be established before the new technology is introduced. With rising international debt, third world nations cannot afford expensive, inappropriate technology. Development organizations and third world governments need a tool to help develop and evaluate appropriate technologies before they are introduced to developing countries. Many development organizations recognize this need and they are developing techniques based on systems analysis where cultural and economic impacts of proposed projects can be included in the project evaluation process. Within agricultural projects, the techniques are often referenced by the term 'farming systems analysis'.

1.3 Farming Systems Analysis

Farming systems analysis views the whole farm as an integrated system. A farming system is a complex interaction of components such as water, soil, plants, labor, culture and environment, as shown in Figure 1.1. Shaner et. al. (1982) describes how a multi-disciplinary approach is used to examine and identify the interdependencies of these components. Analysis "focuses on the interdependencies between farm system components under control of members of the farm household and how these components interact with the physical, biological and socioeconomic factors not under household control" (Shaner et al., 1982).

Harrison (1980) argues that rural development projects dependent on technological transfers have often ended in failure because of technological incompatibility of the project with the environment into which the technology was introduced. Thus farming systems analysis is a tool which can be used to:

a. increase the success rate of technological transfers

Systems Thinking and Appropriate Technology

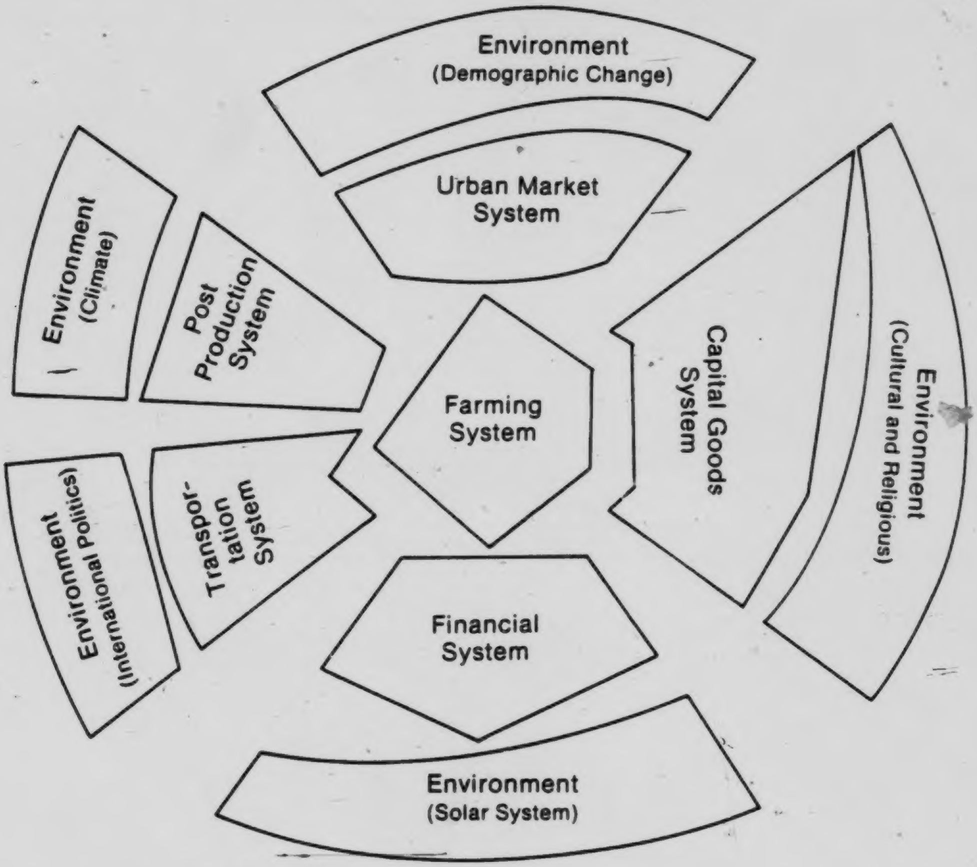
Environment
(Demographic Change)
Urban Market System
Environment
(Climate)
Post Production System
Farming System
Capital Goods System
Environment
(Cultural and Religious)
Environment
(International Politics)
Transportation System
Financial System
Environment
(Solar System)

Considerations:
1. separation at interfaces:
2. compatability of the shape of interfaces:
3. degree of implied internal integration within systems:
4. dimensions beyond two?
5. possibilities of generalizations across different rural situations:

Figure 1.1 Farming system within environment (adapted from L.P.Apedaile AGFOR 320 curriculum)

by identifying those conditions that require change before the technology can be successfully introduced or by identifying required changes to the technology so that it can fit into the local conditions, and

b. aid in the development of new and more appropriate technologies.

The technical complexity and high capital cost of micro hydroelectric systems relative to traditional energy sources combined with the seldom understood intracacies of subsistence agriculture demand the use of farming systems analysis techniques. Farming systems analysis provides a means to identify where, how and in what form energy is consumed in the agricultural sector. This is necessary information when the introduction of new energy sources into a farming system are being considered.

1.4 Energy and Agriculture in Developing Countries

United Nations (1983) statistics show that developing countries use less energy per capita than industrialized nations. Twenty per cent of the world's population living in industrialized nations consume seventy two percent of the world's commercial energy. The term "commercial energy" refers to energy commodities which are bought and sold in world markets. Coal, oil, natural gas and electricity are the most commonly traded commercial energy commodities. Commercial energy commodities have a high value because the energy contained within them can be converted into useful work or heat with a high degree of efficiency. A high efficiency energy source is commonly referred to as a "high ordered" energy. Electricity is a high ordered energy whereas dung and other traditional non-commercial energy sources are low ordered energies.

Makhijami (1975) argues that if one were to include data on non-commercial energy in the United Nation statistics, one would find that developing nations consume more than twice the energy indicated. The relatively small amounts of commercial energy bought by developing nations is consumed by the industrial and transport sectors. The majority of farmers in developing countries cannot afford to purchase commercial energy. This forces the rural sector to meet its energy needs with traditional non-commercial energy sources such as fuelwood, dung, crop residues for heating fuels, animals for draft power and human labor for power and production control. Since traditional non-commercial energy is less energy efficient than commercial energy sources, more non-commercial energy is required to do the same amount of work (Hays, 1977). Electrical energy from micro hydroelectric systems can replace the less efficient energy sources.

1.4.1 Rural Energy Use

The rural sector needs new energy sources to develop and prosper (Lawand, 1981). International aid organizations and international development banks have spent hundreds of millions of dollars on rural electrification programs (World Bank, 1975). Much of this money was spent to establish grid systems that connected isolated rural communities to large hydroelectric dams and thermal generating stations. According to the World Bank (1975), twelve per cent of the rural population in developing countries have access to electrical power but only half of these can afford to buy it. This represents a misallocation of resources, which developing nations cannot afford. Hays (1977) outlines two approaches to avoid this waste. Firstly, energy planners should determine where energy is needed, how much energy is needed and in what form this need can best be met. Secondly, development and investment policies should encourage the use of small decentralized facilities such as micro hydroelectric systems to provide on-site power because most of the population lives in isolated rural areas.

Regardless of how much planning is done, no project will be successful unless "the people want it and unless they are able to assimilate and build on it (Siwatibau, 1981)". Subsistence farmers will want electrical power only when they perceive that positive economic benefit will result from having it.

1.4.1.1 Farming Activities

Stout (1979) claims that agricultural activities involved in subsistence farming systems consume large amounts of non-commercial energy in the form of human and draft power. Despite the high allocative efficiencies of subsistence agriculture, low productivity per hectare prevails because of the poor energy conversion characteristics of traditional non-commercial energy sources. Without additional inputs of energy either in the form of fertilizers or labor saving technologies, productivity per hectare will remain low. Stevens (1977) explains that subsistence farmers are caught in an economic and technical spiral as they cannot easily obtain the technologies to increase productivity per hectare and increase income until they have an increase in income. He goes on to say that technical, economic and institutional changes are needed to break the spiral and increase agricultural productivity.

Eckholm (1975) warns that in some developing nations, the use of dung as a replacement for fuelwood instead of as an organic fertilizer has led to seriously reduced agricultural productivity. Bhatia (1982) believes that "besides the environmental consequences, sheer social costs of collection and transportation of fuelwood by poor people should be enough incentive for a program of improved efficiency of traditional fuels." Some have thought that the need for both fuel and fertilizer could be met with biogas technology but experience has shown that the plants are too expensive for the poor to build and operate. Bhatia (1982) found that biogas plants have a negative impact on the landless rural poor of India. Where these plants were installed, dung, previously collected free by local residents, now has cash value so it is collected by the cattle owner for a biogas plant. People without cattle must use other fuel sources for heating and these fuel sources are scarce and costly.

In many parts of the developing world where a limited amount of water has to serve the needs of many, the potential for conflicting uses of water exists. Irrigation and micro hydroelectric systems both require water with a hydraulic head. Main canals used to transport irrigation water can also serve to convey water for micro hydroelectric systems. Water used to produce hydroelectric power cannot be used to irrigate crops located above the micro hydroelectric plant site. Unless the canal system can be expanded to convey more water, micro hydroelectric development will be limited to using surplus irrigation water. The author observed an unused 75 kW micro hydroelectric system in Peru. It was unused because local subsistence farmers would not forgo food production for the benefits of electricity.

Stout (1979) observed that the use of commercial energy increases sharply in the transition from subsistence farming systems to 'modern` farming systems. Substitution of chemical, mechanical, electrical and fuel energy for non-commercial energy occurs when it becomes relatively more economical to use these sources of commercial energy than to use human or draft energy. This was evidenced in the Punjab region of India where diesel pumpsets and high yielding grain varieties were adopted during the "green revolution" because of their ability to improve farm production (hence, income) per hectare. However, farm production increases dependent on extensive use of commercial energy supplies for production inputs are vulnerable to fluctuations in the prices of world energy commodities. Where feasible, micro hydroelectric systems can be used to replace or reduce dependence on commercial energy commodities. Once built, micro hydroelectric systems are not subject to the commodity price fluctuations and problems of fuel supply associated with systems that depend on commercial energy commodities for fuel to operate the system.

Dramatic changes in productivity can result from the careful introduction of energy efficient appropriate technologies to subsistence farming systems. Szekely (1983) lists some of the farm activities that require energy inputs as being:

a. clearing, plowing, cultivating and seeding,
b. production and application of fertilizers,
c. irrigation,
d. maintainence and care of animals, and
e. harvesting crops and collecting livestock products.

Most of these activities require portable energy sources to facilitate energy distribution across farm fields. Since electrical energy is suited for stationary centralized activities, it is difficult to incorporate into the farming activities Szekely (1983) lists. However, many post-harvest production activities in subsistence farming systems are centralized at the farmstead and therefore many traditional energy sources used for post-harvest production activities could be replaced by electrical energy.

1.4.1.2 Post-Harvest Production Activities

Post-harvest production activities begin after the crop is harvested. Activities include threshing, drying, storing, primary food production and transport. Subsistence farming systems rely heavily on both human and animal power for most of these activities. Micro hydroelectric systems could be used to supplement or replace human and animal power for threshing and to improve the quality of other post-harvest production activities.

While for most of the year, high levels of underemployment in the farming sector exist, there often is a labor shortage for a few weeks during the harvest in regions associated with subsistence farming systems because the time available for harvest and preparing the crop for storage is limited. In many subsistence farming systems, grain is threshed by men and women using flails or by herding animals over the crop. Micro hydroelectric power systems can be used to power small stationary threshers which speed up the threshing process substantially reducing the need for scarce labor.

Forest et. al. (1982) noted that crop losses of up to thirty percent can accumulate throughout the post-harvest production system, the greatest loss resulting from insect contamination during storage. This represents a serious loss for farmers who already suffer from low agricultural productivity. Theshing by flail or by animals walking on the grains causes a large porportion of the crop to be harvested as broken grains. With the tough seed coat broken, the soft endosperm is exposed to insect attack. Forest et. al. (1982) suggests that better threshing techniques could reduce the amount of damaged grains and make them less susceptible to insects. Small threshers and dehullers have been designed which help reduce both the problem of damaged grains and the problem of labor shortage during harvest but they require a source of power to operate them. Electric motors are easier and cheaper to maintain and operate than are diesel or gasoline motors. So, in areas where threshing occurs near the farmstead or near a source of electric power, electrically powered threshers and dehullers could be adopted.

To minimize storage losses, a crop must be dried before storage even if wet conditions prevail during harvest. However, in most developing countries, crops are dried by spreading them on the ground which allows insects access to the crop. Community driers with blowers and/or supplementary heaters powered by micro hydroelectric systems in conjunction with properly designed storage facilities would enable the farmer to store grain in good condition, reducing storage losses.

Subsistence farmers often try to supplement their incomes with high priced cash crops. However, many of these crops are perishable and poor transportation in the rural areas makes getting the crops to market in good condition difficult for subsistence farmers. The farmer thus receives a lower price for the product than he/she would otherwise expect. This economic condition would suggest that there may be some feasibility where small rural industries could be established to process cash crops into a more stable and higher priced product in the areas where they are produced. Mnzana (1981) suggests that such industries could operate with energy provided by micro hydroelectric systems.

1.4.1.3 Domestic Energy Use

Fifty per cent of all energy commodities consumed in developing countries are consumed by household and homecraft activities such as cooking and space heating (Tinker, 1980). This figure can rise up to ninety per cent in warmer countries where space heating is not required.

Cooking over open fires uses the most energy as the practice is inefficient in energy utilization. For example, Arnold and Jongma (1978) found that ninety four per cent of the heat value of fuelwood is wasted in Indonesia. Population growth and the resultant increased need for fuelwood has put a serious strain on the environment and has led to deforestation in many parts of the world. Deforestation is a serious environmental problem. Some of the environmental consequences include rapid soil erosion, high sediment loads in rivers and a reduced ability of the watershed to store water. In addition, the receding forests force women and children to spend up to half a day gathering sufficient fuel for the day's meal. Micro hydroelectric systems, where feasible, can provide energy for cooking and eliminate the need to collect fuelwood. The resulting reduced pressure on the forest, if combined with reforestation projects, should improve the quality of the watershed. This, in return, would benefit the micro hydroelectric system and users of the system by providing a more stable year round water supply. Women and children freed from collecting fuelwood can devote time to other tasks which could be economically productive.

Tinker (1980) points out that "time is the key factor in the utilization of human energy." She argues that the slow adoption of more energy efficient cook stoves by African women was partly due to the need to chop the wood to fit the stove. Chopping wood added more work than the energy efficient cook stove saved to the already long day of most African women. If available, reliable and affordable, electrically powered cook stoves would quickly be adopted as a labour saving device.

Molnar (1980) found that human energy is the input for most other domestic and homecraft activities such as collecting water, child care, spinning, weaving and knitting. Appropriate technologies such as micro hydroelectric systems can provide the additional energy to reduce the drudgery and increase the quality of some of these tasks. Time released could be diverted to more economically beneficial activities, thus improving the standard of living for many families.

1.5 Technical Appropriateness of Micro Hydroelectric Power

Micro hydroelectric systems have yet to gain wide spread acceptance as a source of power for farm and village electrification projects. The technology is often seen as too expensive and complex. Over the last decade, the development of electronic load controllers to replace mechanical governors has reduced the overall cost of micro hydroelectric systems but the controller is still a significant cost factor making micro hydroelectric systems uneconomic for most subsistence farmers.

Governors and load controllers both ensure that output voltage and alternating current frequencies remain constant when electrical loads change. Where electrical loads are constant and the flow of water is constant, micro hydroelectric systems can be designed to operate without a governor. However, this situation rarely occurs as water flows tend to be cyclic according to seasons and electrical loads highly variable.

Electric motors and electronic devices are designed to operate with steady input voltages and frequencies. Many practical applications of electrical power in rural areas of developing countries continue to function where voltage, current and frequency vary. In particular, induction motors and heating elements can operate quite well outside of their design voltage and frequency. If input voltage and frequencies can remain within the tolerances of electrical equipment without requiring electronic load controllers, then the removal of the governor is advantageous as the capital cost of the hydroelectric system would be substantially reduced.

During the summer of 1983, the author observed three multiple jet micro hydroelectric systems operating in the sub-tropical El Dormilon valley of Colombia. A governor was not required on these systems as voltage was maintained within tolerable levels by controlling the runaway speed with multiple jet governing systems. The electric power generated by these systems was used to operate freezers, radios, hot plates, juicers, lights and space heaters. Use of these various appliances throughout the day caused the voltage to fluctuate from 90 to 130 volts. The electrical appliances used were not damaged by the fluctuating voltage because current and frequency varied directly with voltage.

1.6 Micro Hydroelectric Power as an Appropriate Technology

The reliable energy provided, the mechanical simplicity and versatility of the observed micro hydroelectric systems suggest that they would be technically appropriate for rural peoples who live in hilly and alpine terrains where water is abundant. The farming systems analysis of societies based on subsistence farming systems indicate that there are numerous opportunities for people in these societies to use electric power if it were available at a cost that these people could afford.

In summary, micro hydroelectric systems that can be developed for people in subsistence farming systems can provide a number of economic benefits for these people. Micro hydroelectric systems can create jobs in the rural sector where demand for jobs is greatest. This would reduce income disparities between rural and urban sectors of developing countries and slow the rural to urban migration. By supplying inexpensive energy to many small cottage industries which produce goods from locally available raw materials, micro hydroelectric systems would stimulate employment opportunities in sectors of the local economy outside the agricultural sector.

The systems observed indicated that economically efficient micro hydroelectric systems can be built and maintained with locally available materials and can be installed by the users. They can also be financed with local capital which increases the autonomy and self reliance of the users.

Only increased use of this micro hydroelectric system by subsistence farmers can judge its final appropriateness. However, little technical information on design parameters of these systems is available in the literature for engineers wanting to design and install systems in remote rural areas. This research project was an initial effort to develop some information on design parameters.

2. DESCRIPTION OF MICRO HYDROELECTRIC SYSTEM

2.1 Hydraulic Turbines

Over the years, two major technologies have been developed to derive work from water, those being the waterwheel and hydraulic turbines. Waterwheels, the earliest technology, have been used by peoples throughout history for at least three millennium. A characteristic of waterwheels is that there is little or no movement of water with respect to the vanes. The current wheel, where vanes of the wheel dipped into a stream of water and were moved by the stream's current, was the earliest and least hydraulically efficient type of waterwheel. Hydraulic efficiency is defined as the ratio of the energy output from the turbine or waterwheel to the total energy contained in the water before it comes into contact with the turbine or waterwheel. Confining the stream so that water did not escape around or beneath the vanes improved hydraulic efficiencies of these wheels to 30 percent.

Hydraulic turbines, which were later developed, involve the movement of water with respect to the vanes and are designed to cause the velocity of water flowing through the turbine to change both direction and magnitude. Since the turbine buckets must apply a force to change the velocity of the water jet, then an equal and opposite force must be supplied by the water onto the turbine buckets. By this reasoning, Daugherty (1920) defined a hydraulic turbine "as a waterwheel in which a motion of the water relative to its buckets is essential to its action."

Many turbine designs exist which can be used to match an infinite number of operating conditions. Hydraulic turbines are often classed into two broad categories which differ radically one from the other. Impulse turbines use the dynamic or kinetic component in a stream of water, operate in free air at atmospheric pressure and are most hydraulically efficient when the energy in the water is provided by high head and low flowrate. Reaction turbines utilize both the dynamic and pressure action of a stream of water, operate completely surrounded by water and are most hydraulically efficient when the water's energy is provided by low head and high flow rates. As the water sources observed by the author in Colombia had the characteristics of high head and low flow rates, this project evaluated two small impulse turbines generally referred to as Pelton turbines.

2.2 Pelton Turbines

The Pelton turbine, first patented in 1880, is the most common impulse turbine in use today. Pelton turbines are easily recognized as they have many buckets attached to the outer perimeter of the wheel (Figure 2.1). Each bucket consists of two elliptical spoon shaped compartments separated by a straight sharp wedge. A high velocity water jet operating in the plane of the turbine is aimed at the center of a bucket. The water jet is split in two by the wedge and forced to change direction as it flows over each half of the bucket. Each bucket on the turbine is in contact with the water jet for a short period of time. This constant transfer of force from one bucket to the next creates an impulse action, hence the name impulse turbine.

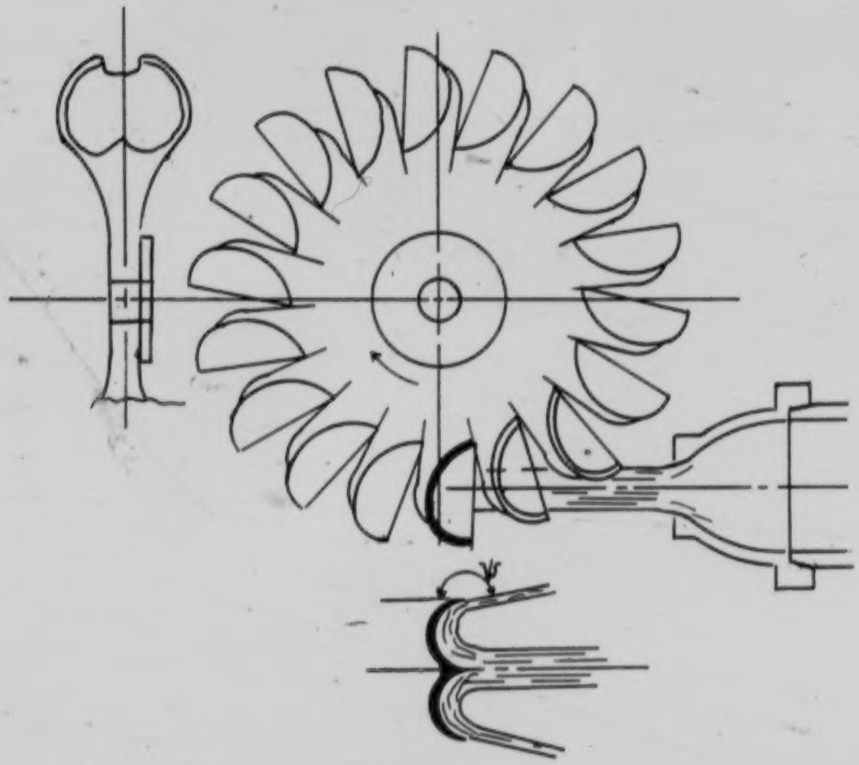

Figure 2.1 Small Pelton turbine

Since 1880, Pelton turbine design improvements have focused on the maximization of hydraulic efficiency. Over 100 years of design has produced a machine capable of obtaining efficiencies of 95 percent. Turbine design is site specific since each hydropower site is unique as far as available volume of flow and head are concerned. The design criteria of Pelton turbines briefly presented in this section are discussed in detail by Daugherty (1920).

Hydraulic efficiency of an impulse turbine depends on the optimum number and size of buckets and the pitch diameter of the turbine. Pitch diameter is measured from the center of the Pelton turbine to the center of the water jet at a point tangent to a circle scribed by the center of a rotating bucket. Optimum pitch diameter depends upon the available water jet velocity at the nozzle and the desired rotational speed of the turbine. Water jet velocity can be calculated using Equation 2.1. For a given hydro site, H_t

$$V_j = C_d(2gH_t) \qquad (2.1)$$

is fixed so waterjet velocity depends upon the discharge coefficient C_d. The discharge coefficient for nozzles can range from 0.61 for a sharp-edged orifice nozzle which is low cost and easy to manufacture to 0.98 for a precisely designed manufactured nozzle which is relatively high cost. Maximum power is developed at the turbine when the tangential velocity of the bucket at pitch diameter is 0.47 times the velocity of the water jet (Daugherty, 1920). Having estimated the tangential velocity of the buckets and knowing the angular velocity with which the turbine should rotate, the optimum pitch radius for the turbine can be calculated using Equation 2.2.

$$x_o = V_b/\omega \tag{2.2}$$

For a given water jet velocity, turbine diameter is inversely proportional to rotational speed.

Weight, size and cost of the turbine determine the upper limit on turbine diameter. The lower limit is determined by shaft size and the minimum amount of space required to attach the buckets to the hub. The size and shape of the buckets is largely a function of water jet diameter. Daugherty (1920) states that bucket width should be approximately three times the jet diameter. Water jets with diameters greater than the recommended size cause the Pelton turbine to lose hydraulic efficiency as incoming water interferes with the free flow of water leaving the buckets. This action is commonly referred to by the term "flooding".

The rate that water leaves the buckets is determined by the angle of return (ψ) imposed on the water jet by the shape of the bucket and the water jet velocity. Maximum force from the water jet is transmitted to the buckets when water returns 180 degrees. With this angle of return, the velocity of water leaving the buckets with respect to an observer facing the turbine perpendicular to the plane of the turbine is zero. However, this condition would cause the water leaving the bucket to strike the backside of the next bucket, thereby reducing the rotational speed of the turbine. Turbine designers use an angle [illegible] return of 165 degrees to allow water to leave the buckets with sufficient velocity to clear the path of the adjacent bucket as illustrated in Figure 2.1.

Daugherty (1920) states that optimal turbine performance requires that the proper number of buckets be mounted on the turbine. Whereas too few buckets result in energy loss because they swing out of the path of the water jet before all the water in the jet has had an opportunity to strike the bucket, too many buckets result in unnecessary disruptions of the water jet, reducing hydraulic efficiency. Bucket requirements for optimal turbine performance can be calculated for a given turbine knowing the velocity of the water jet and desired speed of rotation.

The most common way to maximize hydraulic efficiency of an impulse turbine is to direct water onto the turbine using a single water jet. Single water jet systems have higher hydraulic efficiencies than multiple jet systems and are well suited to large hydro power systems. The incremental cost of a larger, more efficient pelton for a single jet system is less than the incremental revenue produced by more power output from a given water supply. However, use of a single water jet limits the volume of water that can be used efficiently by a specific turbine and hence limits the amount of power that the turbine is capable of developing. In rural areas of developing countries where cost is a limiting factor, maximization of power is very important. Multiple jet systems, although less hydraulically efficient than single jet systems, increase the volume of water striking the turbine and are thus capable of producing more power from a specific turbine.

For micro hydroelectric systems in rural areas of developing countries, multiple jet systems may be able to provide an alternative energy source to present use of non-commercial energy commodities. The cost of the system will be the determining factor. The cost of the turbine, a major component of micro hydroelectric systems, is a function of turbine size and the user will benefit most when the smallest possible turbine is used to produce the required amount of power.

2.3 Electric Power Generation

Hydraulic turbines are used as prime movers to produce either or both electrical and mechanical power. Where not required, electrical power generation should not be introduced as it adds both complexity and cost to any micro hydropower project. However, use of the mechanical power produced by a micro hydropower project is limited to locations near the hydro site while electrical power has the advantage that it can be easily transmitted to sites located some distances from the hydro site. Electrical power has an added advantage over mechanical power of being suitable for use in a wider variety of devices (eg. heating elements and lights). This factor is important if the hydro project is to offer economic benefits within a subsistence farming system.

2.3.1 Electric Generating Equipment

Around the turn of the century, direct current (dc) power was generated by the direct coupling of hydro turbines to dc generators. Direct current generators can operate over a wide range of rotational speeds for the armature so the generators do not require accurate speed control on the input shaft. Voltage regulation is a function of connected load so a rheostat installed on the field winding is used to keep voltage constant. As technology improved and the uses for electricity became more sophisticated, ac power became more common as it is easy to transmit power using transformers. Today, it is difficult to get any dc equipment capable of producing a direct current at voltages greater than 24 volts. Automobile and truck dc generating systems using either 12 volt or 24 volt systems can generate up to 1 kW of dc power (Martin, 1981). If one wants to keep the cost of a micro hydroelectric project low, the design of the system must use as many "off the shelf" components as possible. Most micro hydroelectric projects should be capable of producing 2 to 5 kW of power if they are to be useful so this means that the micro hydroelectric systems are restricted to ac systems.

The choice of ac generating equipment largely depends on whether or not the system is connected to a power grid. When micro hydroelectric systems are connected to a power grid, induction generators are preferred because voltage and frequency are easy to regulate and they are rugged and relatively inexpensive. The grid provides the excitation current and the frequency control to the induction generator which then produces variable current flow at constant frequency and voltage. Power output from induction generators increases as rotational speed increases provided the maximum torque of the generator is not reached. When maximum torque has been reached, electrical output begins to decrease, rotational speed increases, and the generator will "run away" (Fritz, 1984). Therefore, speed control on the input shaft of the generator is required for overspeed protection.

As power grids do not exist in most rural areas of developing countries, synchronous alternators are better suited for micro hydroelectric systems. Normally, a small dc generator provides the excitation current for the rotor of a synchronous alternator (Warnick, 1984). However, Fritz (1984) states that small synchronous alternators are currently available which no longer require a small dc generator. They are self-exciting, incorporate a voltage regulator and are brushless which makes them ideal for micro hydroelectric systems. The dc generator is replaced by a bridge rectifier and filtering system in the stator which creates the direct current needed for excitation which is then boosted by current transformers as the alternator is loaded. This feature makes the alternator almost maintenance free, a desirable feature in isolated locations.

The frequency and voltage output of a synchronous alternator is directly proportional to the rotational speed of the rotor. Synchronous alternators can be connected to a power grid but in order to generate a fixed ac frequency, they must operate at a specific rotational speed known as the synchronous speed.

Synchronous alternators are generally built to meet site specific conditions but off the shelf units are available up to 40 kW. In North America, a two or four pole alternator must operate at 3600 rpm or 1800 rpm respectively to produce an alternating current with a frequency of 60 Hertz at 120 Volts. Under conditions of variable load, the rotational speed of synchronous alternators must be governed to produce electricity with a constant frequency and voltage.

2.3.2 Speed Regulation

As previously discussed, electric power generation by stand alone synchronous alternators frequently requires some form of speed control on the generator. Every hydropower installation must address the problem of speed control. "The size of the problem depends on the type and size of turbine, the loading conditions and whether the plant is isolated or connected to an electrical grid, (Fritz, 1984)."

2.3.2.1 Mechanical Governors

Mechanical governors are most commonly used for Pelton turbine systems larger than 100 kW. Koester (1911) and Daugherty (1920) discuss at great length the design of mechanical governors briefly discussed in this section.

Mechanical governors sense the speed of a turbine using the centrifical forces generated by rotating flyballs. A change in rotational speed of the flyballs causes a subsequent change in their centrifugal force which either increases or decreases their vertical location on their shaft. Vertical movement on the shaft activates a servomotor which causes the control mechanism to either increase or decrease the amount of water striking the turbine depending on the direction of vertical movement by the flyballs.

Two principle methods are used to control the amount of water striking a Pelton turbine. The first method adjusts the flow rate using valves while the second directs the water jet either on or off the turbine. Using valves to control flow has the advantage of saving water (Koester, 1911). Rapidly changing loads increase the possibility of water hammer developing in some systems if the governed valves are closed too quickly. Daugherty (1920) suggests that systems subject to large load fluctuations and having long penstocks would benefit from having a governor that deflects the water jet away from the turbine. This would prevent water hammer from developing and possibly destroying the system.

Regardless of which method is used, mechanical governors are technically complex and very expensive. Fritz (1984) states that the technology is difficult to scale down for micro hydroelectric systems as it was developed for larger hydroelectric systems. Martin (1981) notes that, for micro hydroelectric systems, the governor can easily cost more than the turbine and generator being regulated. Thus, the technical complexity, the difficulty to maintain and repair and the high capital cost of mechanical governors makes them inappropriate for use in isolated regions of developing countries.

2.3.2.2 Load Controllers

Electronic load controllers maintain constant turbine speed by maintaining a constant electrical load on the system using a combination of system loads and a base or "dummy" load. These controllers sense the amount of electrical power demanded by system users and divert unused power to the dummy load. Dummy loads are usually water heaters or space heaters. The controllers are capable of changing the amount of power diverted so rapidly that the alternator operates at a constant load and so no change in speed occurs. Again there is some question as to the appropriateness of electronic load controllers in rural settings of developing countries. Two major faults are technical complexity and relatively high cost. An electronic load controller suitable for micro hydroelectric systems smaller than 20 kW presently costs $CAN 1,386.00. It is produced in Canada by Thomson and Howe Energy Systems Inc. Kimberley, British Colombia. This price would more than triple the cost of a 5 kW micro hydroelectric system, putting micro hydroelectricity beyond the reach of subsistence farmers in developing countries.

A simpler load controller can be used where each system load is matched with an equivalent dummy load on a two way switch. When one load is turned off, its equivalent dummy load is turned on at the same time, thereby keeping constant load on the turbine. The only difficulty with this system occurs when resistive dummy loads are matched with inductive loads (i.e. electric motors). The power factor of the motor and the start up power requirements demand special consideration in the design of the system for matching dummy loads.

Induction motors cause current to lag voltage so a lagging power factor is created. Referring to Figure 2.2, one can see that by offsetting voltage from current by angle θ, the apparent power, P_A, measured in kVA, is greater than ordinary resistive power, P, measured in kilowatts, by a factor of $\cos\theta$ (the power factor). Capacitors cause voltage to lag current which creates a negative reactive power. A capacitor installed in series with an induction motor should be capable of producing a negative reactive power, P_X, equal in magnitude to the positive reactive power of an induction motor. This will cancel the effect of the inductive motor and restore the power factor to one (cosθ=0).

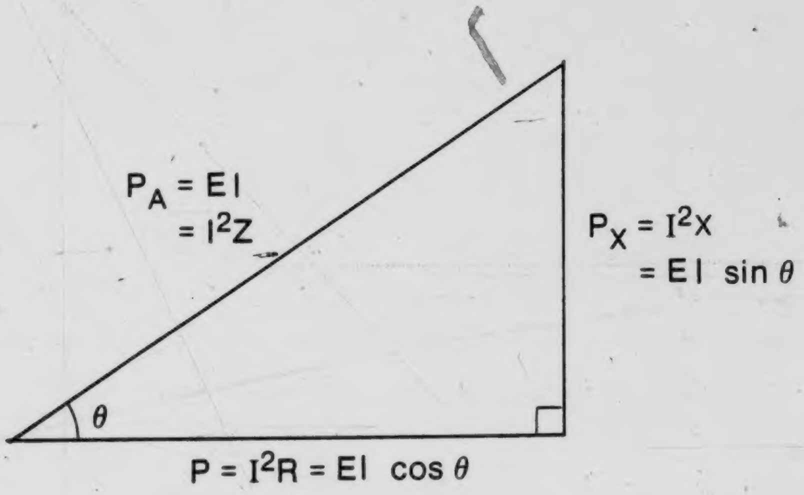

Figure 2.2 Power triangle showing effect of inductive loads on power factor.

Another problem is that induction motors generally require twice their rated power to start. Provisions can be made in the switching system to temporarily transfer power normally directed to resistive loads from those loads to the induction motor during the start up period.

For both the manual and electronic load control systems, the power output of the alternator must always exceed the useful demand. Martin (1981) states that this condition wastes the energy in the water during periods of low demand. This would be a problem if water was limited and stored in a reservoir. However, many micro hydroelectric power plants are "run-of-river" (meaning they have little or no storage capacity) so designers need not be concerned with this loss of energy.

2.3.2.3 Runaway Speed

As with any man made device, mechanical or electrical governors do occasionally fail. If, for whatever reason, load on the generator were disconnected and the governor failed on a single jet Pelton turbine, overspeed conditions would prevail on the generator. The generator and turbine speed would increase until runaway speed were reached. For Pelton turbines, this runaway speed is the rotational speed of the turbine that results when the force of the water jet striking the buckets is equal to the force of windage and bearing friction in the system. The force required to overcome windage and bearing friction in micro hydroelectric systems is usually low so runaway speeds in single jet configurations of these systems occur when the tangential velocity of the buckets nearly equals the velocity of the water jet.

Since centrifugal forces increase as a square of rotational speed, generators in these systems must be able to withstand centrifugal forces that occur at runaway speed. Martin (1981) claims that these forces can be up to 400 per cent higher than the centrifugal forces that occur at normal speed. Operating at runaway speed for extended periods of time can cause damage to the system. To avoid generator damage caused by the system operating at runaway speeds, developers buy oversized generators which are more capable of handling the extreme centrifugal forces generated but which increase the cost of the hydroelectric system (Reddy, 1966).

Damage to loads on the micro hydroelectric system can occur if the system is not operated at design speeds. As previously mentioned, the frequency and voltage produced by synchronous generators varies directly with rotational speed. As a synchronous generator driven by a Pelton without speed control approaches runaway speed, frequency and voltage increase to the point where they will damage loads connected to the alternator. Voltages from an ungoverned single jet Pelton turbine system could easily exceed 130 volts and thus exceed the ability of most electrical devices to cope. A mechanism that reduces runaway speed is essential to keep voltage and frequency within acceptable levels that will not destroy either the generator or the loads on the system.

Many electrical devices can operate within a range of current, voltage and frequency without hindering the operation or permanently damaging the device. The voltage output from the multiple jet micro hydroelectric system operating at El Dormilon in Colombia has fluctuated between 90 and 130 volts for the last five years with no damage to either resistive loads (lights and heating elements) or inductive loads (small induction motors). Light bulbs dim when voltage drops to 90 volts and brighten when power surges upward. Small appliance induction motors have not burned out because the frequency and voltage input vary simultaneously.

2.3.2.4 Runaway Speed Reduction

The past two decades have seen many approaches taken to reduce the runaway speed of Pelton turbines. Most methods involve the placement of a failproof (non-mechanical, non electrical) device around or behind the turbine. Each of these devices reduce runaway speed with varying degrees of success. With the exception of Toro (1980), all speed reduction devices discussed below were tested as single water jet systems.

Reddy (1966) and Shirgur (1968) utilized the portion of the water jet that at overspeed conditions, (i.e. the pelton operating above the optimal design speed), passes through the turbine without contacting the buckets. This water is commonly called wastewater. A horn shaped device was placed behind a Pelton turbine to catch and direct wastewater onto the back of the buckets perpendicular to the direction of bucket travel. Shirgur (1968) tested two devices. One device turned the wastewater 190 degrees and the other device turned the wastewater 230 degrees in the plane of the turbine. He found that with each device the runaway speed was reduced to 72 and 78 percent of initial runaway speed respectively. The most significant find was that the reduction in runaway speed was achieved without any change in hydraulic efficiency at maximum power.

Gavirria (1977), Genes (1978) and Toro (1980) all tried to redirect the water leaving the buckets at different angles to the plane of the turbine onto the backs of the buckets when the turbine was operating in overspeed conditions. The angle of the water leaving the plane of the turbine depends upon the ratio of the tangential speed of the turbine buckets over the velocity of the water jet. The turbine could operate in any of the following conditions:

a. $V_b/V_j < 1/2$ $\delta>90°$ (overload condition)

b. $V_b/V_j = 1/2$ $\delta=90°$ (optimal operating speed)

c. $V_b/V_j > 1/2$ $\delta<90°$ (overspeed condition)

The angle δ is the angle formed between the water leaving the turbine and the plane of the turbine (Figure 2.3). Photograph 2.1 shows that when a Pelton turbine is operating at maximum power, the water leaves the bucket perpendicular to the plane of the turbine obliterating the turbine from view. Photograph 2.2 illustrates that at runaway speed, water leaves the buckets at an obtuse angle leaving a clear view of the turbine.

Gavirria (1977) tested a tubular device designed to collect the water leaving the buckets when δ was less than 90 degrees and redirect that water onto the backs of buckets. The device surrounded 25 percent of the turbine starting at the point where water leaving the buckets during overspeed conditions could be captured. Use of this device

Photograph 2.1 Pelton turbine operating at maximum load with four water jets (δ=90 degrees)

Photograph 2.2 Pelton turbine operating with four jets under runaway speed conditions ($\delta<90$ degrees)

resulted in a 5 percent reduction in runaway speed but the overall hydraulic efficiency at optimal speeds was reduced by another 4 percent.

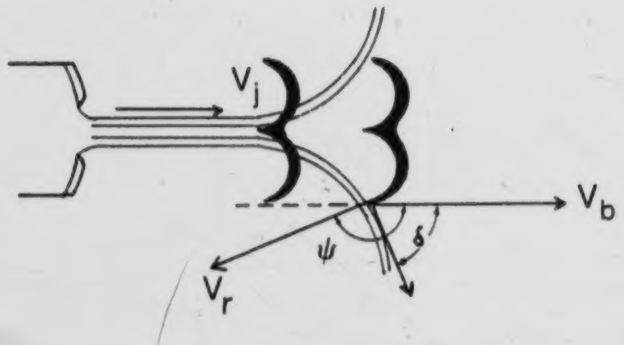

Figure 2.3 Velocity relations at discharge

Genes (1978) used the work of Gavirria to develop and test several speed control devices. The first device tested was constructed from a car tire cut to surround 75 percent of the circumference of the turbine. Water leaving the turbine was confined and collected by the tire. Buckets would strike the collected water as they passed through the device. With similar results to Gavirra's device, Genes constructed a second device by placing ten equally spaced plates inside the tire. The plates were designed to allow the buckets to pass through with a minimum of clearance. This device managed to reduce runaway speed by 29 percent.

However hydraulic efficiency at optimal operating speed was reduced to 48 percent from a hydraulic efficiency of 65 percent without the device. This is an unacceptable reduction in efficiency so a third device was developed. This device, rather than being tubular, was funnel shaped covering 25 percent of the turbine circumference. The device was widest at the point where water leaving the buckets at an angle δ greater than 90 degrees could be captured and narrowed until the buckets would just clear as they passed through. Water would collect at the end of the device and could only be removed as little packets of water in between two adjacent buckets. This device reduced runaway speed to 81 percent of runaway speed without the device and reduced hydraulic efficiency at optimum operating speed to 55 percent from a hydraulic efficiency of 65 percent without the device. Genes concluded that the reduction in hydraulic efficiency at maximum power was caused by water prematurely entering the device.

Toro (1980) redesigned the funnel shaped device of Genes (1978). Toro developed a short cup shaped device to reduce the chance of water entering the device before overspeed conditions prevailed. Formed out of polyvinyl chloride (PVC) pipe, the device was wide enough to capture water escaping from the buckets during overspeed conditions and it quickly narrowed to a width that would only allow passage of the buckets. Using one jet, Toro's cup device reduced runaway speed to 70 percent of the runaway speed without the device while hydraulic efficiency of optimal operating speeds was reduced to 55 percent. With the shortened cup device, there was more room to place other cup devices on the turbine. With three equally spaced jets and cup devices, runaway speed was reduced to 60 percent of the runaway speed without the device with the hydraulic efficiency at optimal operating speeds dropping to 55 percent from a hydraulic efficiency of 65 percent without the device. Toro speculated that the drop in runaway speed with three jets and cup devices was due to the collision of water leaving the braking device with the adjacent water jet, thereby reducing the quality of the subsequent jet, where jet quality refers to the coherence of the water jet. A good quality water jet will have uniform diameter and no spray.

The multiple jet, multiple cup system developed by Toro (1980) was installed on a 1.75 kW micro hydroelectric system and used on a small Colombian farm (Lobo and Burton, 1980). A hotplate, lights and various audio-visual appliances have successfully used power generated and regulated by this micro hydroelectric system for five years.

Lobo and Burton (1980) recognized the importance of jet quality on the reduction of runaway speed. They conclude that the untouched wastewater segments leaving the turbine could sufficiently reduce the quality of the water jets for multiple jet systems having more than three jets. Lobo found that runaway speeds could be reduced to 70 percent of the runaway speeds without the device with no reduction of hydraulic efficiency at optimal operating speeds (personal communication). Multiple jet micro hydroelectric systems were built and have been functioning successfully now for four years on small farms in Colombia.

3. THEORETICAL FRAMEWORK

3.1 Introduction

Most research and development of Pelton turbine systems has been conducted with the objective of developing turbine designs that maximize hydraulic efficiency. Since multiple jet systems reduce hydraulic efficiency, they are seldom considered when designing high head hydropower projects. However, when designing micro hydroelectric systems for use in isolated rural areas where electric power is nonexistent, the ability of the system to provide reliable power inexpensively is more important than the achievement of maximum hydraulic efficiency.

Research for this project was undertaken to explain how multiple jet systems work. Three steps were necessary to generate the data needed to analyze multiple jet performance. First, as explained in this chapter, a theoretical model was developed for a computer using observed physical relationships to describe the operation of a multiple jet micro hydroelectric system. A good theoretical model can be used by micro hydroelectric developers to study the effect of design changes on power output. Hypothetical flowrates and orifice sizes were used in this theoretical model to evaluate the effect of jet configuration on power output from a pelton turbine.

Secondly a micro hydroelectric system was then built to test four variables according to the experimental method outlined below in section 3.2. The components of this micro hydroelectric system are described in chapter four. Hydraulic head, flowrate and runaway speed were recorded for 250 experimental runs.

Next, the accuracy of the theoretical model for predicting runaway speed was tested. The hydraulic head and flowrates recorded during the experimental runs were inserted into the theoretical model to predict runaway speeds for each of the 250 runs which would later be compared with the actual runaway speeds determined in step two. These runaway speeds are recorded in Tables A.3.1 to A.3.10.

The analysis of results appears in Chapter five. Discussion in Chapter five focuses on the three areas of importance identified in the objectives for this research: 1) the effectiveness of the theoretical model for predicting runaway speed, 2) the examination of the importance of each variable on runaway speed, 3) and the comparison of turbine performance curves. Chapter six contains the conclusions of this research based on observations and the results discussed in chapter five.

3.2 Experimental Method

Explanation of the experimental method is presented at this time to facilitate an understanding of the development of the theoretical computer model in section 3.3. To determine optimal operating conditions for multiple jet micro hydroelectric systems, four variables which have the greatest influence on power production were tested: turbine, jet configuration, head and flow rate.

The performance of an inexpensive handcast turbine from Colombia was compared to that of a relatively expensive manufactured turbine from England. The physical characteristics of these two turbines are described in Table 3.1. The significance of bucket number was also tested as the handcast turbine had 18 buckets and the manufactured turbine 16.

TABLE 3.1 TURBINE CHARACTERISTICS

	Turbine Type	
Characteristic	Handcast Colombian	Manufactured English
Weight(gm)	120	450
Diameter(cm)	12	13
Pitch diameter(mm)	106	106
Number of buckets	18	16
Angle of return ψ	170	165
Bucket width(mm)	36	33
Composition	Aluminum	Brass

The five jet configurations selected are illustrated in Figure 3.1. The single-jet system represented the normal operation of a Pelton turbine and was expected to operate

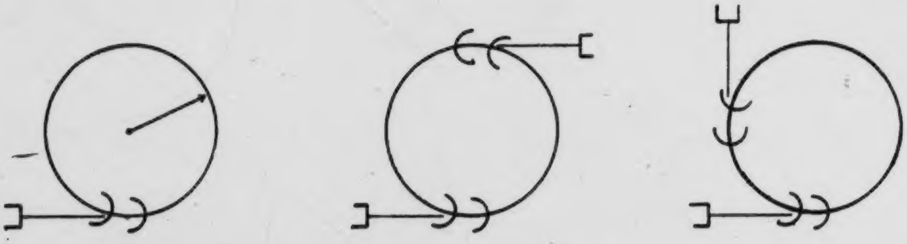

a) 1 Jet b) 2 Jet no interference c) 2 Jet

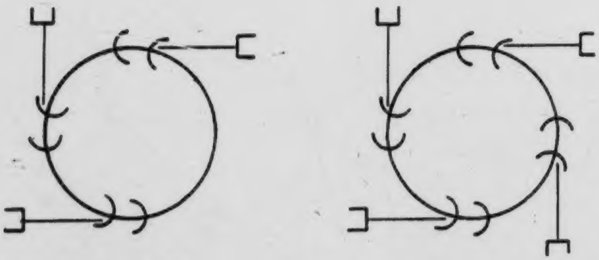

d) 3 Jet e) 4 Jet

Figure 3.1 The five water jet configurations evaluated in this research.

the turbine at the highest rotational speed possible. Two two-jet configurations, (one with interference, one without interference) were used to estimate the amount of water removed by the interference which was caused when wastewater segments struck an adjacent jet. This was done by using the no interference configuration as a standard against which the performance of the other two-jet configuration was compared. The three-jet configuration was used to calculate the amount of wastewater produced by interference at two points and the four-jet configuration introduced the maximum amount of interference possible, reducing runaway speed the most.

The five hydraulic heads tested ranged from thirty to fifty meters. Thirty meters of hydraulic head was chosen as the lower limit on hydraulic head. The low rotational speeds and low power outputs associated with this head (Table 3.2) and the flowrates used in this experiment make development of micro hydroelectric systems below this head impractical.

TABLE 3.2 CHARACTERISTICS OF WATERJET AT 30 AND 50 METERS OF HYDRAULIC HEAD

Hydraulic Head (m)	Waterjet Velocity (m/s)	Rotational Speed Of Turbine With Pitch Diameter of 0.1016 m (rpm)	Theoretical Power With Flowrate of 3.3 l/s (watts)
30	24	2100	971
50	31	2726	1618

Standard polyvinyl chloride (PVC) pipe, which is available in third world countries, cannot withstand pressures greater than that which exists at fifty meters of head. Higher heads would demand thicker walled and, hence, more expensive PVC pipe or simply other more expensive pipe.

The five flow rates used in the experiments were arbitrarily chosen to include the operating range for the handcast turbine. Flow rate is directly dependant on the orifice diameter of the nozzles used. Orifice diameters were chosen on the recommendation by Daugherty (192[illegible]) that waterjet diameter not exceed one third the bucket width. This criteria was maintained for all orifice diameters except the single-jet configuration. If the single-jet orifice diameter was decreased to less than one third the bucket width, then the water jet diameters for the four-jet configuration would have been too small to represent realistic operating conditions. The two-jet-no-interference configuration served to replicate the operating conditions of a single-jet system operating at the same flow rate. Each flow rate was established using one of five nozzle "series". The term "series" refers to a group of water jet nozzles where each jet configuration has the same total crosssectional area. Series 1 orifices have the smallest total area. Each orifice series is approximately 23 percent larger than the previous series. To evaluate the effect of jet configuration on runaway speed, the power input to the turbine must be equal for each configuration. Flow rate and power input will be equal only when the total orifice cross sectional areas for each configuration are the same.

TABLE 3.3 ORIFICE SIZE DEVIATION

Series	Number of Orifices	Orifice dia.(mm)	Total Area (mm)^2	Average Area (mm)^2	Increase %
1	1	16.00	201	195	0
1	2	11.00	190	195	0
1	3	9.06	193	195	0
1	4	7.90	196	195	0
2	1	17.85	250	248	27
2	2	12.50	245	248	27
2	3	10.28	249	248	27
2	4	8.90	249	248	27
3	1	19.88	310	298	20
3	2	13.72	295	298	20
3	3	11.00	285	298	20
3	4	9.85	304	298	20
4	1	22.12	384	375	26
4	2	15.44	374	375	26
4	3	12.49	367	375	26
4	4	10.92	375	375	26
5	1	24.21	460	454	21
5	2	16.94	451	454	21
5	3	13.96	459	454	21
5	4	11.89	444	454	21

Two hundred and fifty runs were undertaken to test each possible variable configuration. Each of the 250 experimental and theoretical runs was identified by a run identifier (C1J340) which was six characters long and separated into four fields. The first field is one character long and a letter is used to identify whether the turbine used was the handcast Colombian (C) or manufactured English (E) turbine or theoretical (T) indicating the use of the computer model (Figures 3.7-3.9). The second field is also a one character field which is used to identify the orifice series number. These numbers may range from 1 to 5. The exception to this rule occurs in Figures 3.7, 3.8 and 3.9 representing the use of the computer model where the numbers "1" and "2" refer to the handcast turbine and manufactured turbine respectively. The third field is 2 characters in length where the first character is always a "J". The second character is used to identify one of the five jet configurations where the number corresponds to the number of jets. Since there are two configurations with two jets, the two-jet-no-interference configuration is identified by the absence of the second character. The final field, two characters long, is used to indicate at what hydraulic head the test was run.

3.3 Theoretical Model Development

A theoretical model was developed to predict runaway speed of the turbine. The model is based on two principles. The first is that when a Pelton turbine operates in overspeed conditions, water passes through the turbine without imparting its force onto the turbine buckets. Such water was identified by Reddy (1966) as wastewater. Reddy notes that the wastewater volume increases as the rotational speed of the turbine increases, thus decreasing the effective power of the waterjet. The second principle is that friction generated at the bearings and friction due to windage act to slow the turbine down. This windage and bearing friction increases with speed until, at runaway speed, the power of the water striking the buckets equals the power absorbed by friction.

Two sets of curves were developed in this model. The first set represented the power produced by the turbine. The downward trend with increasing rotational speed represents the loss of ability of turbine to take power out of the water jet. The second set represented the power required to overcome friction. This power requirement increases as rotational speed increases, hence the upward trend. The power curves were developed assuming that power at the turbine equaled the power of water striking the turbine. The amount of water striking the turbine was calculated by subtracting the wastewater flow from the total water flow leaving the nozzles. The power absorbed due to friction was calculated using a motor draw test and was calculated under two conditions; 1) where the alternator was connected to the turbine, causing a high friction energy loss and 2) where the alternator was disconnected from the turbine, resulting in a low friction energy loss.

3.3.1 Determination of Wastewater Volume

Reddy (1966) calculated wastewater volume using graphical methods. His results were satisfactory for his work but the method is awkward and time consuming. An equation derived from basic principles is required to accurately determine wastewater volumes. The equation developed below was first derived by Dilip et al. (1972). In comparing his results with those of Reddy (1966) and Shirgur (1968), Dilip found that his equation was an accurate means of calculating wastewater volumes.

The logic used to derive his equation is based on the dimensions shown in Figure 3.2. Figure 3.2a represents the lower half of a Pelton turbine operating under the influence of one water jet. The procedure for multiple jets of uniform diameter is exactly the same, with the exception that the total wastewater volume is calculated by multiplying the wastewater volume from one jet by the number of water jets. If the water jets are of different diameter, then the calculation is repeated for each jet of differing diameter and the total wastewater volume is the sum of the wastewater generated by each jet.

The model assumes that the centerline of the water jet is tangent to the pitch diameter and lies in the plane of the turbine. The volume of the wastewater segment is determined by dividing the water jet from top to bottom into several horizontal slices and then summing the water volume calculated in each horizontal slice as shown in Figure 3.2b and 3.2c. The length and width of each slice depends on its perpendicular distance from the hub, the rotational speed of the buckets and the velocity of the water jet.

The volume of wastewater from a single jet depends upon the relative velocity velocity of the water jet relative to the bucket and the number of buckets on the pelton. As shown

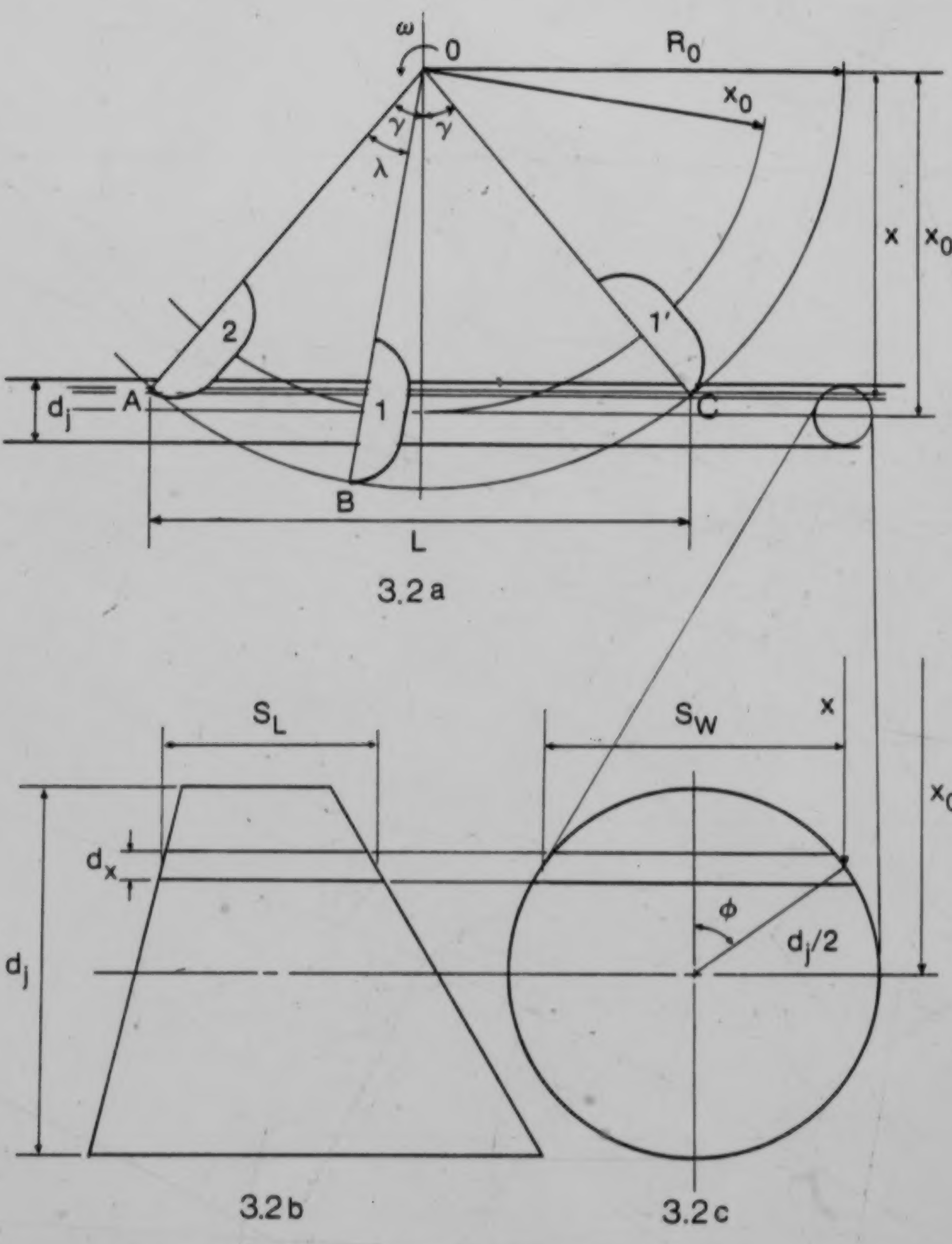
ω
0
R₀
x₀
γ
γ
λ
2
1
1′
A
B
C
dj
x
x₀
L
3.2 a
SL
SW
x
x₀
dx
dj
ϕ
dj/2
3.2 b
3.2 c

Figure 3.2 Waste water determination

in Figure 3.2a, the instant bucket number 2 moves past position A, some water to the left of bucket number 2 is prevented from striking bucket number 1. The drop of water immediately to the right of bucket number 2, at position A, must intercept bucket number 1 before bucket number 1 passes position C and moves out of the drop's path if that drop is to transfer its energy to the bucket. The time, t_w, required for the drop of water to travel from A to C is given by Equation 3.1. The time,

$$t_w = (2R_o \sin\gamma)/V_j \tag{3.1}$$

t_b, required for bucket 1 to move from position B to C is defined by Equation 3.2. When the turbine operates in

$$t_b = (2\gamma-\lambda)/\omega \tag{3.2}$$

overspeed conditions, t_w will be greater than t_b and a segment of water in the jet will pass through the turbine unable to act upon the turbine. The length of these segments will depend on the difference $t_w - t_b = t_l$ described by Equation 3.3. The length of the wastewater segment is given

$$t_l = ((2R_o \sin\gamma)/V_j)-((2\gamma-\lambda)/\omega) \tag{3.3}$$

by Equation 3.4 while the width of the segment, S_w, is

$$S_l = V_j t_l \tag{3.4}$$

defined by Equation 3.5. If the thickness of the segment is

$$S_w = d_j \sin\phi \tag{3.5}$$

defined as dx, then the volume of the wastewater in each slice is given by Equation 3.6. Equation 3.6 cannot be

$$dV = V_j((2R_o \sin\gamma)/V_j)-(2\gamma-\lambda/\omega))(d_j \sin\phi)dx \tag{3.6}$$

integrated to determine the total volume of the wastewater segment until the angles are replaced by an equivalent linear function. Referring to Figure 3.1 and basic geometry $\sin\phi$ can be defined by Equation 3.7. Equations 3.8 and 3.9

$$\sin\phi = ((d_j/2)^2-(x-x_o)^2)^{1/2}/(d_j/2). \tag{3.7}$$

$$\gamma = \arccos(x/R_o) \tag{3.8}$$

$$\sin\gamma = (R_o{}^2-x^2)^{1/2}/R_o. \tag{3.9}$$

are developed to solve for γ and $\sin\gamma$ respectively. Substituting Equations 3.7, 3.8 and 3.9 into Equation 3.6 and simplifying yields Equation (3.10). The total volume of

$$dV = 2((R_o{}^2-x^2)^{1/2}-((V_j/\omega)(\arccos(x/R_o)-\lambda))\,(d_j{}^2-4(x-x_o)^2)^{1/2}dx \tag{3.10}$$

wastewater found between any two buckets is determined by integrating Equation 3.10 over the Pelton wheel radius impacted by the water jet (Equation 3.11). Equation 3.12

$$V = \int_{(x_o - d_j/2)}^{(x_o + d_j/2)} 2((R_o{}^2-x^2)^{1/2}-((V_j/\omega)(\arccos(x/R_o)-\lambda))\,(d_j{}^2-4(x-x_o)^2)^{1/2}dx \tag{3.11}$$

serves to convert the volume of wastewater from each jet

$$Q_j = ZVN/60 \tag{3.12}$$

into a flow rate per second of wastewater, Q_j. The total flow of wastewater generated depends on the number of water jets focused on the turbine and the relative position of those jets to each other. Although the volume of wastewater at each jet is the same for the configurations shown in Figures 3.1b and 3.1c, a greater total wastewater volume is generated by configuration 3.1c due to interference between the two jets. As the wastewater segments for jet configurations shown in Figures 3.1c, 3.1d, and 3.1e pass through the turbine, they strike an adjacent jet. The momentum of the wastewater segment striking the adjacent water jet is assumed to be sufficient to divert an equivalent volume of water in this jet away from the turbine. The total amount of water missing the turbine (Q_v) can be calculated with Equation 3.13 where K equals the

$$Q_v = (K+L)V_j \tag{3.13}$$

number of jets and L equals the number of interference points per turbine. Subtracting the amount of water missing the turbine from the total water flow in the jets yields the volume of water actually striking the turbine, Q_t. The volume of water striking the turbine directly influences the amount of power generated.

3.3.2 Power Calculations

The first step for calculating power is to determine the force with which the water strikes the turbine buckets. The volume of water striking the turbine, determined in section 3.2, is converted to mass. For most conditions, it is convenient to use a mass density of water of 1000 kg/m^3 or 1 kg/ℓ. Thus, a flow rate of one liter per second is equal to a mass flow of one kilogram per second. Flow rate expressed in liters per second will serve to express mass in kilograms per second for the force equations.

The force produced by water striking the buckets is directly dependant upon the velocity with which water strikes the buckets. Since both the water and the buckets are moving, the relative velocity, V_r, of the water with respect to the buckets is used.

When the turbine is in equilibrium, at constant velocity, then the force (moment) applied by the bucket on the water must equal the force (moment) of water on the bucket. Where the force of the water is equal to the mass of the water striking the bucket multiplied by the velocity with which the water strikes the bucket. Figure 3.3 illustrates the action of water on a bucket. Only forces parallel to the waterjet contribute to turbine rotation. Using the convention illustrated in Figure 3.3 and summing all forces in the x direction, we find that:

$$F_s = Q_s(V_j-V_b)2(Q_s/2)(V_r\cos\psi). \qquad (3.14)$$

Simplifying, we get Equation 3.15 where the force, F_s, is

$$F_s = Q_s(V_r)(1-\cos\psi) \qquad (3.15)$$

measured in newtons.

The perpendicular distance from the center of the turbine to the center of the water jet is the moment arm X_o, over which the force of the jet acts. Force multiplied by the length of the moment arm yields torque expressed in joules. Power is then calculated by multiplying torque by angular velocity. Multiplying angular velocity, ω, by the moment arm, x_o, and by Equation 3.15 yields the power Equation 3.16, where power is calculated in terms of watts.

$$P = Q_sV_r(1-\cos\psi)x_o\omega \qquad (3.16)$$

At this stage, one should point out that although Equation

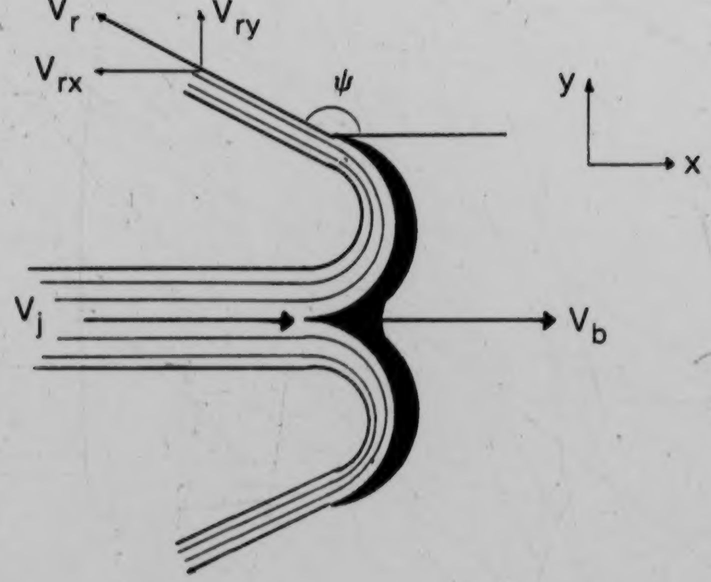

Figure 3.3 Velocities acting on a single Pelton turbine bucket (view is a cross sectional slice perpendicular to plane of Pelton turbine at a point where the water jet is perpendicular to the bucket)

3.16 neglects some losses, it is a good approximation of power. The power would decrease slightly if one were to account for power lost due to friction of the water passing over the buckets and if one were to consider the small portion of water just touching the bucket but not able to flow over the bucket before it swings out of position. However, Figure 3.4 shows that the tangental velocity of the buckets is not always parallel to the direction of water flow. The component of bucket velocity parallel to flow would be less by a factor of cos β. This would increase slightly the relative velocity, V_r, and cause power to increase. This increase in power will offset the initial decrease in power described earlier.

3.3.3 Runaway Speed Determination

Reddy (1966) and Shirgur (1968) predicted turbine runaway speed using a procedure based on a balance of moments. When the turbine is operating at a constant speed, moments are balanced. For Reddy (1966) and Shirgur (1968), runaway speed occured when the moment of the waterjet was equal and opposite to the combined moments of bearing and windage friction and the wastewater being returned onto the backside of the buckets.

As demonstrated in section 3.3.2, power is the product of the moment (or torque) and angular velocity of the turbine. As the governing system tested has no braking device, runaway speed occurs when the power of the water

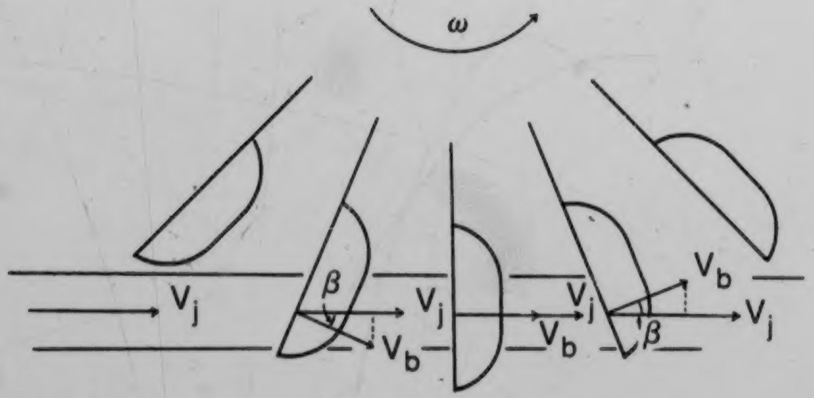
ω
V_j
β
V_j
V_b
V_j
V_b
V_b
β
V_j

Figure 3.4 Components of velocity at Pelton turbine bucket (cross sectional view in the plane of the Pelton turbine)

striking the turbine is equal to the power absorbed by bearing and windage friction.

The experimental apparatus had two configurations where power absorbed by bearing and windage could be tested. One configuration consisted of the turbine operating on a shaft without any load connected to the shaft. This configuration represents the minimum power required to spin the turbine on it's shaft. The other configuration consisted of the turbine operating on the shaft which was connected to an alternator through pulleys and a V-belt. The alternator was not connected to an electrical load. A motor power draw test was used to define the power absorbed by bearing and windage in both configurations.

The motor power draw test was used to determine the actual amount of power required to overcome bearing and windage friction at several speeds. An electric motor uses a fixed amount of power to operate a constant load at constant speed. Part of the load on the motor is caused by windage and bearing friction of the motor itself. Some power is also lost because of inefficiencies within the motor's windings, often referred to as flux losses. The power used by the motor is calculated by subtracting the power leaving the motor from the power available to the motor.

Motor power draw tests were performed for five turbine speeds in order to collect enough data points to establish a precise relationship between turbine speed and power absorbed by bearing and windage friction. Three conditions were tested at each of the selected speeds:

a. The motor disengaged from any load.

b. The motor directly coupled to the turbine shaft without any other load connected to the turbine shaft.

c. The motor directly coupled to the turbine shaft with a load connected to the turbine shaft in the form of an alternator driven from the turbine shaft through pulley's connected by a V-belt.

The first condition establishes losses due to bearing friction and electromagnetic flux within the motor itself. Subtracting this loss from each of the remaining two observations yields the actual amount of power required to overcome friction for each of those conditions. Table 3.4 summarizes the data collected for this test. These data were then plotted and a regression program used to derive Equations 3.17 and 3.18, where Equations 3.17 and 3.18

$$P_{HF} = 20.26027e^{0.00133(rpm)} \tag{3.17}$$

$$P_{LF} = -31.8605 + 0.06554(rpm) \tag{3.18}$$

represent the bearing and windage friction losses for the system both with the alternator connected (high friction system) and without the alternator connected (low friction system) to the turbine. Bearing and windage friction loss curves eventually increase exponentially, as shown in Equation 3.17. Equation 3.18, although linear, is valid within the region tested, but will take on exponential characteristics at higher turbine speeds. Figure 3.5 clearly

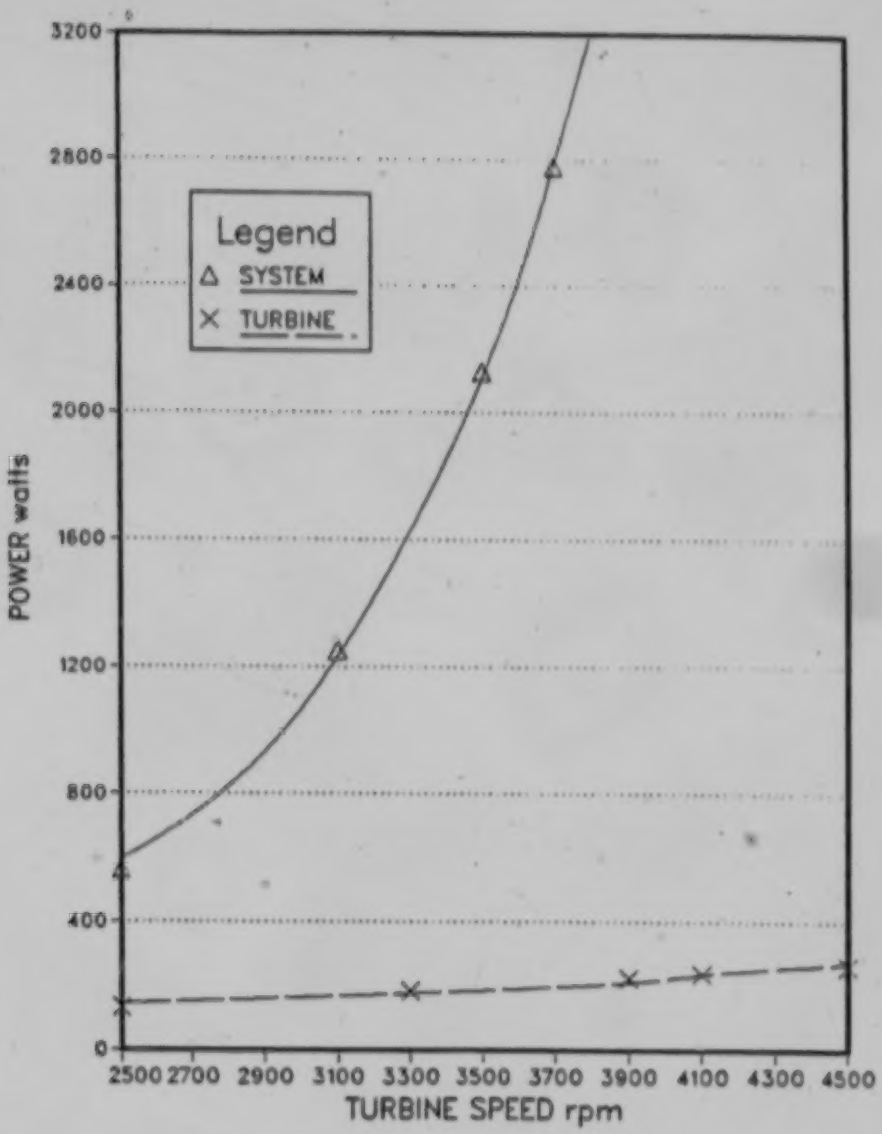

Where Equation 3.17 defines SYSTEM (high) friction and Equation 3.18 defines TURBINE (low) friction.

Figure 3.5 High friction and low friction curves

illustrates the differences between the two friction curves.

TABLE 3.4 MOTOR DRAW TEST RESULTS

	Total power draw (watt)			System power draw (watt)	
rpm	Motor	Motor Turbine	Motor Turbine Alternator	Low Friction Turbine	High Friction Turbine Alternator
1410	37	98	180	61	143
1640	50	120	225	70	175
1840	57	148	260	91	203
2040	70	175	405	105	335
3550	275	480	1560	205	1285

3.4 CSMP Model Description

The many equations needed to determine for power output of the system (section 3.3.2) were used in a computer based simulation model using the Continuous System Modeling Program (CSMP), a software package available on the University of Alberta's Amdahl computer. As CSMP (Speckhart and Green, 1976) is designed to simulate dynamic systems over time, it was well suited to model the interaction of a waterjet on a Pelton turbine. CSMP is a powerful program as demonstrated by the conciseness of the model (Appendix A.1). The three stage format of CSMP models shall be used to explain model setup.

The first section, refered to by CSMP as the INITIAL section, is used to specify the constants particular to the problem being solved. In this section, the turbine and the conditions under which it operates are defined. Computer time can be reduced if the calculations which are needed for the model and which only need be done once are placed in this section.

CSMP uses numerical integration procedure to solve differential equations. All simulation statements needed for the integration of Equation 3.11 are placed in the second (or DYNAMIC) section. The size of the integration step and the integration procedure to be used is outlined in the final (or TERMINAL) section. Choosing the numerical integration method and integration step size is important for the minimization of error and will be discussed in greater detail in section 3.8. Equations requiring results from the integration, such as Equation 3.16 which was used to calculate power, are also placed in the TERMINAL section.

3.5 CSMP Model Verification

The integration of Equation 3.16 is such an important part of the model that the ability of the model to accurately calculate the wastewater volume had to be established before the model could be used to predict runaway speeds. The CSMP model and hand calculations were compared by calculating the volume of a single wastewater segment generated using the theoretical conditions established for a 10mm diameter water jet from the three-jet configuration outlined in section 3.3 and a rotational speed of 420 radians per second.

To limit hand calculations to a reasonable number of iterations, the wastewater segment was sliced horizontally into ten 0.1 centimeter thick slices. Roundoff error was minimized by carrying all calculations to 8 significant digits and using centimeters for dimensions (the CSMP model used meters). For each slice, Equations 3.4 and 3.5 were used to determine the length and width, respectively. Equation 3.5 estimates width at the midpoint of each slice, as seen in Figure 3.6. An estimate of the volumetric error expected (due to the estimation of the volume of a cylindrical shape using rectangles) was established by comparing the actual cross sectional area of the wastewater segment, A_{act}, with the summation of the cross sectional areas of the ten slices, A_{est}. This comparison showed that A_{est} overestimated A_{act} by 0.967 percent.

To determine slice volume, the cross sectional area of each slice was multiplied by the calculated slice length (Table 3.5). The summation of these volumes can be used to estimate total wastewater segment volume which is of 0.859 cm^3 for the 10 mm jet system in question. This volume is 0.930 percent greater than the volume calculated by the CSMP model of 0.851 cm^3 for the same jet system.

The 0.930 percent difference in volume calculations is a direct result of the 0.967 percent difference in cross sectional area calculations. The irregular shape of the wastewater segment accounts for the slight differences between area and volume calculations. These results indicate

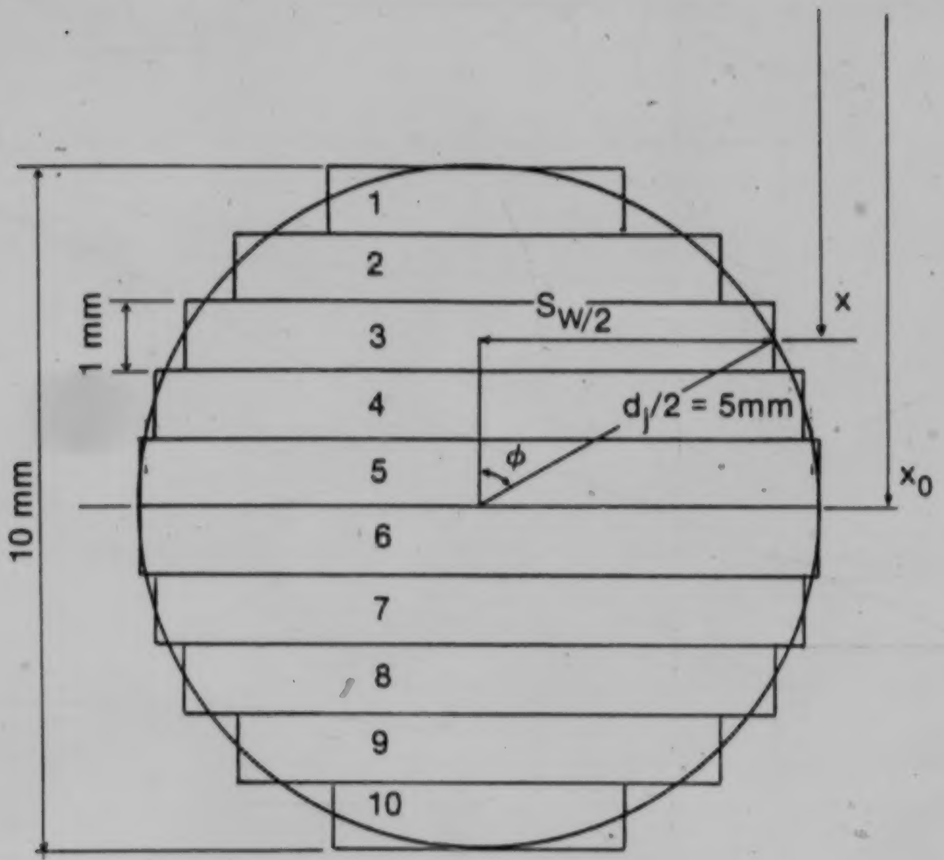
1
2
3
4
5
6
7
8
9
10
1 mm
10 mm
S$_{W/2}$
$d_j/2 = 5$mm
ϕ
x
x_0

Figure 3.6 End view of wastewater segment for verification of wastewater volume calculations

that the CSMP model accurately predicts wastewater volume according to Dilip's (1972) Equation 3.11.

TABLE 3.5 WASTEWATER SLUG VOLUME CALCULATION

Segment number	Segment depth (cm)	Width Sw (cm)	Area (cm^2)	Length SL (cm)	Volume (cm^3)
1	0.100	0.436	0.044	0.586	0.026
2	0.100	0.714	0.071	0.701	0.050
3	0.100	0.866	0.087	0.814	0.070
4	0.100	0.954	0.095	0.925	0.088
5	0.100	0.995	0.100	1.034	0.103
6	0.100	0.995	0.100	1.142	0.114
7	0.100	0.954	0.095	1.248	0.119
8	0.100	0.866	0.087	1.352	0.117
9	0.100	0.714	0.071	1.455	0.104
10	0.100	0.436	0.044	1.556	0.068
		TOTAL	0.794	TOTAL	0.859

3.6 CSMP Model Results

To evaluate the theoretical solution, the CSMP model was used to estimate power curves for the handcast Colombian and the manufactured English turbine when they were subjected to the same head and flow conditions. The diameter of the waterjets was adjusted so that the same total volume of water was aimed at the turbine regardless of whether there were 1, 2, 3 or 4 jets. The power produced by the turbine was calculated for speeds ranging from 2500 to 4000 revolutions per minute for each combination of waterjets and for each turbine. Table 3.6 summarizes the test parameters. Theoretical power curves for the manufactured and handcast turbines are plotted on Figures 3.7 and 3.8 respectively while the runaway speed reduction results are summarized in Table 3.7.

TABLE 3.6 PARAMETERS FOR THEORETICAL POWER CURVES

Number of jets	Jet diameter (mm)	Area per jet (mm^2)	Combined jet area(mm^2)
4	9.000	63.617	254.470
3	10.392	84.820	254.470
2	12.728	127.230	254.470
1	18.000	254.470	254.470

TABLE 3.7 THEORETICAL POWER CURVE SPEED REDUCTION SUMMARY

Run Identifier	Runaway speed w/ alt. rpm	Runaway speed w/o alt. rpm	Reduction of Speed w/ alt. %	Reduction of Speed w/o alt. %
T1J140	3164	3860	0.0	0.0
T1J40	3155	3852	0.3	0.2
T1J240	3121	3585	1.4	7.1
T1J340	3115	3525	1.6	8.7
T1J440	3090	3429	2.3	11.2
T2J140	3113	3731	0.0	0.0
T2J40	3099	3701	0.4	0.8
T2J240	3052	3439	2.0	7.8
T2J340	3038	3379	2.4	9.4
T2J440	3017	3283	3.1	12.0

Several similarities exist between Figures 3.7 and 3.8. As expected, there was little difference between the curves where no interference occured. The volume of water passing through one jet of 18 mm diameter and two jets of 12.73 mm diameters is exactly the same as the model assumes that

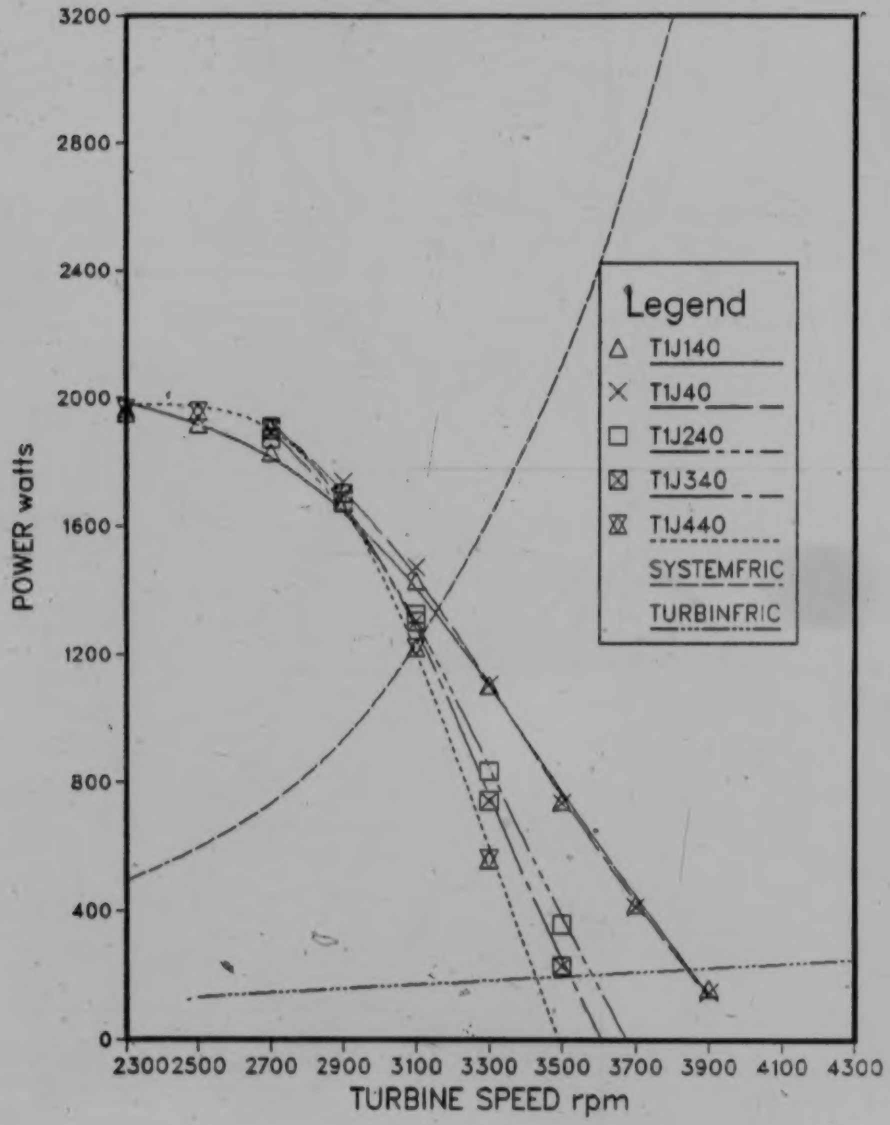

Figure 3.7 Theoretical power curves for handcast Colombian turbine

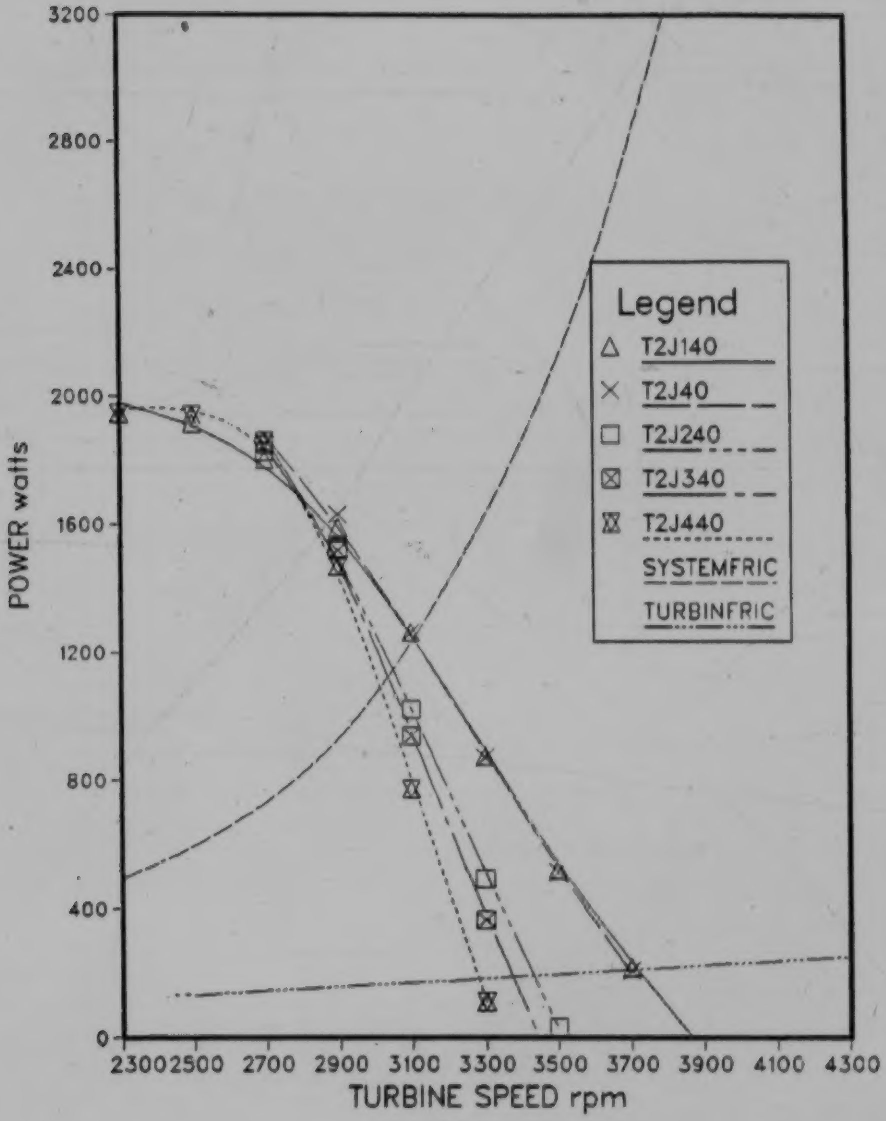

Figure 3.8 Theoretical power curves for manufactured English turbine

their velocities are the same. The model does not account for the possibility of flooding the turbine if jet diameter is too large because the only means to determine reliable values would involve extensive testing, which was beyond the scope of this research. Also, runaway speed decreases with the introduction of water jet interference. As the number of interference points increases, power decreases because less water strikes the turbine.

Figures 3.7 and 3.8 show that the influence of the windage and bearing friction is quite high when it comes to determining runaway speed. If the only objective is to decrease runaway speed, then it appears that increased friction is desirable as the runaway speeds with the high friction system are all lower compared to the low friction system. However, increasing friction decreases the amount of power available for practical use. It is most desirable to decrease the runaway speed rapidly without losing large amounts of power to friction.

Figure 3.9, formed by combining Figures 3.7 and 3.8 shows that the manufactured turbine decreased its runaway speed more quickly than the handcast turbine for the head and flow conditions used. The manufactured turbine differs from the handcast turbine in that it has an 8.3 percent larger diameter, 5 degrees less return angle, ψ, in the bucket and two fewer buckets. In theory, the number of buckets has the greatest effect on the amount of water missing the turbine and the amount of power produced. Runs

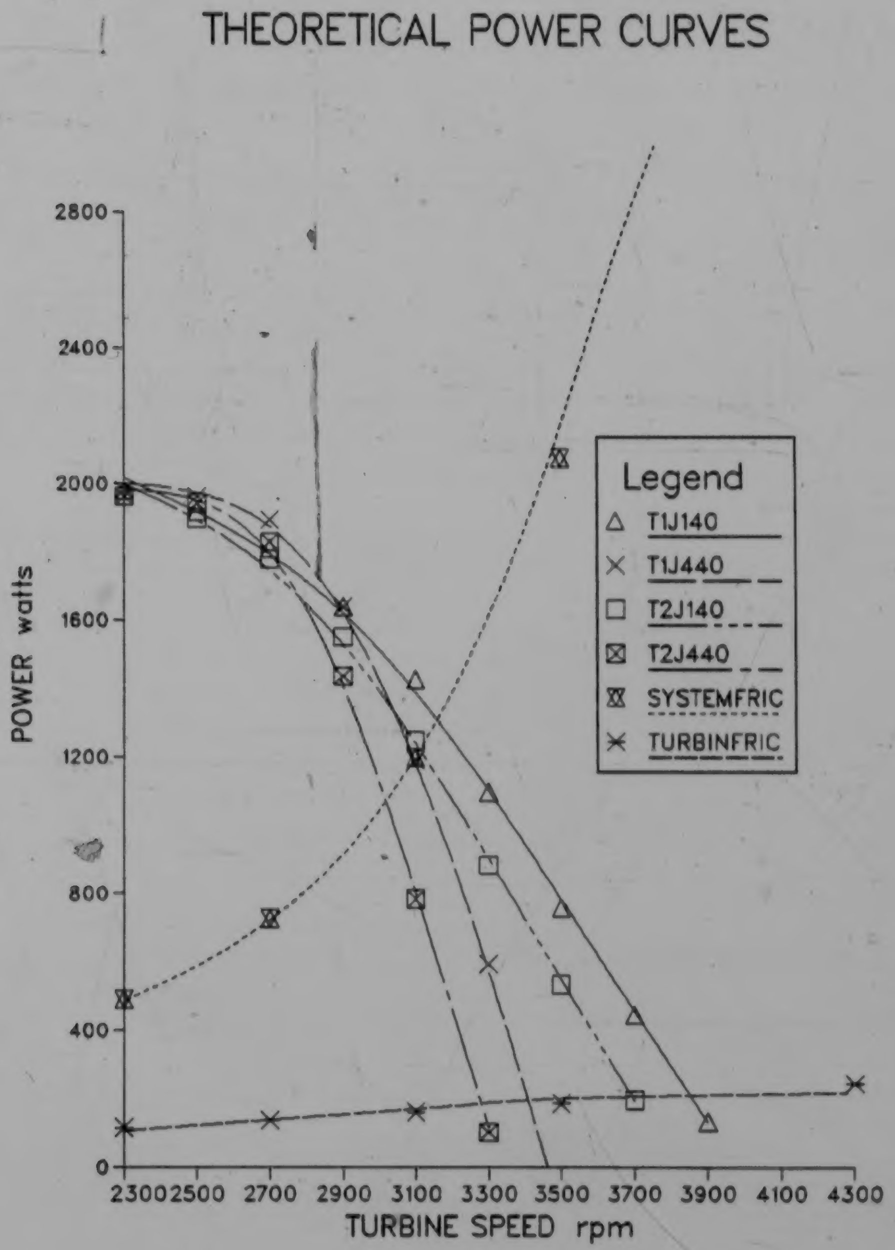

Figure 3.9 Comparison of handcast and manufactured Pelton turbine power curves for the single-jet and four-jet configurations

keeping all factors the same except the number of buckets gave almost identical results. As far as the model is concerned, increasing the turn angle in the bucket increases power. It is difficult to quantitatively account for the loss of power caused by exiting water striking the backside of the adjacent bucket as so much depends on the shape of the back of each bucket and the amount and velocity with which the exiting water strikes it.

The CSMP simulation package allows the user to choose amongst different integration methods. One chooses the integration method that uses the least amount of integration steps, and therefore computer time, to achieve an acceptable level of error. As mentioned earlier, the Runge-Kutta method allows the computer to choose integration step size. By specifying, for each integration step, the absolute value of the estimated integration error and the relative magnitude of the estimated error, the computer will choose the step size for each integration to keep error within the bounds specified (Speckhart and Green, 1976). A value of 5.0×10^{-11} was used for each parameter to insure an error of less than 0.1 percent between the calculated and actual solution.

4. EXPERIMENTAL PROGRAM

4.1 Introduction

Permanent facilities to test medium to high head Pelton turbines do not exist at the University of Alberta. The equipment assembled and used to evaluate the performance characteristics of two Pelton turbines under the influence of multiple jet systems and varying head and flow conditions are described in this chapter.

The apparatus was set up to determine turbine efficiency for each combination of head, flowrate and jet configuration where efficiency is defined as actual power out of the system over theoretical power into the system. Power out (P_{out}) was measured while theoretical power (P_{in}) was calculated using Equation 4.1 (adapted from Fritz, 1984). Reddy (1966) describes good speed control as being

$$P_{in} = \rho g Q_t H_t \qquad (4.1)$$

characterized by high efficiency at maximum power with rapidly decreasing efficiency in overspeed conditions (Figure 4.1).

4.2 Apparatus Utilized

4.2.1 Overview

To facilitate explanation, the equipment used for this experiment was classified into four categories: power input components, power output components, infrastructure and

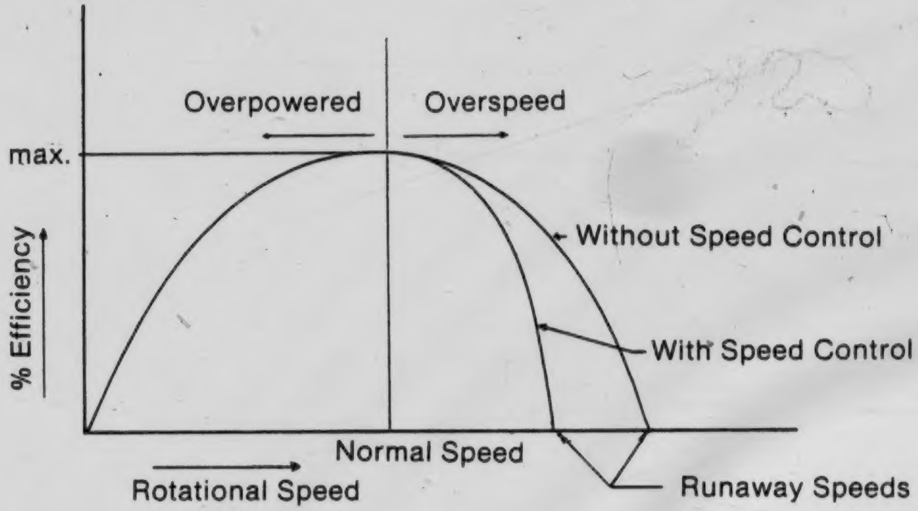
Overpowered
Overspeed
max.
% Efficiency
Without Speed Control
With Speed Control
Normal Speed
Rotational Speed
Runaway Speeds

Figure 4.1 Effect of efficiency on runaway speed reduction

data acquisition components. Power input components includes the equipment needed to determine the amount of theoretical power in the water being supplied to the Pelton. The equipment used to convert water power into hydroelectric power is discussed in the "power output components" section. Infrastructure refers to the support structure required to hold the experimental apparatus together. Equipment in this category will be discussed briefly for, although functionally important, equipment design is not critical to the experiment. A description of the computer and program used to collect data is contained in the data acquisition section. The location of most of the equipment outlined in the following sections may be seen in Figure 4.2.

4.2.2 Power Input Components

Head for the water jets was provided by a small irrigation pump, (Rain Master model SS-34-15 manufactured by Construction Machinery Company of Iowa) shown in Photograph 4.1. Adjusting the throttle of the electric start, 18.6 kW (25 horsepower), 4 cylinder gasoline motor varied the flowrate of the centrifugal pump.

Water entered the pump through a 7.62 cm (3 in) diameter suction hose and discharged into a 7.62 cm (3 in) diameter nipple, which reduced to a 5.08 cm (2 in) diameter pipe. Water for each of the four nozzles was split at the water divider (Photograph 4.2). Flow was controlled with the hand valves to ensure that H_t was the same at each of the

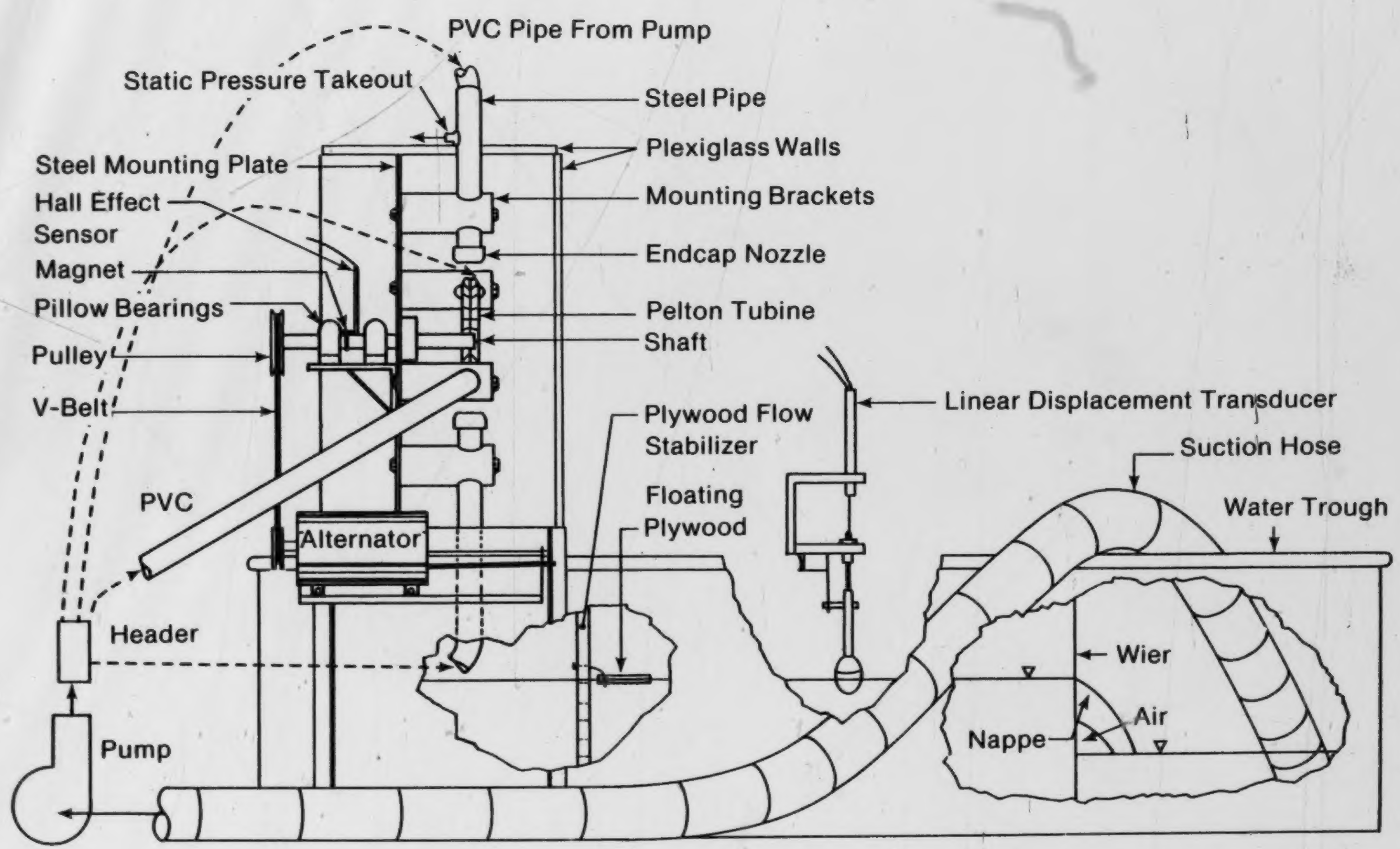
PVC Pipe From Pump
Static Pressure Takeout
Steel Pipe
Plexiglass Walls
Steel Mounting Plate
Mounting Brackets
Hall Effect Sensor
Endcap Nozzle
Magnet
Pillow Bearings
Pelton Tubine
Shaft
Pulley
V-Belt
Linear Displacement Transducer
Plywood Flow Stabilizer
Suction Hose
Floating Plywood
PVC
Water Trough
Alternator
Header
Wier
Air
Nappe
Pump

Figure 4.2 Major Components of Experimental Apparatus

Photograph 4.1 Gasoline powered irrigation pump used to simulate hydraulic head

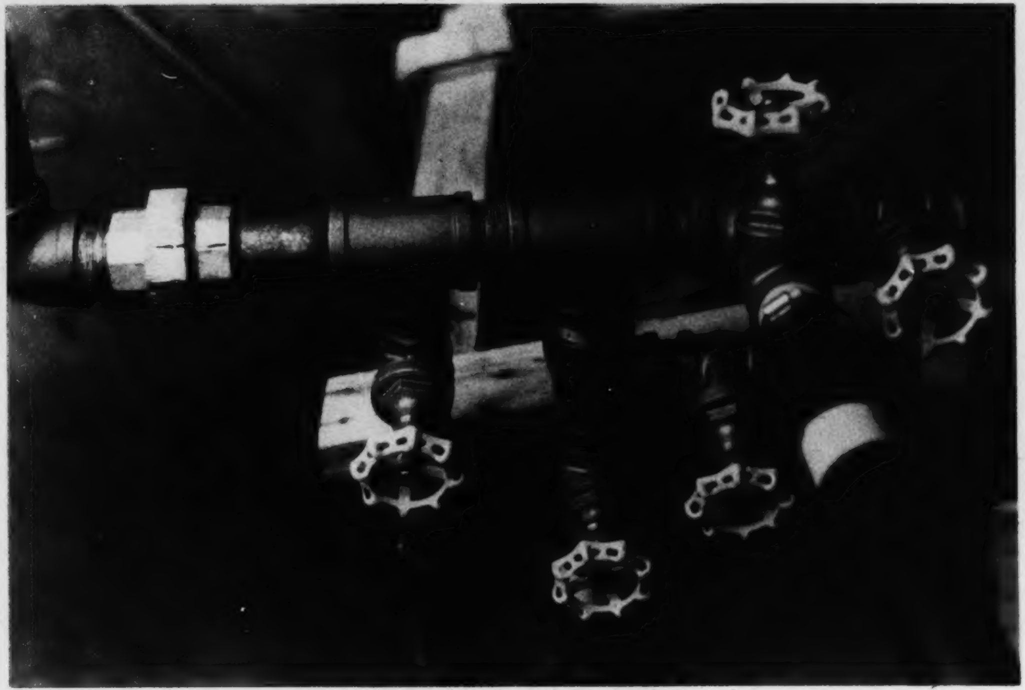

Photograph 4.2 Water divider to evenly distribute water to all four nozzles.

nozzles. The closest valve to the union joint was a bypass valve which accommodated minor pressure adjustments. Bypass water was carried behind the weir so that the flow of bypass water was not combined with the flow of water from the turbine that passed over the weir.

Turbine performance was tested with total hydraulic head (H_t) varying from 30 meters to 50 meters. Equation 4.2 describes Bernoulli's equation for calculating H_t.

$$H_t = H_e + H_v + H_p \tag{4.2}$$

Figure 4.3 describes the relationship between these components.

Water velocity in the pipe immediately before the nozzle was calculated by dividing the volume of water flowing through the nozzle by the cross-sectional area of the pipe. Velocity heads were seldom greater than 1 meter as flowrates per nozzle seldom exceeded 5 litres per second.

The pressure (or static) head was determined using a Multiple Range Pressure Transducer, (Model DP15TL manufactured by Validyne Engineering Corporation, California). The transducer was fitted with a diaphram rated to 550 KPa. Standard laboratory proceedures were used to tap each nozzle for a static pressure (Figure 4.4). The 3.18 mm (0.125 in.) diameter reinforced plastic hose transmitted the static pressure from each nozzle to a valve, as illustrated in Photograph 4.3. Each valve was attached to a header which allowed the pressure transducer to monitor static pressure from the four nozzles either individually or as a group.

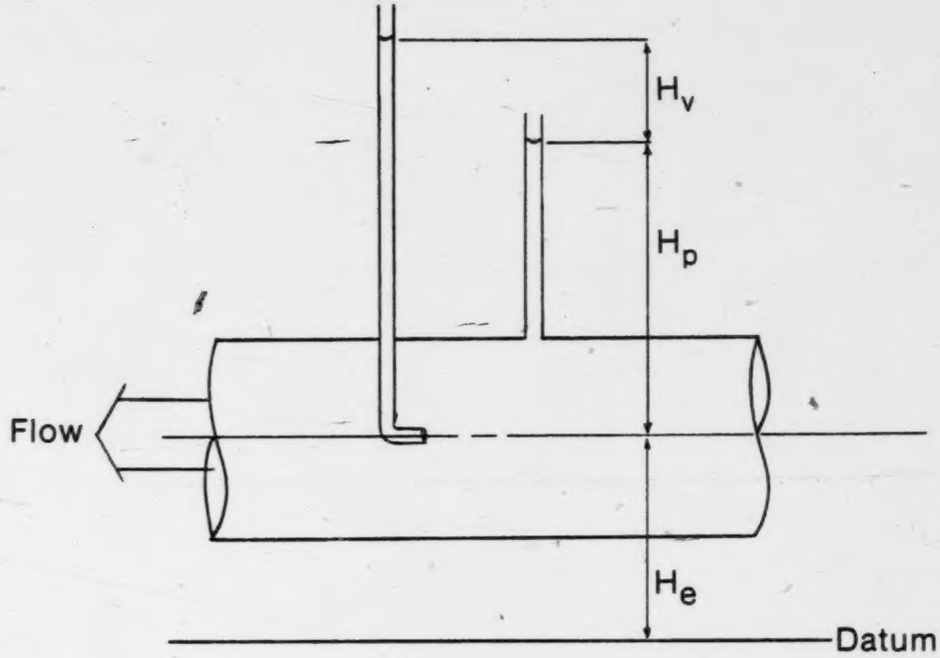
Hv
Hp
Flow
He
Datum

Figure 4.3 Components of total head

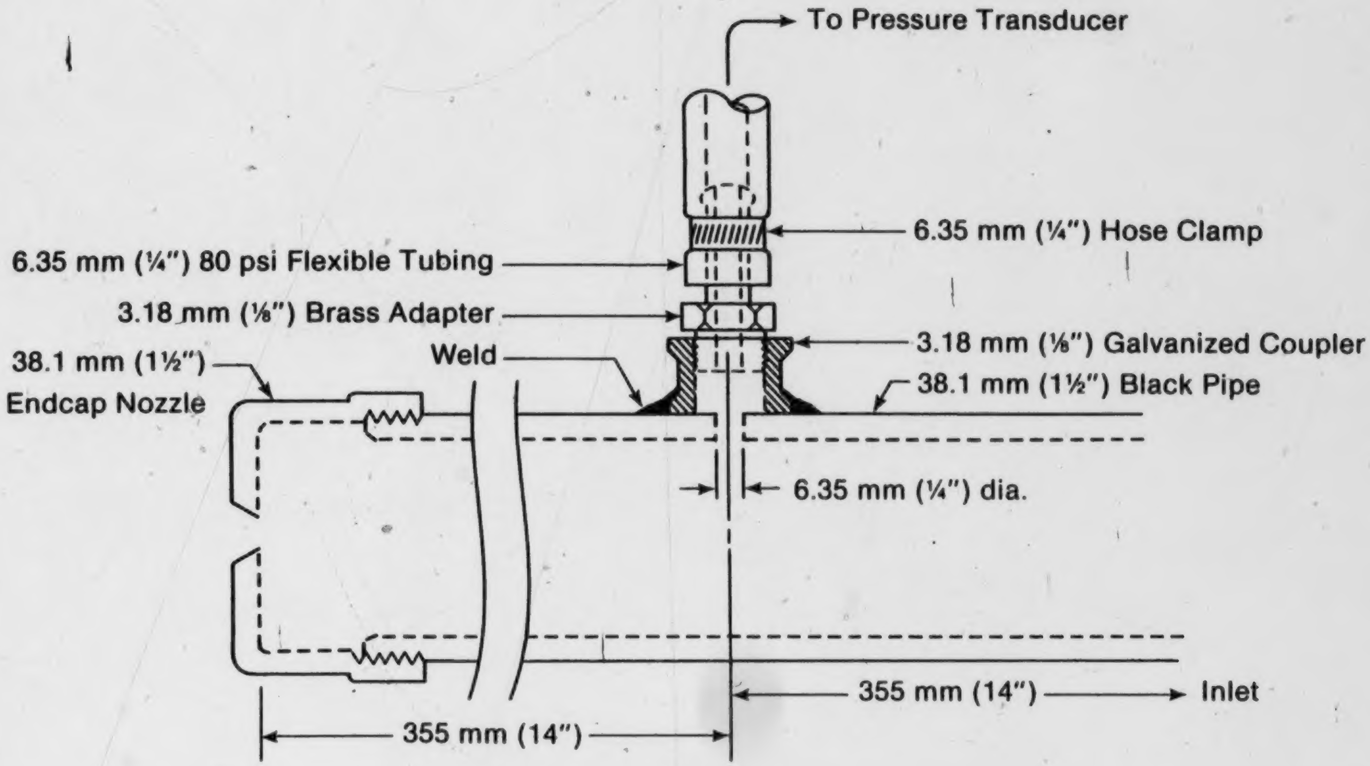
To Pressure Transducer
6.35 mm (¼") Hose Clamp
6.35 mm (¼") 80 psi Flexible Tubing
3.18 mm (⅛") Brass Adapter
3.18 mm (⅛") Galvanized Coupler
38.1 mm (1½") Endcap Nozzle
Weld
38.1 mm (1½") Black Pipe
6.35 mm (¼") dia.
355 mm (14")
Inlet
355 mm (14")

Figure 4.4 Static Pressure Assembly

Photograph 4.3 Pressure transducer mounted on header

By positioning the pressure transducer at the same elevation as the center of the upper horizontal nozzle, the elevation head became zero. Total head was calculated by adding pressure head to the calculated velocity head.

To avoid errors caused by fluctuations in atmospheric pressure, the pressure transducer was calibrated daily using a Standard Dead Weight Tester (Model #23-1 manufactured by Chandler Engineering Company, Oklahoma) (Photograph 4.4). A small program (Appendix A.2.1) was written to perform a linear regression on ten data points read by the data acquisition computer from the pressure transducer. The linear regression coefficient (r) had to be greater than 0.9995 before the calibration was accepted and the slope and y intercept values were used in the main data acquisition program (A.2.4).

The flow rate of water passing through the nozzles was perhaps the most important parameter to measure as flow rate is critical for the calculation of power. The standards defined in Brater (1959) use a triangular or V-notch sharp crested weir as an accurate way to measure fluid flow rates under 25 liters per second. The standards defined in Nelson (1976) stress the importance of meeting the following standard conditions for accurate flow measurement from a weir:

a. Smooth laminar flow conditions of water must exist prior to discharge over weir.

b. Waterflow over the weir or nappe must be completely

Photograph 4.4 Calibration of pressure transducer using hydrostatic apparatus

surrounded by air (Figure 4.2).

c. Measurement of water elevation (H_w) over the v-notch must occur at a distance no less than 2.5 H_w upstream from the weir.

d. Both the smooth flat surface and the sharp edge of the weir must face upstream.

The aforementioned conditions were met within the confines of a large animal watering trough 2.44 m long by 0.74 m wide and 0.60 m deep.

Smooth laminar flow was achieved by installing a plywood screen made with 40 mm diameter holes drilled on 80 mm centers, (Figure 4.5) beneath the front cover of the turbine cabinet confining turbulent flow behind the screen. Small waves were eliminated with a floating piece of plywood 16mm X 16cm X 60 cm attached immediately downstream from the screen.

The water behind the weir was maintained at a level low enough to allow the nappe to discharge into free air and yet high enough to prevent air from entering the pump's suction hose. Changing the flow rate between runs either by adjusting head and orifice series often meant that water was added or removed from the system to control the water level behind the weir. Water was added to the system with a garden hose while water removal was done by opening a small valve on the pump's discharge line.

Hansen, et. al. (1980) used Equation 4.3 to calculate

$$Q_t = 0.0138H_w^{2.5} \qquad (4.3)$$

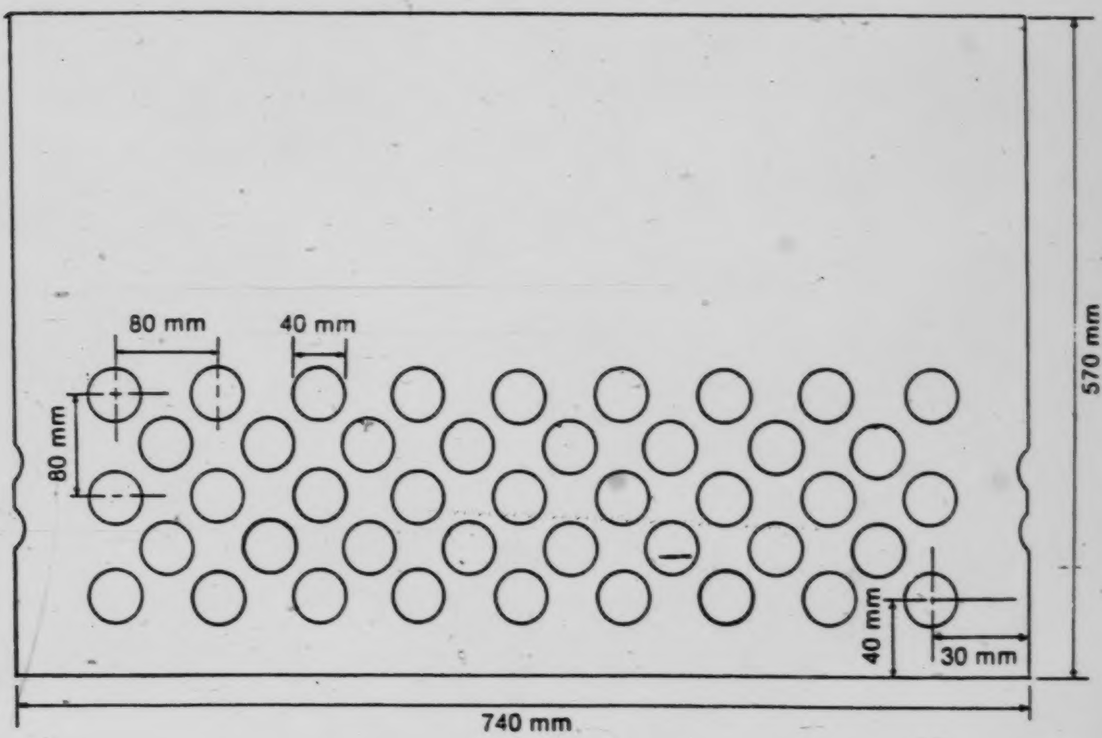
80 mm
40 mm
80 mm
570 mm
40 mm
30 mm
740 mm

Figure 4.5 Plywood screen used to create laminar flow

the flow of water over a sharp crested V notch weir. Since the maximum expected flow rate (10 liters per second) occurs when H_v equals 13.93 cm, the apparatus used to measure the surface elevation of the water was placed 50 cm upstream from the weir.

Photograph 4.5 illustrates the apparatus used to measure the water surface elevation. Any change in water surface elevation would be detected by the float. This change manifests itself at the bearing plate with vertical and slight horizontal movement. A well lubricated 9.53 mm (0.38 in) diameter, stainless steel rod riding on the bearing plate and passing through a 4 cm sleeve eliminated all horizontal movement. A linear variable displacement transducer (LVDT) converted the position of the rod into a dc voltage which provided an analog voltage imput to the data acquisition computer. The LVDT was calibrated once every 25 runs to ensure proper performance. A program was written (Appendix A.2.2), where the data acquisition computer read the LVDT voltages at 10 different water surface elevations before a linear regression was performed. When the regression coefficient value was greater than 0.9995, indicating a strong linear relationship, the slope and y-intercept would be used for the data acquisition runs.

The weir (Photograph 4.6) was installed perpendicular to both the walls and floor of the trough. Shaped from 16 gauge galvanized sheet metal and reinforced with a 25 mm x 25 mm x 3.2 mm (1 in x 1 in x 0.125 in) angle iron (Figure

Photograph 4.5 Water level measurement apparatus

Photograph 4.6 Water flow measurement system, from turbulent flow to suction hose

4.6), the upstream side of the weir remained smooth and flat ensuring proper flow over the weir (Brater,1959). The weir was secured in position and sealed with liberal amounts of silicone sealant. To insure that all water flowed through the V-notch of the weir the sides of the trough were supported by two 3 meter long, 38 mm x 89 mm wooden beams bolted together at each end to prevent the trough walls from flexing and breaking the seal around the weir.

The rotational speed of the turbine was determined using a magnetically-activated electronic switch which utilizes the Hall Effect for sensing a magnetic field. The Hall Effect sensor detects the magnetic field produced by a small magnet attached to the turbine shaft (Photograph 4.7). The Hall Effect sensor was held in place by a wooden bracket to within 1 millimeter of the magnet to ensure accurate readings at high rotational speeds. A frequency to voltage circuit (Appendix A.3) converted current pulses to a dc voltage capable of been read by the data acquisition computer.

The Hall Effect sensor was calibrated daily using a stroboscope. While connected to the data acquisition computer a calibration program (Appendix A.2.3) recorded voltages at ten distinct turbine speeds before performing a linear regression on the data. The y-intercept and slope were used in the data acquisition program when the regression coefficient was greater than 0.9995.

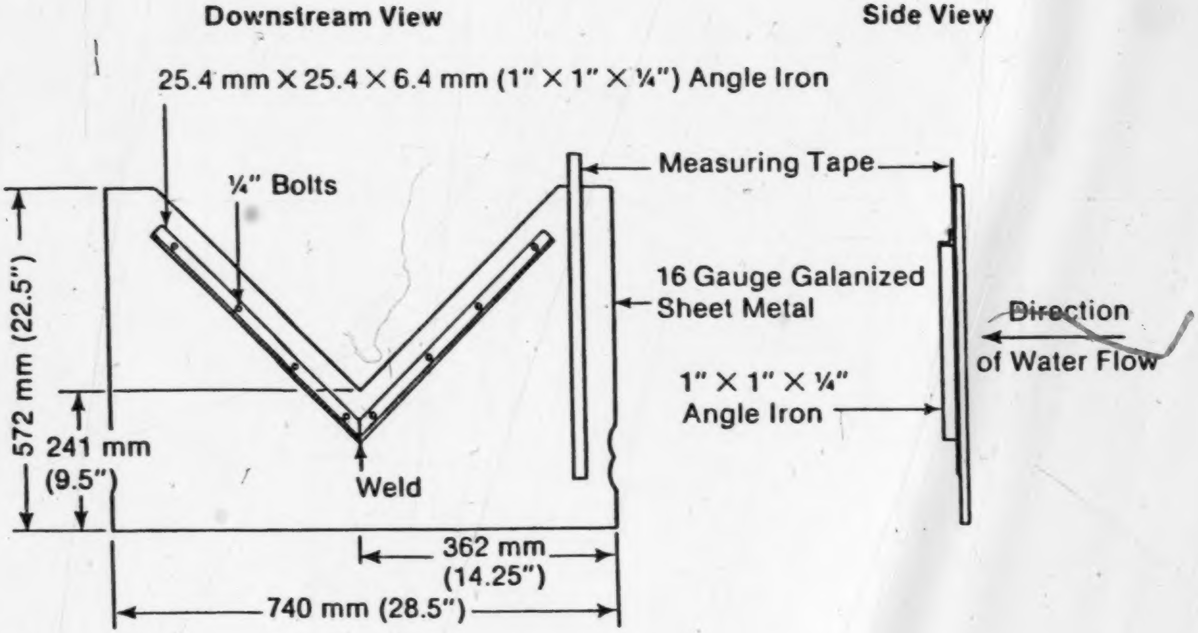
Downstream View
Side View
25.4 mm × 25.4 × 6.4 mm (1" × 1" × ¼") Angle Iron
¼" Bolts
Measuring Tape
16 Gauge Galanized
Sheet Metal
Direction
of Water Flow
1" × 1" × ¼"
Angle Iron
572 mm (22.5")
241 mm
(9.5")
Weld
362 mm
(14.25")
740 mm (28.5")

Figure 4.6 Weir

Photograph 4.7 Hall effect sensor in wooden support and magnet mounted to shaft

4.2.3 Power Output Components

Mechanical energy in the shaft of the turbine was transferred to a two pole, brushless alternator capable of producing 3.6 Kilowatts at 120 volts ac and 60 Hz. at a rotational speed of 3600 rpm using pulleys and a belt. This type of alternator is ideally suited for operation in developing countries as a brushless machine requires virtually no maintainance while the relatively light weight of 29.6 kilograms facilitates transportation to remote locations. The alternator produces single phase voltage which eliminates the need to balance loads and allows the alternator to operate at maximum efficiency.

Throughout the experiment, output power was measured in watts. Alternating current power generated by the alternator was measured with a portable standard wattmeter. The wattmeter (Photograph 4.8) was accurate to within 0.05 percent of full range value, or 1 watt over a range of 2 kilowatts.

Power can also be described as the product of voltage and amperage. A Beckman model HD 150 multimeter was used to measure alternator voltage (Photograph 4.8). Monitoring the voltage gave some indication as to how well the system was controlled. Since voltage is directly proportional to rotational speed, the higher the rotational speed of the alternator, the higher the voltage.

Equation 4.4 was used to determine amperage given power

$$I = P/E \qquad (4.4)$$

Photograph 4.8 Voltmeter (left) and wattmeter (right)

and voltage. This equation is valid as long as the power factor is zero. Having calculated amperage, Equation 4.5—

$$P_L = I^2R \tag{4.5}$$

was then used to calculate power losses within the alternator so as to determine alternator efficiency.

Electrical loads were placed on the alternator using a large set of resistors (Photograph 4.9). Nine knife switches connected all thirty six 12 ohm resistors. A wide range of electrical loads were possible with manipulation of the switches.

4.2.4 Infrastructure

The turbine cabinet was constructed primarily to provide a solid base for mounting the turbine and the nozzles. However, the cabinet also served to keep all the water within the system and permit the observation of turbine operation. The cabinet was supported on its own base over the water trough.

The back of the cabinet was constructed from a 6.35 mm (0.25 in) thick steel plate rigidly fixed in a vertical position. The mounting plate provided solid support for the nozzle mounts, bearing blocks and shaft. The two sides and top of the cabinet were made of 12.7 mm (0.5 in) thick plexiglass sheets. An effective watertight seal was created by bolting the plexiglass to the frame with a rubber seal. A vertical slot was cut in each sheet to allow movement of the pipe connected to the nozzles in the plane of the turbine.

Photograph 4.9 Resistor bank

The slot was sealed with a small plexiglass collar around the pipe and clamped to the side piece of plexiglass.

The front of the cabinet featured a 6.35 mm (0.25 in) thick plexiglass removable door. The door was held in place by eleven hand tightened "T" bolts which facilitated the changing of the nozzles.

Nozzle mounts were designed to rigidly support the four nozzles and permit adjustments in the plane of the turbine. Adjustments were necessary to change pitch diameters with a change of Pelton turbine. Four pieces of steel pipe 7.62 cm (3 in) in diameter and 25.4 cm (10 in) long were machined flat at one end. A 4.8 cm (1.9 in) diameter opening was machined 15.24 cm (6 in) from each of these ends (Figure 4.7).

Eight small steel plates 38.1 mm (1.5 in) X 73.7 mm (2.9 in) X 9.525 mm (0.375 in) thick were drilled and tapped for a 19.05 mm (0.75 in) diameter bolt. The plates were then welded into each end of the nozzle mount, one to secure the nozzle in place and the other to secure the mounting bracket to the mounting plate.

Waterjet velocities were calculated using Equation 4.6.

$$V_j = Q_N/A_j \qquad (4.6)$$

Figure 4.8 shows that the diameter of the water jet is less than the diameter of the orifice. The diameter of the water jet was determined using measurements taken by the apparatus shown in Figure 4.9. A detailed description of the procedure used to measure is described by Reddy (1966). When the two

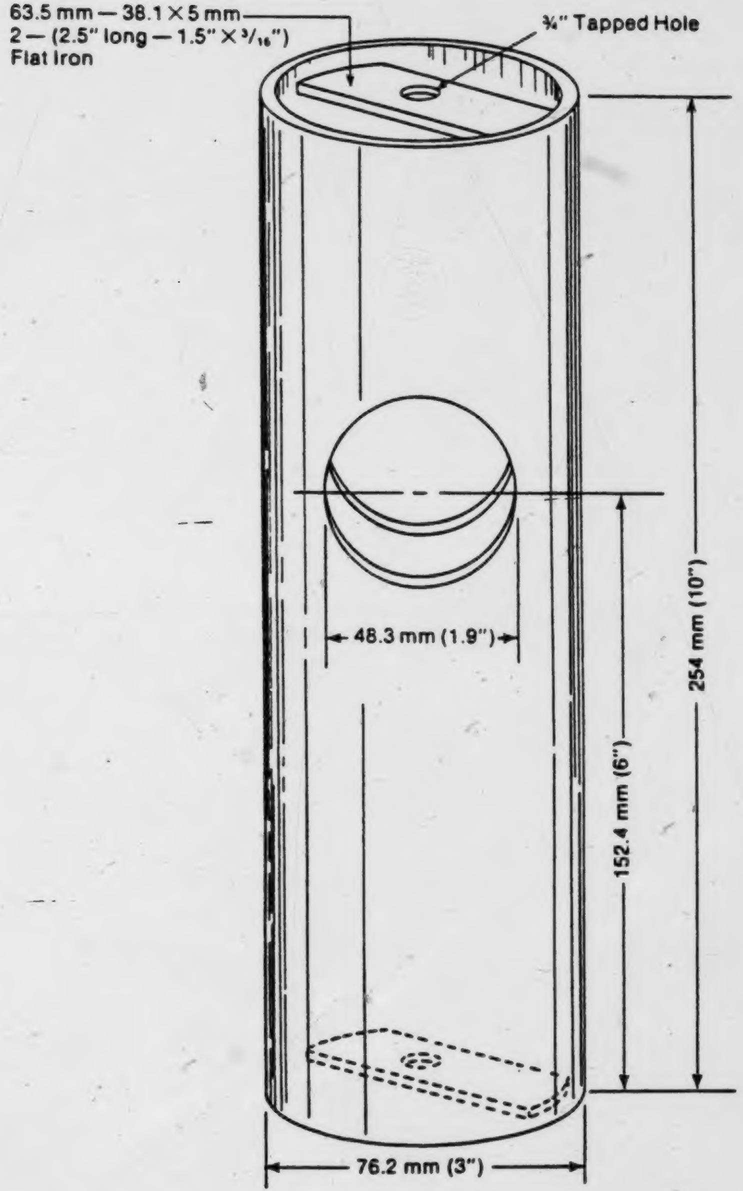
63.5 mm — 38.1 × 5 mm
2 — (2.5" long — 1.5" × 3/16")
Flat Iron
¾" Tapped Hole
48.3 mm (1.9")
254 mm (10")
152.4 mm (6")
76.2 mm (3")

Figure 4.7 Nozzle mount

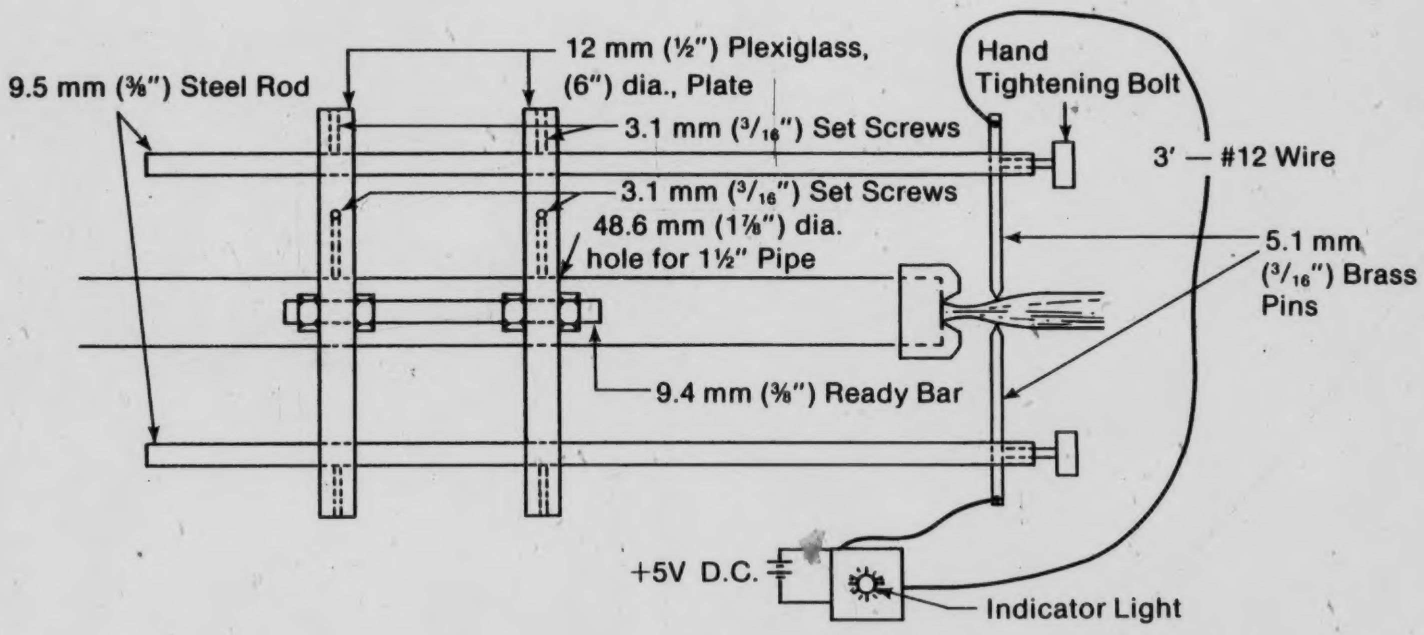
12 mm (½") Plexiglass,
(6") dia., Plate
9.5 mm (⅜") Steel Rod
3.1 mm (3/16") Set Screws
3.1 mm (3/16") Set Screws
48.6 mm (1⅞") dia.
hole for 1½" Pipe
9.4 mm (⅜") Ready Bar
Hand
Tightening Bolt
3' — #12 Wire
5.1 mm
(3/16") Brass
Pins
+5V D.C.
Indicator Light

Figure 4.9 Water jet diameter measurment apparatus

conducting points touched each side of the water jet, electrical current passed though the water jet as indicated by the light.

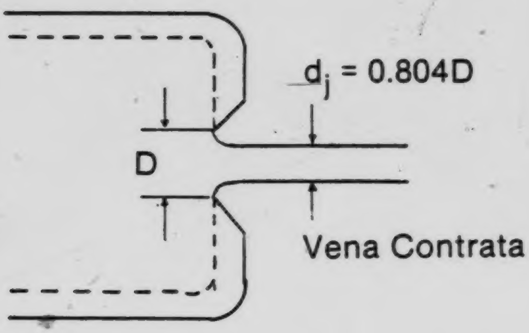

Figure 4.8 Orifice - water jet diameter relationship

The diameter of the water jet produced by each orifice was measured 6 mm from the orifice opening while the system was operated at a head of 40 meters. The results are summarized in Table 4.1. The mean water jet diameter was 19.80 percent less than the orifice diameter. Thus, the cross sectional area of the water jet was calculated from the water jet diameter which was calculated by multiplying the orifice diameter by 0.802. water jet velocity was then calculated by dividing the flow rate of the water jet by the cross-sectional area of the water jet.

Nozzles are rated according to their discharge coefficient, (C_d). The discharge coefficient is defined as

TABLE 4.1 JET DIAMETER REDUCTION MEASUREMENT SUMMARY

Series number	Number of jets	Orifice (mm)	Waterjet dia (mm)	Change in dia %
1	4	7.90	6.48	18.00
1	3	9.07	7.11	21.50
1	2	11.00	8.56	22.20
1	1	16.00	13.00	18.70
2	4	8.90	7.49	15.70
2	3	10.29	7.87	23.50
2	1	17.86	14.35	19.60
3	4	9.86	7.92	19.60
3	2	13.72	11.00	19.80
3	1	19.89	16.51	17.00
4	4	10.92	8.43	22.70
4	3	12.50	9.78	21.80
4	2	15.44	12.57	18.60
4	1	22.12	18.92	14.40
5	4	11.89	9.48	20.30
5	3	13.77	11.10	19.30
5	2	16.94	13.46	20.50
			MEAN	19.60 *

* The percent mean of diameter change had to be determined experimentally prior to collecting runaway speed field data and prior to performing subsequent CSMP simulations. The mean diameter change was used to calculate water jet velocities in both the CSMP (A.1) and data acquisition program (A.2.4) programs. However, the reduction factor used in these programs was the result of a miscalculation where 18.60 was used instead of 19.60. The 1.24 percent error decrease in the reduction factor results in a 0.83 percent increase in water jet velocity and ultimately a 0.39 percent increase in power. Test 3 in Table 5.1 indicates that a slight increase in power enhances the ability of the CSMP model to predict runaway speed. However, the original data was used in the analysis because the error was not sufficient to justify repeating the analysis.

the ratio of the actual flow rate over the ideal flow rate (Baumister & Marks, 1967). The ideal flow rate was calculated using Equation 4.7 whereas the actual flow rate

$$Q_N = A_o(2gH_t)^{0.5} \qquad (4.7)$$

was determined experimentally. A high quality nozzle can have a discharge coefficient as high as 0.98 whereas a sharp edged orifice type nozzle typically has a discharge coefficient of 0.61 (Hansen et.al., 1980).

Two factors cause the actual flow rate to be less than the ideal flow rate. The first is the reduction of the cross sectional area of the water jet caused by the momentum of the water flowing out of the orifice (i.e. the vena contracta effect) as seen in Figure 4.8. Hydraulic inefficiency due to turbulent flow at the orifice is the second factor reducing the ideal flow rate. Hydraulic inefficiency reduces the effective head which in turn reduces jet velocity.

The experimental procedure used permitted the estimation of the discharge coefficient. The mean discharge coefficient calculated from 250 experimental runs was 0.625. Of the 0.375 reduction in ideal discharge coefficient, 0.357 is the result of the vena contracta effect leaving the 0.018 difference due to head loss. Equation 4.6 was adjusted to reflect the difference due to head loss resulting in Equation 4.8 which was used to calculate jet velocity.

$$Q_N/A_j = V_j = 0.982(2gH_t) \qquad (4.8)$$

In this experiment, reduction of the diameter the water jet was acccommodated for by making the endcap orifice diameter 19.8 percent larger than the desired water jet diameter. As water jet reduction can be adjusted for, it need not be considered when discussing nozzle efficiency. However, the inefficiency caused by head loss across the nozzle can only be accomodated by increasing the static head of the system by 3.6 percent. Since static head cannot always be increased the efficiency of the endcap nozzle is 98.2 percent (100.0-(3.6/2)).

Galvanized endcaps 3.81 cm (1.5 in) in diameter were used as nozzles to form the water jet. Endcaps with standard pipe thread are common and inexpensive in most developing countries but the resulting nozzles are less efficient in terms of hydraulic flows.

The objective of using five orifice series was to vary flow rate so that each turbine could be tested over a wide range of flows. To determine the effect of jet configuration on speed control, the flow rate and total head must remain constant for each jet configuration within a series. The orifice Equation 4.9, shows that the flow rate is directly

$$Q_N/A_o = V_j = C_d(2gH_t)^{0.5} \tag{4.9}$$

proportional to the cross sectional area of the orifice. To insure that the same volume of water passes through each of the five jet configurations, the total cross sectional area of the orifice nozzles for each jet configuration must be equal. For example, the cross sectional area of a single-jet must be the same as the sum of the cross sectional areas of the nozzles for the four-jet configuration within the same series. The orifice sizes within a series were determined by calculating the total orifice area of the four-jet system which was then divided by the number of jets, leaving the desired area of the orifice. Equation 4.10 was used to determine the diameter of the orifice. Orifice holes

$$d = (4A_o/\pi)^{0.5} \qquad (4.10)$$

were drilled into the center of the endcap. The front of the hole was then countersunk creating a sharp edged orifice as seen in Photograph 4.10. Actual orifice diameters are discussed in section 5.2.1.

The handcast turbine was bought as a rough casting. Several casting flaws had to be repaired with an argon welder before a hub could be machined, as shown in Photograph 4.11. Where possible flashings were removed with a file from the buckets to insure that the inside surface of the buckets were as smooth as possible. The small size and proximity of the buckets to each other made the removal of flashings from the inside surface of each bucket difficult. The manufactured turbine was already prepared for mounting as shown in Photograph 4.12.

The handcast turbine was not dynamically balanced prior to use. Serious vibrations occured when it was operated at rotational speeds over 3500 rpm resulting in the eventual destruction of six hall effect sensors. Unless properly balanced, a turbine mounted directly on the shaft of the alternator will shorten the life of the alternator.

Each turbine was mounted on a shaft. The shafts were identical except for the mounting configuration. To ensure that the shafts were balanced, 47.6 mm (1.875 in) diameter

Photograph 4.10 Measuring the diameter of the orifice of an endcap nozzle

Photograph 4.11 Preparation of handcast Pelton turbine

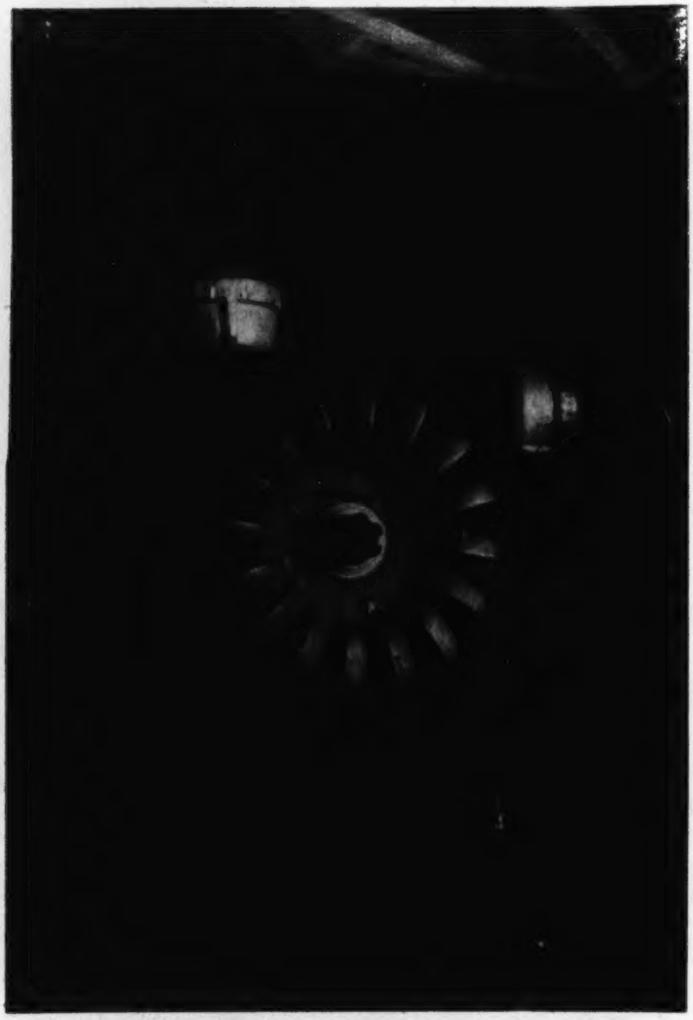

Photograph 4.12 Manufactured turbine mounted on shaft positioned with a two-jet configuration

round steel bar was machined down to 3.81 cm (1.5 in). One end was machined to accomodate the turbines while the other end was machined down to 22.2 mm (0.875 in) to accomodate the power transfer sheave.

The shafts were held in place by two sets of bearings 3.81 cm (1.5 in) in diameter. Single track ball bearings mounted in pillow blocks were used because they are low friction bearings. The dust covers and the original grease were removed from the bearing before it was mounted on the shaft to further reduce friction. A small amount of lightweight oil in the bottom of the pillow block kept the bearings lubricated.

A water seal (Figure 4.10) was designed to prevent water from entering the bearings without increasing the rotational friction of the system. The water seal prevented water from passing through the shaft opening in to ways. 1) The water seal cover slipped over the shaft and was securely bolted to the mounting plate. This arrangement prevented water from splashing directly through the shaft opening. 2) A wedge shaped ring was positioned on the shaft, next to the mounting plate, on the turbine side. Water creeping along the shaft was thrown off at the wedge due to higher centrifugal forces at the thin outer edge of the wedge. The aluminum cover would collect and then drain off this water. This method was successful at stopping water from entering the bearings without any friction contact points.

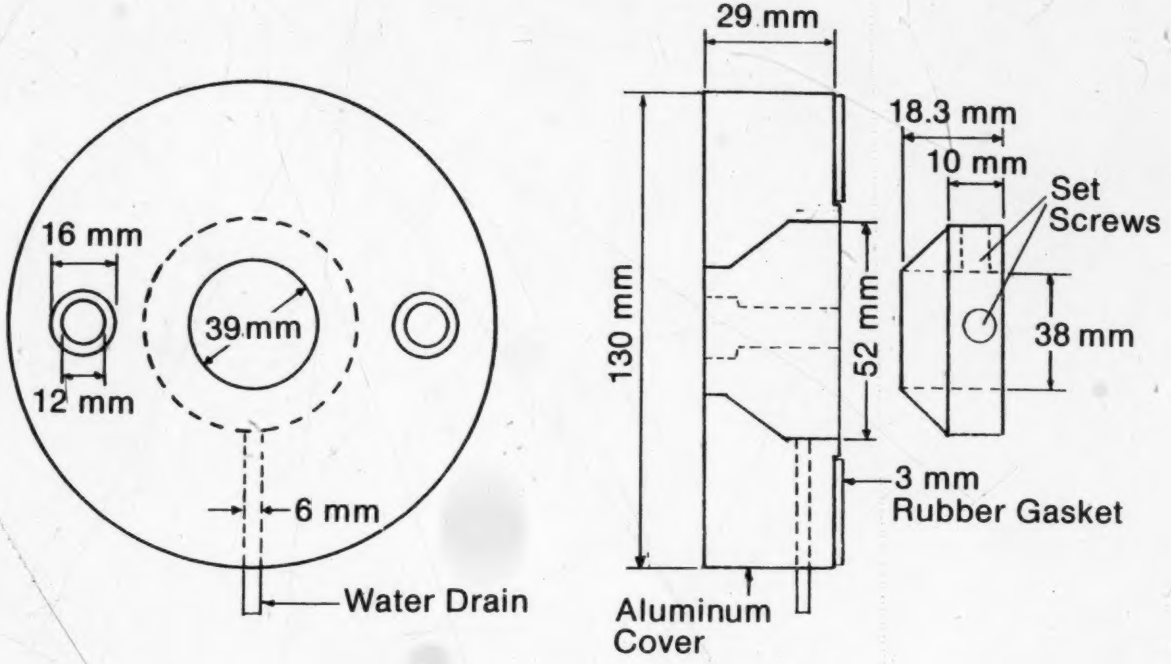
16 mm
12 mm
39 mm
6 mm
Water Drain
29 mm
130 mm
52 mm
Aluminum Cover
3 mm Rubber Gasket
18.3 mm
10 mm
Set Screws
38 mm

Figure 4.10 Water seal

Power from the turbine was transmitted to the alternator using a B section V-belt and two sheaves; a 15.24 cm dia. (6 in) sheave on the turbine shaft and a 10.16 cm (4 in) sheave on the alternator (Photograph 4.13). With an A-section belt, these pulleys have effective diameters of 13.21 cm (5.2 in) and 8.12 cm (3.2 in) respectively (Wood's, 1981), thus increasing the speed of the alternator to 1.62 times that of the turbine. The alternator operated at approximately 3600 rpm, when the turbine operated at normal speed, where normal speed is defined by Reddy (1966) as the rotational speed at maximum power.

To eliminate belt slippage, a 22.64 kg weight was suspended from the alternator base which itself weighed 29.66 kg. The combined mass of the alternator and weight transmitted a force of 425 N through the belt to the shaft and bearings. This load on the bearings generated a large amount of friction, which could have been eliminated with the alternator directly coupled to the turbine shaft.

4.2.5 Data Acquisition

The modular instrument computer, (MINC), manufactured by Digital Equipment Corporation, was used for data acquisition, performing computations and producing graphic displays for the experimental component of this research project.

Computer programs were written using an interactive programming language called MINC Basic. Programs and data

Photograph 4.13 Alternator connection to shaft with v-belt and pulleys

were stored on 8.5 inch floppy diskettes. The program (Appendix A.2.4) is divided into 4 main sections. Section one initializes the values of constants. Instrument voltages are converted to head, rpm and flow rate values in section two. Total head is calculated and displayed to insure that the system is operating at the desired head. Adjustments could then be made to the pump and/or the water divider when required and section two rerun to recalculate head.

The data collection sequence contained in the third section began when head was at desired level. Eleven data points were taken for each run. The run began by overloading the alternator with the resistor bank and forcing the turbine to operate with both speed and efficiency below optimal conditions. To minimize the effect of slight variations in the analogue signal voltage, each instrument voltage was read one hundred times (once every 1/50th of a second for two seconds.) The arithmetic mean of each instrument's voltage was used for subsequent calculations. The computer then waited for manual data input of the power (in watts) and the voltage values to be entered from the keyboard. On completion of these entries, the electrical load on the alternator was reduced. This resulted in increased rotational speed at the turbine as the amount of power produced matched the load. Ten separate data points were observed as load was reduced ten times for each run in relatively even increments. The last data point was taken when load was zero making the final speed of the turbine equal to runaway speed.

The final section of the program contained the logic to calculate the results obtained from the run and to display a graph of the power curve. A smooth power curve as seen in Photograph 4.14 meant a good run and the data was saved for additional analysis. An irregular spiked curve indicated that the data was incorrect and the run was redone. Irregularity could be caused by either misread instrument voltages or more commonly by incorrect keyboard entries of power values. On average one run in ten had to be redone.

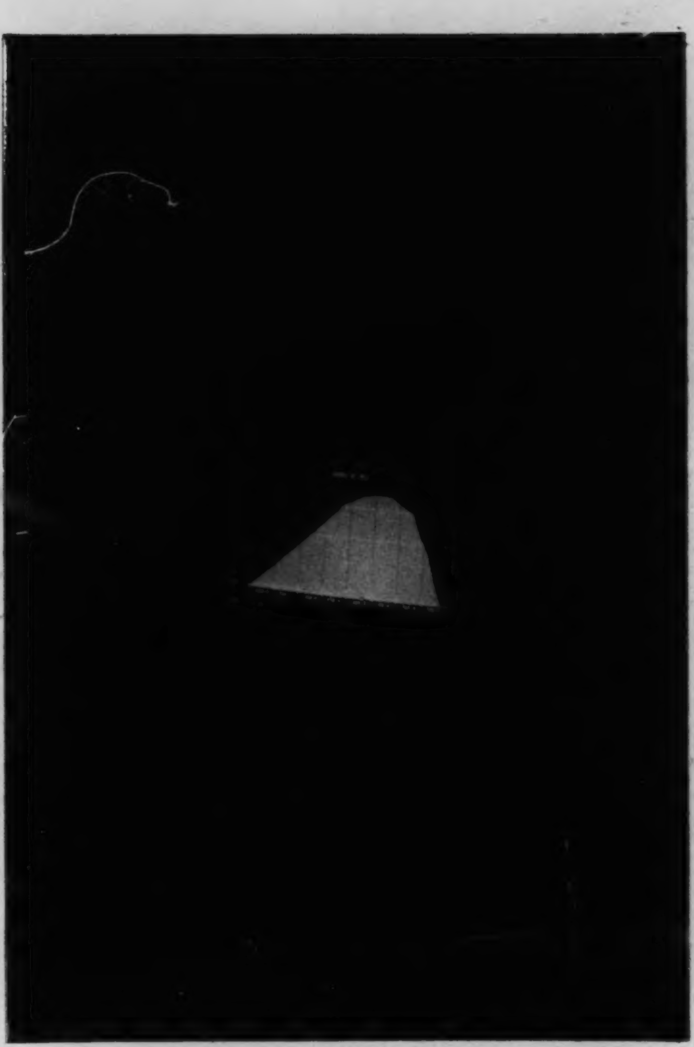

Photograph 4.14 MINC terminal demonstrating power curve

5. RESULTS AND DISCUSSION

The effect of jet configuration on Pelton turbine performance was evaluated in three stages. The first stage compared the CSMP model predictions of runaway speed with experimental data. The objective was to identify which performance characteristics and assumptions were valid. Stage two used common statistical methods to compare the means of different combinations of experimental data. This method identified Pelton turbine design parameters critical for runaway speed reduction. The third stage explored the relationship between jet configuration and the hydraulic efficiency of the micro hydroelectric system tested.

5.1 CSMP Model Prediction and Evaluation

The CSMP model was tested by setting the values of the appropriate constants in the program equal to the observed flow rates and observed head with the turbine and the jet configurations used in each of the experimental runs. The model calculated the values for power output at a given turbine speed which were then plotted along with power loss curves for the high friction and low friction micro hydroelectric systems. Runaway speeds were predicted by calculating the rotational speed corresponding to each of the intersection points between the calculated power curves and the power loss curves, as illustrated in Figures 5.1 and 5.2. These runaway speeds are recorded in Tables A.4.1

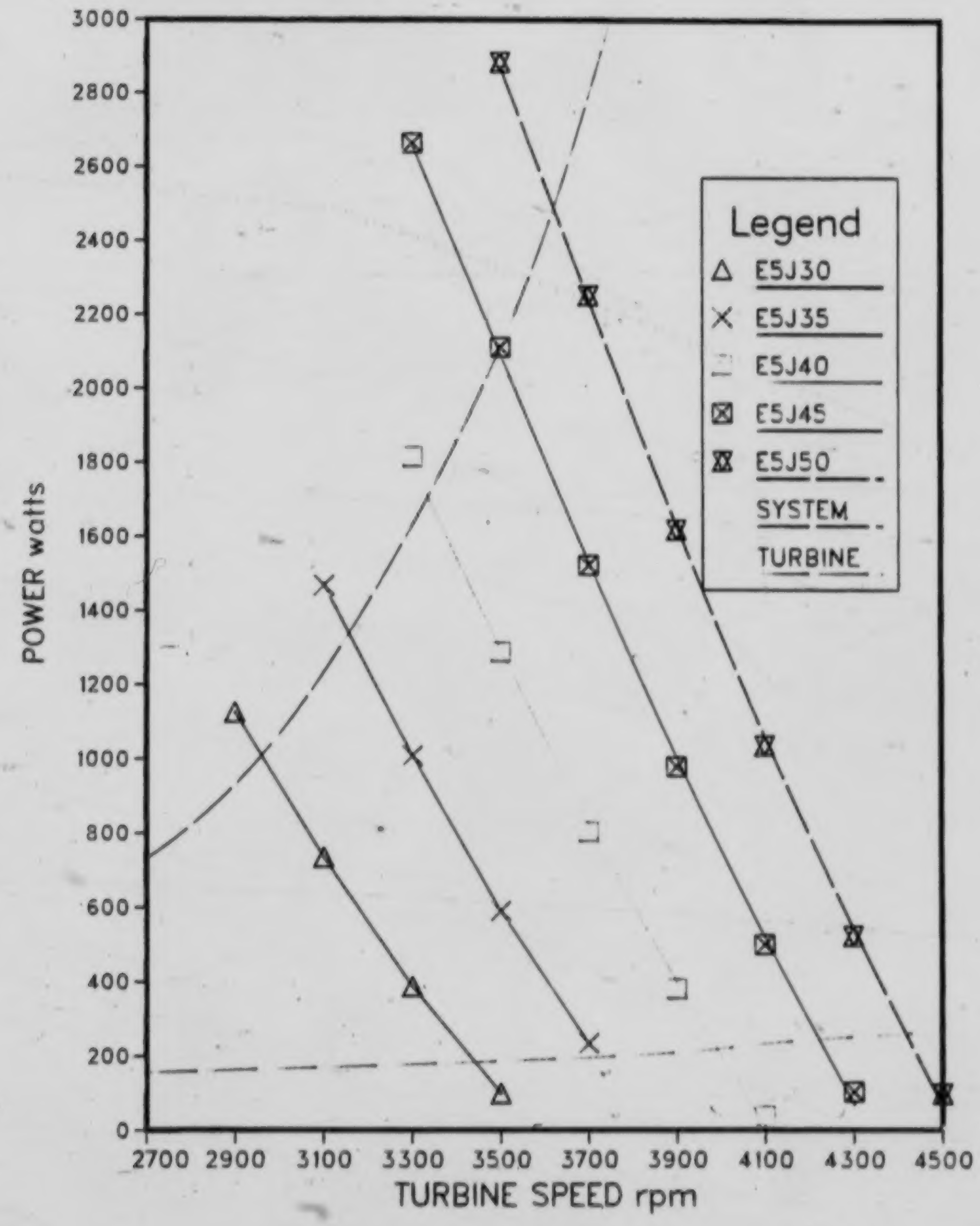

Figure 5.1 Theoretical power curves for a two-jet-no-interference configuration

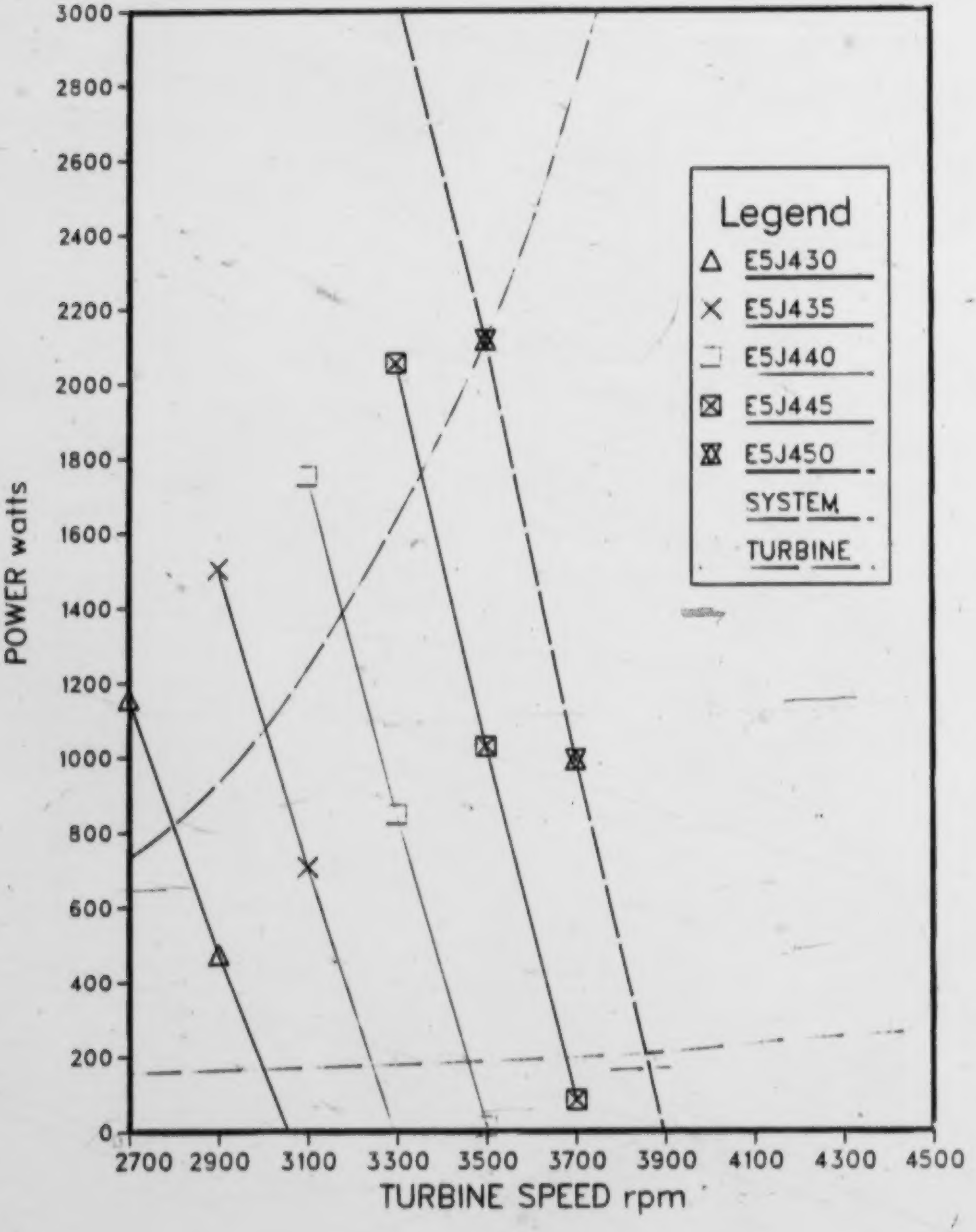

Figure 5.2 Theoretical power curves four-jet configuration

to A.4.10 (Appendix A.4); where the runaway speeds for the high friction, with generator system and the runaway speeds for the low friction, no generator system are recorded in columns 7 and 8 respectively. The experimentally measured runaway speeds were recorded in column 9 for the high friction system and column 10 for the low friction system.

The observed data were not consistent because of small differences in flow rates and head between tests. Thus, statistical comparisons were made between the predicted values and the actual values to see how well the CSMP model predicted runaway speed. Since there was no way of knowing what the runaway speeds should be, comparisons were made between the experimental observations and calculated data from the CSMP model. The Student's t-test permits the comparison of means from two sample populations (Steel & Torrie, 1980). The null hypothesis for all comparisons made was, $H_0:\mu_1=\mu_2$, where the mean of group 1 belongs to the same set of data as the mean of group 2. Equation 5.1 is used to calculate a t value for the comparison of the sample means.

$$t_s = (\mu_1-\mu_2)/(2s^2/n)^{0.5} \qquad (5.1)$$

Sokal and Rohlf (1969) refer to the calculated t value as t_s to avoid confusion with the t value found in the Student's t-table, with which t_s is compared. Once t_s has been calculated, one determines t from Student's t-tables for a two-tailed test at a significance level of $\alpha=0.05$ and n-1 degrees of freedom. Sokal and Rohlf (1969) claim that a significance level of $\alpha=0.05$ or five percent is generally accepted as an appropriate value for determining statistical significance. When the t_s value is less than t, the null hypothesis is not rejected. Hence, one can conclude with reasonable confidence that the data from the two groups being compared are from the same data population.

The Statistical Package for the Social Sciences (SPSSx) was used for all t-test comparisons carried out. The program used to compare data is listed in Appendix A.5. Nie et. al. (1975) contains the documentation explaining SPSSx.

Table 5.1 summarizes the results of all t-test comparisons made. The final column of Table 5.1, "2-tail probability" indicates the level of significance, α, that the two means have. One need only compare the calculated α with the selected level of significance of $\alpha=0.05$, rather than search the Student's t-tables for a t value and then compare t and t_s values. Either method is equally valid. The following discussion is based on the t-test results summarized in Table 5.1.

The first test compared all theoretical runaway speed values against all experimental data. The t_s value of 3.68 would be less than t, if and only if $\alpha=0.001$. With a significance level of $\alpha=0.05$, the null hypothesis was not accepted, indicating that the CSMP model inaccurately predicted runaway speed for both turbines. Two more t-test comparisons were made to determine if the CSMP model was better able to predict runaway speed for either one of the two turbines tested. Test 2 compared actual to theoretical

TABLE 5.1 STUDENT'S t-TEST COMPARISONS OF RUNAWAY SPEED DATA

Test	Variable	No. of cases	Mean rpm	Standard deviation	Diff mean	Standard deviation	t-Value	df	2 Tail probability
	theory		3431	169					
1	(total)	50			111	214	3.68	49	0.001
	experimental		3320	207					
	theory		3543	319					
2	(turbine 1)	119			203	216	10.28	118	0.000
	experimental		3340	353					
	theory		3276	337					
3	(turbine 2)	113			-7.9	142	-0.59	112	0.557
	experimental		3284	330					
	run1		3127	329					
4	(T2 J1)	24			-85.9	165	-2.55	23	0.018
	run3		3214	270					
	run2		3766	412					
5	(T2 J1)	20			68	246	1.23	19	0.233
	run4		3698	352					
	run1		3064	323					
6	(T2 J2)	25			-152	86	-8.84	24	0.000
	run3		3216	316					
	run2		3714	415					
7	(T2 J2)	23			13.6	174	0.38	22	0.711
	run4		3700	335					

TABLE 5.1 STUDENT'S t-TEST COMPARISONS OF RUNAWAY SPEED DATA (continued)

Test	Variable	No. of cases	Mean rpm	Standard deviation	Diff mean	Standard deviation	t Value	df	2 Tail probability
	run1		3032	313					
8	(T2 J3)	25			-0.5	89	-0.03	24	0.98
	run3		3700	335					
	run2		3463	359					
9	(T2 J3)	23			-96	96	-4.77	22	0.000
	run4		3559	335					
	run1		3013	298					
10	(T2 J4)	25			85	116	3.68	24	0.001
	run3		2928	291					
	run2		3418	365					
11	(T2 J4)	24			-100	106	-4.59	23	0.000
	run4		3517	361					
	run1		3052	279					
12	(T2 J5)	25			241	129	9.35	24	0.000
	run3		2811	249					
	run2		3348	315					
13	(T2 J5)	23			-19	143	-0.63	22	0.535
	run4		3367	327					

data for the Colombian (handcast) turbine while test 3 compared similar data for the English (manufactured) turbine. The results of test 2, indicated that the means of the theoretical and experimental runaway speeds were significantly different to not accept the null hypothesis for the handcast turbine. Test 3 results showed that the CSMP model was capable of predicting runaway speed for the manufactured turbine with a relatively high level of probability. The difference in the level of prediction for each turbine was not surprising. Physical imperfections of the handcast turbine such as flashings, holes and pits on the interior surface of the buckets absorbed energy and slowed the flow of water over the buckets while misaligned buckets coupled with a high angle of return forced considerable quantities of water to strike the backside of the proximate bucket. As well, serious vibrations created inefficiencies at rotational speeds over 3600 rpm. All these imperfections acted to reduce the turbine speed and, without extensive testing, are difficult to include in a simulation model.

Accepting the accuracy of the CSMP model for predicting runaway speeds for the manufactured turbine permitted further t-tests to determine the strengths and weaknesses of the model. Two comparisons were made for each jet configuration; one between the predicted and actual runaway speeds for the high friction system (run one and three respectively) and the other between the predicted and actual runaway speeds for the low friction system (run two and run four respectively). Evaluation of t-tests 4 to 13 helped re-examine some of the assumptions upon which the model is based.

Results of t-tests 4, 6, 8, 10 and 12 showed that for four of the five jet configurations, the high friction runaway speeds were not predicted. Runaway speeds were underpredicted for t-tests 4 and 6, overpredicted for t-tests 10 and 12 and accurately predicted for t-test 8. These results could be explained by an incorrect positioning of the high friction system curve. Figure 5.3 shows that runaway speed prediction could be enhanced if the existing curve was rotated slightly, clockwise about the intersection of the curve E4J240 and the high friction curve. Estimation of the power loss effects of the high friction system would have been much more accurate if larger variable speed motors were available for the motor draw test. Thus, the inaccuracy may not be with the CSMP model but could be in the procedure used to estimate the power loss in the high friction system.

Student's t-tests on the low friction system show that the model had difficulty predicting runaway speeds for the two- and three-jet interference patterns, t-tests 9 and 11 respectively. The accurate prediction of runaway speeds for the one-jet and two-jet-no-interference configuration infers that the model accurately calculated the quantity of wastewater and power produced. The underprediction of runaway speeds by t-tests 9 and 11 indicates that more water

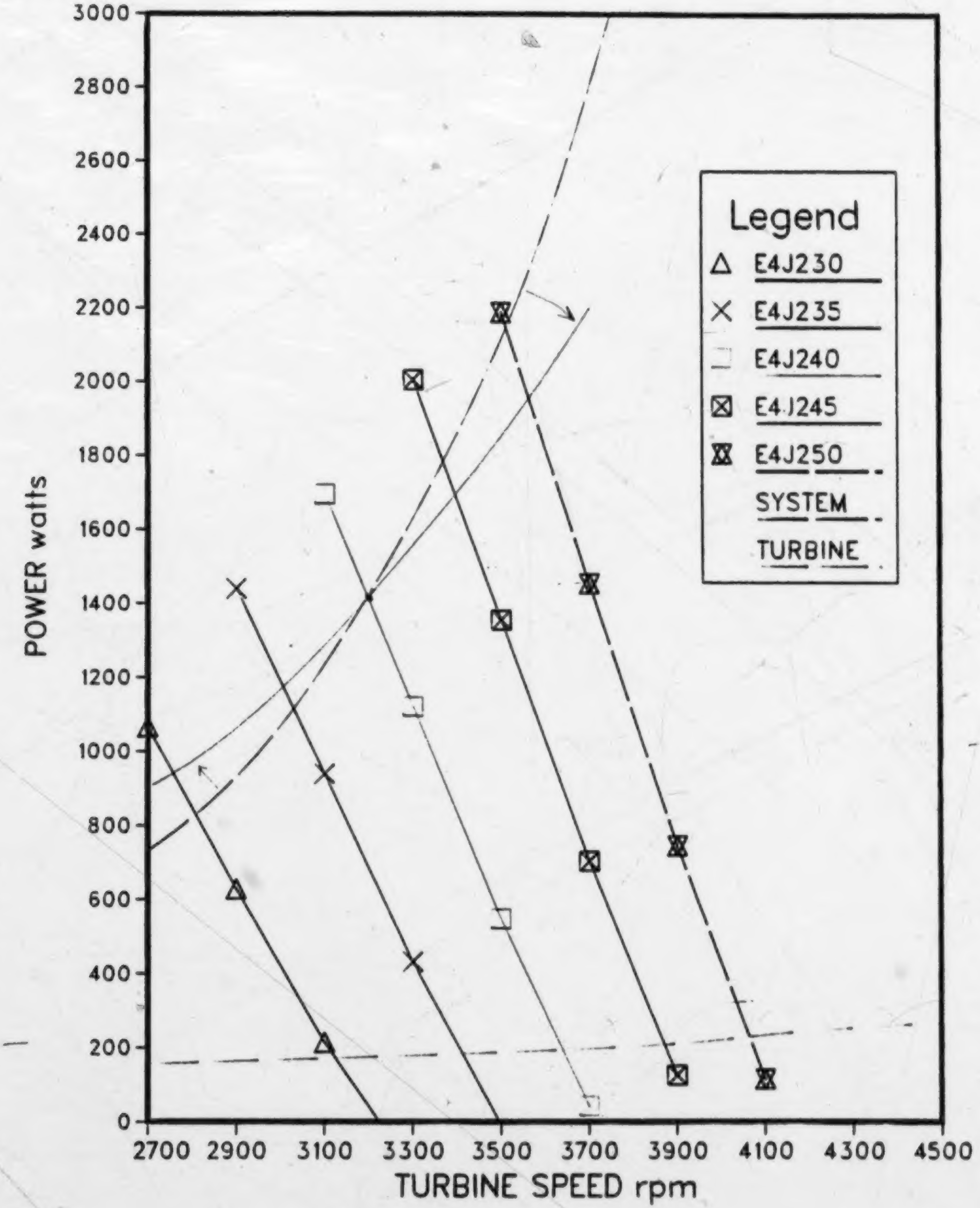

Figure 5.3 High friction curve adjustment

struck the turbine than predicted.

The introduction of jet interference into the CSMP model, as in t-tests 9 and 11, was based on the assumption that the segment of wastewater passing through the turbine will displace from the adjacent jet a segment of water of equal size. In addition, the model was based on the assumption that the displaced segment of water was not part of the wastewater segment of the second jet so the displaced segment of water would have struck the turbine had it not been removed from the water jet.

As more water struck the turbine than predicted, the above assumptions were incorrect. Firstly, it seems unlikely that the wastewater segment was able to remove an equal sized portion of water from an adjacent water jet. Immediately after leaving the nozzle, friction between the air and the water jet causes the water jet to slow down. In order to pass the same volume of water, the water jet is forced to widen. The further the water jet travels from the nozzle, the wider it becomes. The segment of wastewater travels the diameter of the turbine before striking the next water jet which has just left its nozzle. The segment of wastewater, having traveled further, will be incapable of removing an equal volume of water as a portion of the wider segment will completely bypass the narrower water jet. Secondly, more water would strike the turbine if the portion of the water jet removed or disturbed as a result of collision with a wastewater segment were that portion of the water jet that would have gone on to miss the turbine. The length of wastewater segments increase as rotational speed increases as does the probability of removing water that would have missed the turbine. Further work would be required to resolve how much of the water jet struck by a wastewater segment is prevented from striking the turbine.

Even though the assumptions predicting wastewater volume may have been technically inaccurate, they did help the model correctly predict the runaway speeds for the four-jet configuration, (t-test 13.) A possible explanation could be that the high level of splashing associated with the four jet system must have interfered with turbine performance sufficiently to equal the effect of calculated wastewater. Reduced runaway speeds could also result from the greater influence of bucket surface friction on the smaller water jet diameters associated with the four-jet system. This phenomena was important for slowing down the handcast turbine.

The CSMP model developed for this thesis can predict runaway speeds for no interference jet patterns. However, more work is required to determine the nature of water jet interference before a model can be developed to predict runaway speeds of micro hydroelectric systems using multiple jet arrangements to govern rotational speed.

5.2 Effect of Jet Arrangement on Runaway Speed

The effect of jet arrangement on runaway speed is facilitated when comparisons are made between different jet configurations operating under similar flow rate and head conditions. As previously discussed in section 3.2, the mechanism for runaway speed reduction depends on the volume of wastewater generated when the turbine operates above normal speed. Daugherty (1920) claims that normal speed occurs when the tangential speed of the buckets at pitch radius is 0.47 times the velocity of the water jet. Since no wastewater is generated at normal speed and given equal flow rate and head conditions, each jet configuration will achieve maximum power at the same normal speed. Assuming the turbine is being operated within boundary conditions, changes in head or flow rate or both will cause subsequent changes in normal speed and runaway speed. Dividing runaway speed by normal speed yields the Speed Ratio, θ_n (Reddy, 1966). Jet configuration evaluation is facilitated by the use of speed ratio to quantify performance.

Columns 3 and 5 of Tables A.4.1 to A.4.10 show that for a given head, the flow rate and head varied by as much as twelve and two percent, respectively, between jet configurations (Appendix A.4). Figure 5.4 and 5.5 show typical efficiency curves for the handcast and manufactured turbine comparing the effects of five jet configurations at approximately the same head. The analysis of the impact of jet configuration on runaway speed of the turbine is improved if differences in head and flow rate were

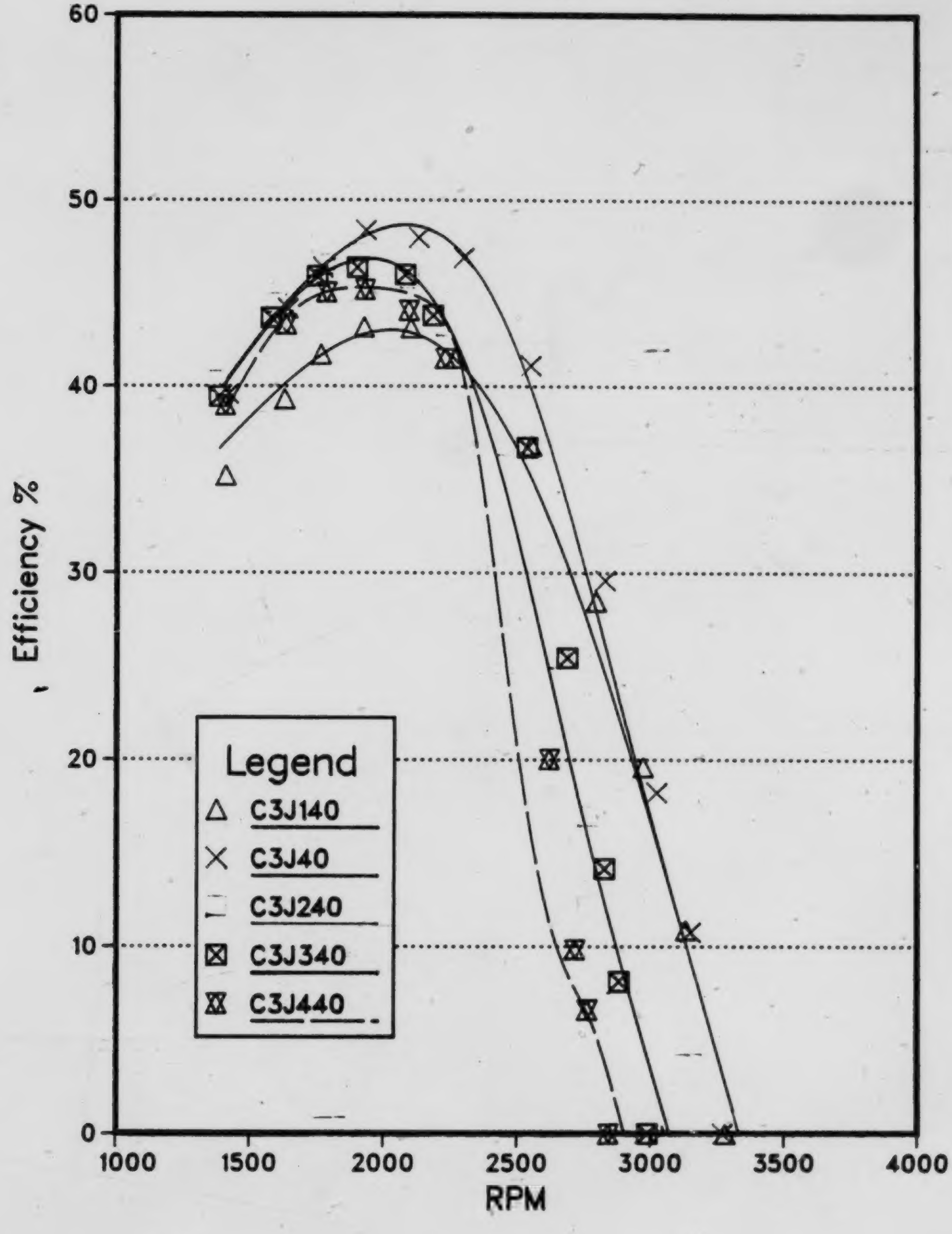

Figure 5.4 Efficiency curves for handcast turbine (series 3 flow rate at 40 meters total hydraulic head)

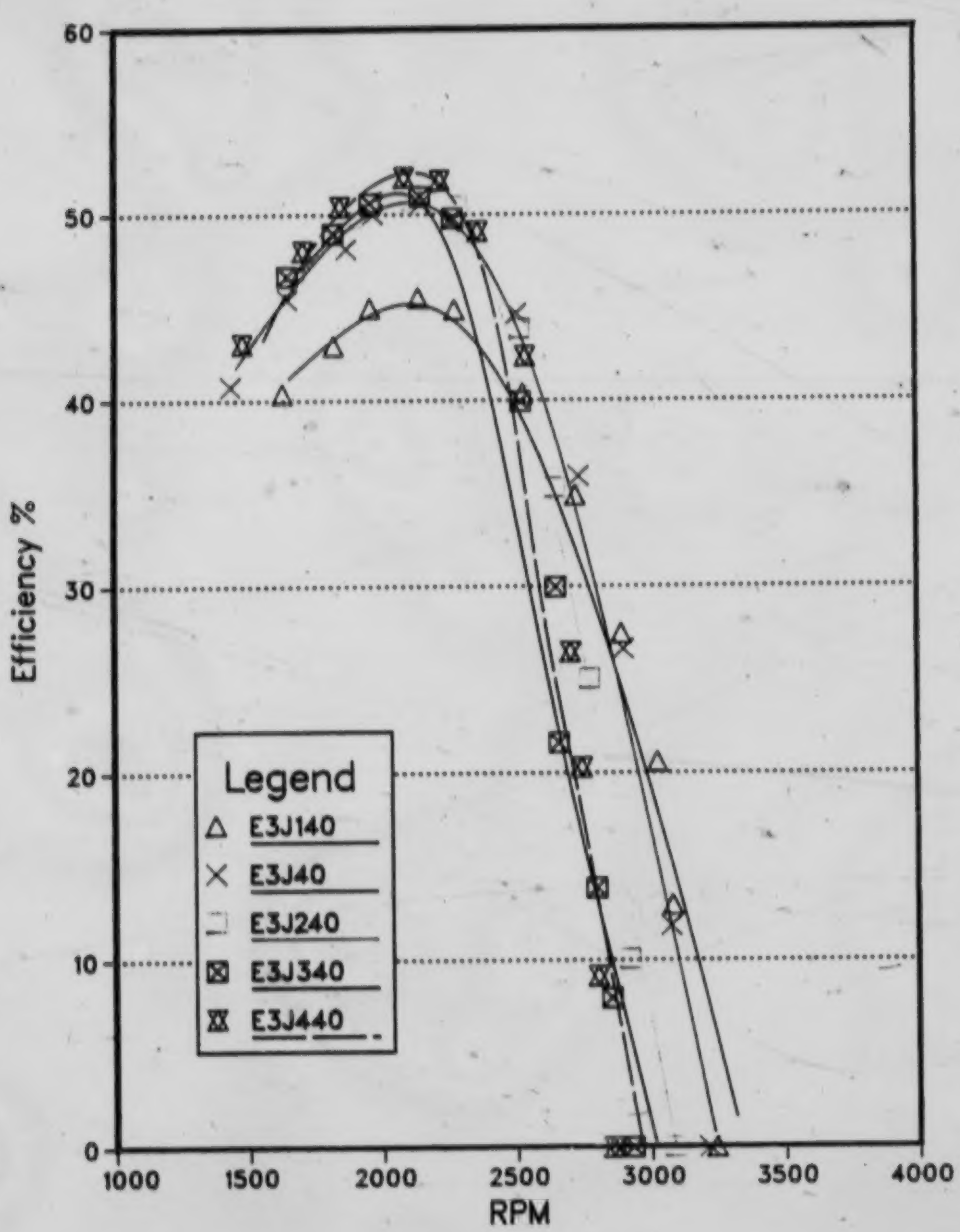

Figure 5.5 Efficiency curves for manufactured turbine (series 3 flow rates at 40 meters of total hydraulic head)

eliminated.

As discussed in Chapter four, the orifice Equation 4.2 shows that flow rate is directly related to both head and cross sectional area. However, variations in cross sectional area have more influence on flow rate than the square root of variations in head. Table 5.2 illustrates that total orifice area varied by as much as eight percent within series groups. The variance was due to the difficulty of getting drill bits to match the desired orifice diameter. Since larger flow rates are associated with larger orifice areas, the effect of variance amongst flow rates can be minimized by the following procedure. For each run, water jet velocity was calculated using Equation 4.8. Normal speed was then calculated using Equation 5.2. Dividing rotational

$$N_r = (14.10V_j)/(x_o\pi) \qquad (5.2)$$

speed by normal speed yields speed ratio, θ_N. With variations in flow rate and head minimized, runaway speeds expressed as a speed ratio could then be compared and evaluated.

5.2.1 Analysis of Variance of Runaway Speed

Speed ratios were calculated and then evaluated using the SPSSx statistical package. Data from each series was analysed separately. The experimentaly measured runaway speed data for the high friction and low friction systems, three and four respectively, were studied on an individual basis. A three-way analysis of variance (ANOVA, Steel and

TABLE 5.2 ORIFICE SIZE DEVIATION

Series	Number of Orifices	Orifice dia. (mm)	Total $(mm)^2$	Area Desired $(mm)^2$	Diff. %
1	1	16.00	201	201	0.0
1	2	11.00	190	201	5.5
1	3	9.06	193	201	3.8
1	4	7.90	196	201	2.5
2	1	17.85	250	250	0.0
2	2	12.50	245	250	2.1
2	3	10.28	249	250	0.5
2	4	8.90	249	250	0.5
3	1	19.88	310	310	0.0
3	2	13.72	295	310	5.0
3	3	11.00	285	310	8.2
3	4	9.85	304	310	1.8
4	1	22.12	384	384	0.0
4	2	15.44	374	384	2.6
4	3	12.49	367	384	4.3
4	4	10.92	375	384	2.4
5	1	24.21	460	460	0.0
5	2	16.94	451	460	2.1
5	3	13.96	459	460	0.2
5	4	11.89	444	460	3.5

Torrie, 1980) was performed on each run followed by a multiple classification analysis, (MCA, Nie et. al., 1975). The SPSSx program used to carry out the ANOVA is outlined in Appendix A.5.1.

ANOVA was used to determine the level of significance each of the main effects; turbine type, jet arrangement and head had on runaway speed. The SPSSx ANOVA subprogram uses an F-test to determine the level of significance amongst treatments. The F value is calculated by dividing each treatment mean square by the residual mean square. The residual mean square was used instead of error mean square to calculate the F value. A large factorial design was the basis of this experiment. Time constraints permitted one replication of each treatment combination. The lack of treatment replications made it impossible to calculate the error mean square. However, Davies (1967) points out that

> "in factorial experiments in which there is no replication and for which no prior estimate of error is available it is customary to employ an estimate of error variance based on the higher-order interactions."

Cockran and Cox (1957) suggest that,

> "if certian high-order interactions are negligible, their mean squares in the analysis of variance will behave exactly like components of the error mean square and therefore can be used to provide an estimate of error."

A three-way ANOVA was conducted on the experimental data for each orifice series. As there was no two-way interaction between jet configuration and head the three-factor interaction with 16 degrees of freedom was used to estimate the residual standard deviation (Cox, 1958).

The calculated F value is then compared to a tabular F value with m and n degrees of freedom and α=0.05, where m and n represent the degrees of freedom of the dividend and the divisor respectively. "A significant F implies that the evidence is sufficiently strong to indicate that all treatments do not belong to populations with a common mean (Steel and Torrie, 1980)."

There is little difference between the t-test and F-test. When determining if two sample means have the same population mean, a two-tailed t-test was used with an $\alpha/2$ probability level. Since $t^2_{(n)} = F_{(1,n)}$ the same comparison can be done using a one-tailed test with an α probability level. Sokal and Rohlf (1969) prefer F-tests "because of their simplicity and elegance and because they tie in well with the overall ANOVA." The F values and significance levels for the main effects for all five ANOVAs are summarized in Table 5.3. Analysis and discussion of results were based on α=0.05. Therefore, effects were deemed significantly different when the calculated significance levels were less than 0.05.

Turbine type proved to have a significant effect on runaway speed in six of the eight cases, in Table 5.3. With relatively large differences in design and quality, between the two turbines, one expected all eight tests to be significant. The high level of similarity found in series 4

TABLE 5.3 ANOVA SUMMARY

Main Effects		Orifice Series Number 1		2		3		4		5	
		F Value	α	F Value	α	F Value	α	F Value	α	F Value	α
	Turbine	3080.4	0.000	191.8	0.000	5.5	0.032	0.05	0.827	189.5	0.000
Run3	Jet	337.1	0.000	98.2	0.000	315.3	0.000	132.3	0.000	415.2	0.000
	Head	1.8	0.177	3.9	0.022	1.0	0.425	1.5	0.249	0.8	0.543
	Turbine	2570.5	0.000	92.2	0.000	171.4	0.000	16.0	0.001	3.3	0.088
Run4	Jet	618.2	0.000	119.0	0.000	380.8	0.000	13.6	0.000	61.5	0.000
	Head	24.5	0.000	3.7	0.026	11.7	0.000	0.14	0.964	4.1	0.026

run three cell is difficult to explain. However, referring to the discussion in section 5.1, one explanation could be that the flow rates used in series 4 caused partial flooding of the handcast turbine at the slower runaway speeds of the high friction speeds, reducing reducing runaway speed to, coincidentally, the same speed as observed for the manufactured turbine. This same explanation applies for the higher flow rates and higher runaway speeds associated with the series 5 run four data block.

The relatively large F values for both high and low friction runs of series 1 data is likely due to low flow rates. The handcast turbine is susceptible to low efficiencies at low flow rates because of misaligned buckets and flashing and pits on the inner bucket surface, whereas the manufactured turbine's efficiency seemed to be relatively stable regardless of flow rate.

The effect of jet configuration on runaway speed was found to be significant for all five orifice series and both friction levels. However, further analysis was required to determine the effect of each jet arrangement on speed. This analysis and its results are discussed in section 5.2.2.

ANOVA results show that head seemed to have little influence on the speed reduction process. Half the cells showed that head was insignificant, with four of the five occuring within the run three data. One might conclude that high friction masks any effect the head has on runaway speed reduction. Again, further analysis of the data was required before any assumptions are confirmed.

5.2.2 Multiple Classification Analysis (MCA)

MCA tables were developed using the STATISTICS ALL option with the ANOVA subprogram (Appendix A.5.2) and they were used to examine the pattern of a treatment's relationship to runaway speed. As the treatments (turbine type, jet configuration and hydraulic head level) are orthogonally different, the MCA tables can determine what portion of the variation in speed ratio is due to each treatment. These tables were summerized and they are located in Appendix A.6.

As determined in the previous section, turbine selection affects runaway speed. However, the ability of a turbine to reduce runaway speed can, under certain conditions, depend upon the flow rate of water striking the turbine. Brief analysis of the experimental data indicated that there was a relationship between turbine type and orifice series, as flow rate seemed to have a strong effect on speed reduction. Study of the importance of flow rate and turbine design on a micro hydroelectric systems ability to reduce runaway speed was facilitated by the wide range of flow rates generated by the five orifice series.

When the volume of water striking the turbines was low, as with the series 1 and 2 orifice sets, the handcast turbine was slower than the manufactured turbine. This was attributed to the effect of bucket misalignment and bucket surface irregularities because an increase in flow rate reduced the effect of these irregularities. The five percent lower power output of the handcast turbine was a result of these irregularities causing a decrease in hydraulic efficiency. Increasing average flow rate 23 percent from series 1 nozzles to series 2 nozzles diminished the effect of turbine irregularities on the runaway speed of the handcast turbine. This in turn increased the effect of the number of buckets on runaway speed. Being less hydraulically efficient the handcast turbine continued to have a lower rotational speed than the manufactured turbine, even though the overall difference between the two turbines was reduced by over 50 percent.

A further increase of 23 percent in flow rate with the series 3 nozzles resulted in the manufactured turbine having a slightly greater ability to reduce runaway speed than the handcast turbine. This result continued with series 4 data. The low runaway speeds associated with the high friction system and the flow rates associated with the series 3 and 4 nozzles combined to minimize the effect of turbine design on runaway speed. This is reinforced by the lack of variation in series 3 and series 4 high friction data, (0.36 and 0.00 percent respectively) as illustrated in Figure 5.6. At lower rotational speeds the ability of the Pelton turbines to generate waste water is reduced. However, at higher rotational speeds the effect of fewer buckets accounts for 9.6 and 26.0 percent of the respective variation in series 3

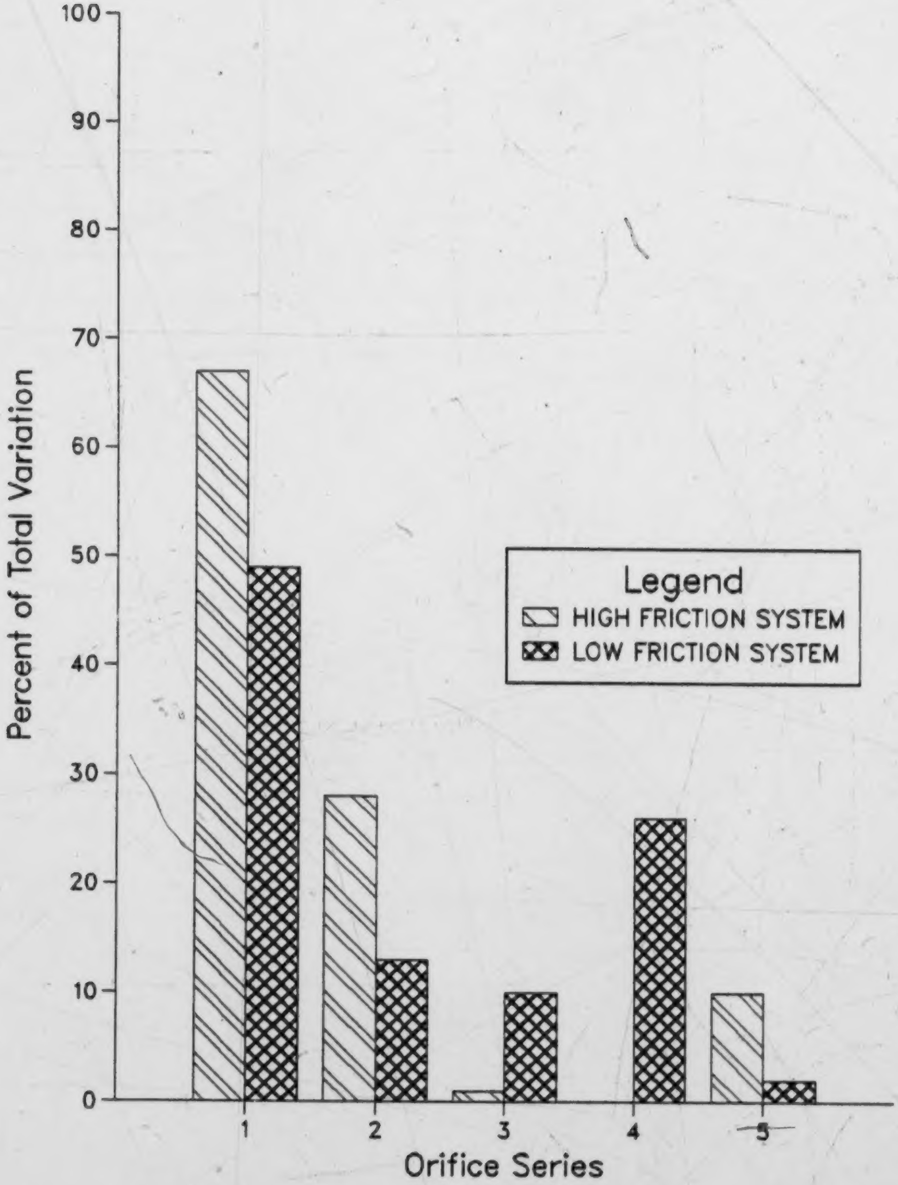

Figure 5.6 Effect of turbine selection on runaway speed as a percent of total speed variation

and series 4 low friction data. These results concur with the principles used to develop Equation 3.11 where wastewater volume is directly proportional to rotational speed.

The high flow rates associated with the series 5 nozzles caused the handcast turbine to operate at lower rotational speeds than the manufactured turbine. The larger volumes of water generated by the series 5 nozzles flooded the handcast turbine because the high return angle of 170 degrees did not allow exiting water to clear the turbine. Water unable to clear the turbine struck the backside of the next bucket which decreased hydraulic efficiency and reduced the rotational speed of the turbine.

Multiple classification analysis was also used to determine the influence of jet arrangement on speed reduction. Figure 5.7 illustrates the MCA analysis for each of the five orifice series and the overall effect of jet configuration on speed reduction. Speed ratios from the MCA were used to calculate the effect of each jet configuration on runaway speed reduction.

Speed ratios were compared by calculating the percent deviation (reduction) from the maximum value of five jet configurations for the other four jet configurations within each series and friction type. Therefore, the jet configuration having the largest speed ratio (because it had the fastest runaway speed) was considered par and had zero percent reduction in speed. As normal speed is different for

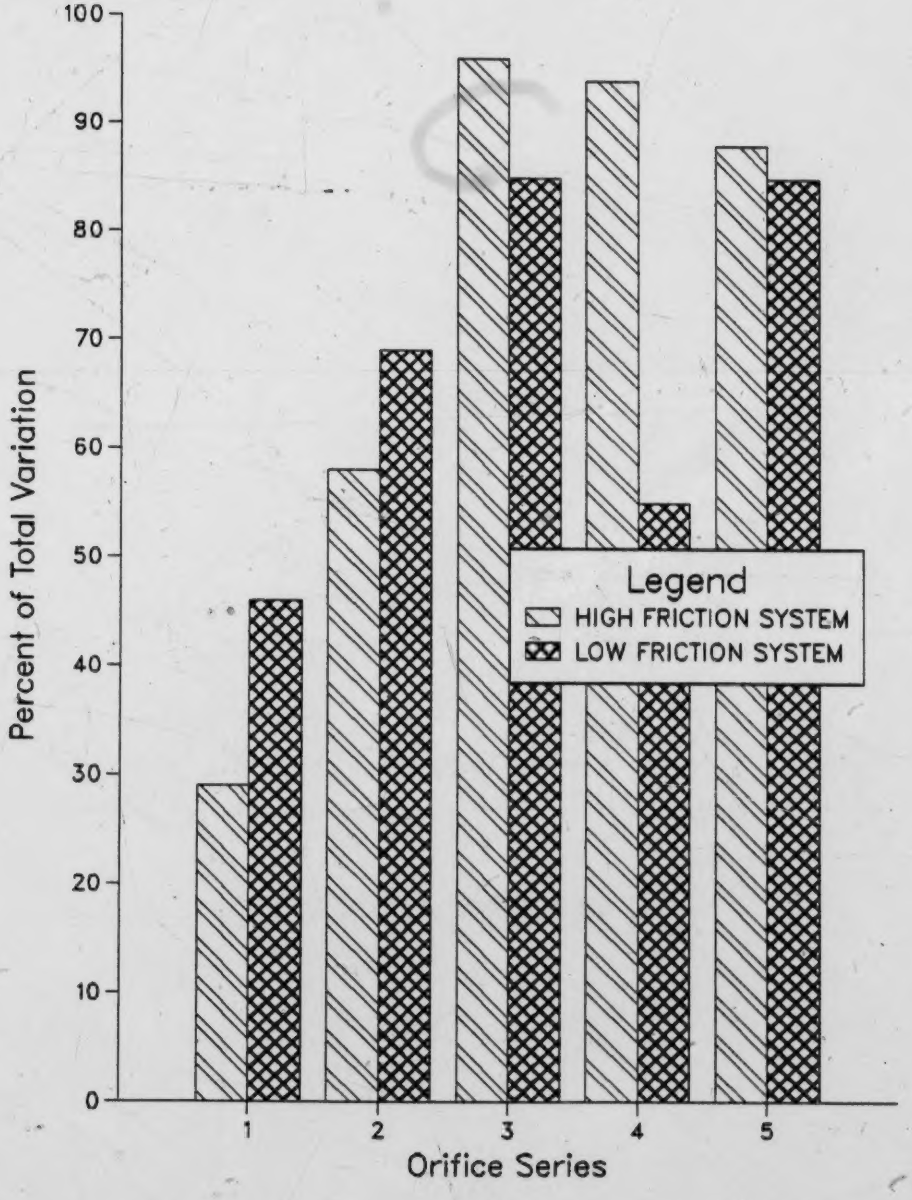

Figure 5.7 Effect of jet configuration on runaway speed as a percent of total runaway speed variation

every site specific situation, the speed ratio was used to compare results. The normal speed is always represented by a speed ratio of 1.0. Speed reduction begins after normal speed is reached. Percent reduction represents the change in speed ratio from θ_n=1.0 (normal speed) to runaway speed, θ_{max}, between two configurations divided by the maximum speed ratio, θ_{max} minus normal speed (θ_{max}-1.0). This approach permits the comparison of reduction results with other systems.

The most common jet configuration used on commercial Pelton turbines is the single-jet. Even though high nozzle efficiencies can be obtained from specifically designed manufactured nozzles, overall system efficiency maximization demands the minimum number of jets be used. The only way to increase the power output of a single-jet system, constrained by head, is to increase jet diameter. As mentioned in section 2.2, jet diameter should not exceed 0.33 times the bucket width. Exceeding this diameter causes inefficient flow over the bucket surface and can cause the turbine to flood. Results of the single-jet configuration show that maximum performance was only obtained for the orifice series 1 data (Figure 5.8). Turbine performance on the whole became increasingly less efficient with increased flow rate, suggesting that the single-jet diameters for series 2 through 5 were too large for the turbines used. Maximum runaway speeds were obtained by the two-jet-no-interference configuration except for series 1

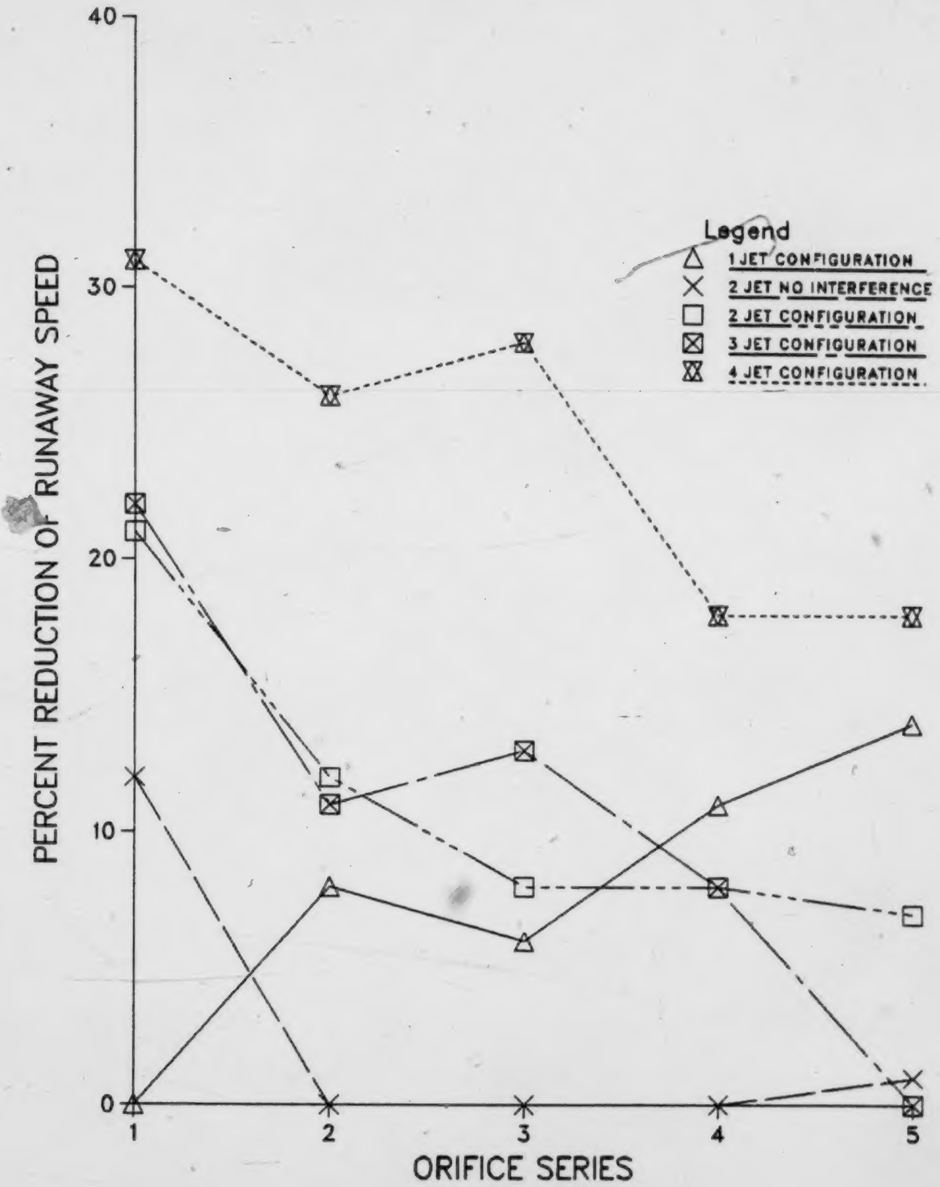

Figure 5.8 Effect of jet configuration on runaway speed as a percent reduction of runaway speed (with respect to normal speed) for the low friction system (generator disconnected)

data and for some unknown reason series 4 data. Flooding was not experienced for the two-jet configurations because their water jet diameters were below the single-jet, series 2 diameter of 14.35 mm.

In general, runaway speed decreases as the number of water jets and interference points increase, thereby increasing percent reduction. For all ten data groups represented in Figure 5.7, maximum speed reduction occurred with the four-jet configuration as illustrated by Figure 5.8. For the high friction (run three) data, runaway speed was reduced by an average of [illegible]6.2 percent, whereas average runaway speed reduction for run four data was 28.2 percent, excluding values for series 4 and series 5 (as many missing data points made MCA comparisons difficult). The actual physical reduction in runaway speed is greater for run four data, even though the percent reduction is lower than run three data.

Jet configuration alone accounted for 96 percent and 85 percent of the variation in series 3 data for run three and run four respectfully. Optimum performance of jet configurations in series 3 data implies that the balance between too low a flow rate (unable to mask turbine irregularities) and too high a flow rate (yielding flooding) exists here. No other treatment was as important as jet configuration for determining runaway speed.

The five data groups (in Table A.6.3) which account for over two percent of the variation in runaway speed, due to hydraulic head are the same groups which show that head was significant in the ANOVA Table 5.3. Careful examination of these cells failed to yield any patterns that might suggest anything regarding the influence of hydraulic head on speed control. The relatively low variations in percentage for cells where α <2.5 percent, indicates that changes in head had little influence on changing the speed ratio.

5.3 Turbine Efficiency

Turbine efficiency (or Hill) curves are used by manufactures of turbines to predict prototype performance from the turbine constants (Warnick, 1984). Efficiency curves are used in this thesis to summarize power curve data for each turbine and to illustrate the effect a four-jet arrangement has on overall system performance. As efficiency curves were developed using data derived while the alternator was connected to the turbine, curves only exist for the high friction system.

Turbine efficiency was calculated by dividing the power produced by the alternator (P_{out}) by the amount of power theoretically available to the turbine (P_{in}) calculated using Equation 4.1.

Efficiency curves are three parameter curves constructed by plotting unit power (P_{ed}) against the speed ratio, θ_n, for each calculated efficiency value on the power curve. Unit power was calculated using Equation 5.3.

$$P_{ed} = P_{out}/(\rho D^2 (gH)^{1.5})\pi \qquad (5.3)$$

Hill curves were developed using SURFACE II (Sampson, 1978).

Comparing the two-jet-no-interference system of the manufactured turbine, Figure 5.9, with the four-jet system, Figure 5.10, one can see that there is a shift in turbine efficiency to the upper right. This illustrates that the introduction of a four-jet arrangement reduces runaway speed without a corresponding loss in the ability to produce power. Little change in contour density on the left hand side of maximum efficiency indicates that turbine efficiency did not decrease between the two-jet-no-interference and the four-jet systems. However, the higher density of contour lines to the right of maximum efficiency indicate that the four-jet system has a more rapid decrease in runaway speed then the two-jet system. The almost closed shape of the 50 percent contour on Figure 5.9 indicates that the turbine was tested to the limits of flow rate. Any further attempt to increase power by increasing the amount of water striking the turbine would decrease the amount of power. The vertical structure of this contour indicate that this turbine has relatively constant performance characteristics, in terms of speed ratio, over a wide range of flow rates. This can be explained in part by the number of buckets and the relatively shallow return angle as both factors allow water to clear the turbine and not interfere with performance. The open-ended maximum efficiency contour of Figure 5.10 indicates that the four-jet system is capable of handling flow rates higher than those tested in this

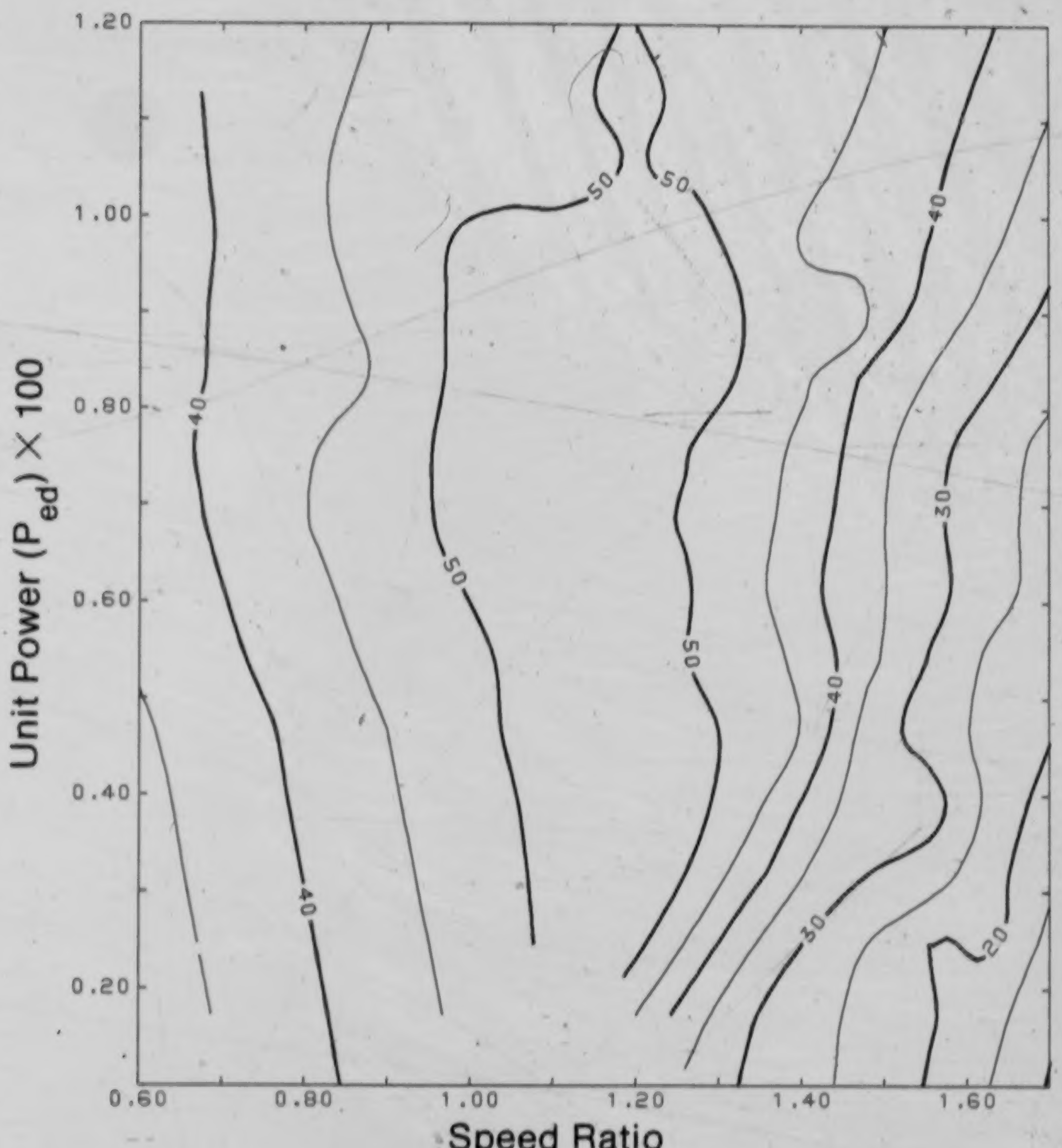

Figure 5.9 Hill curve for manufactured turbine under influence of a two-jet-no-interference configuration

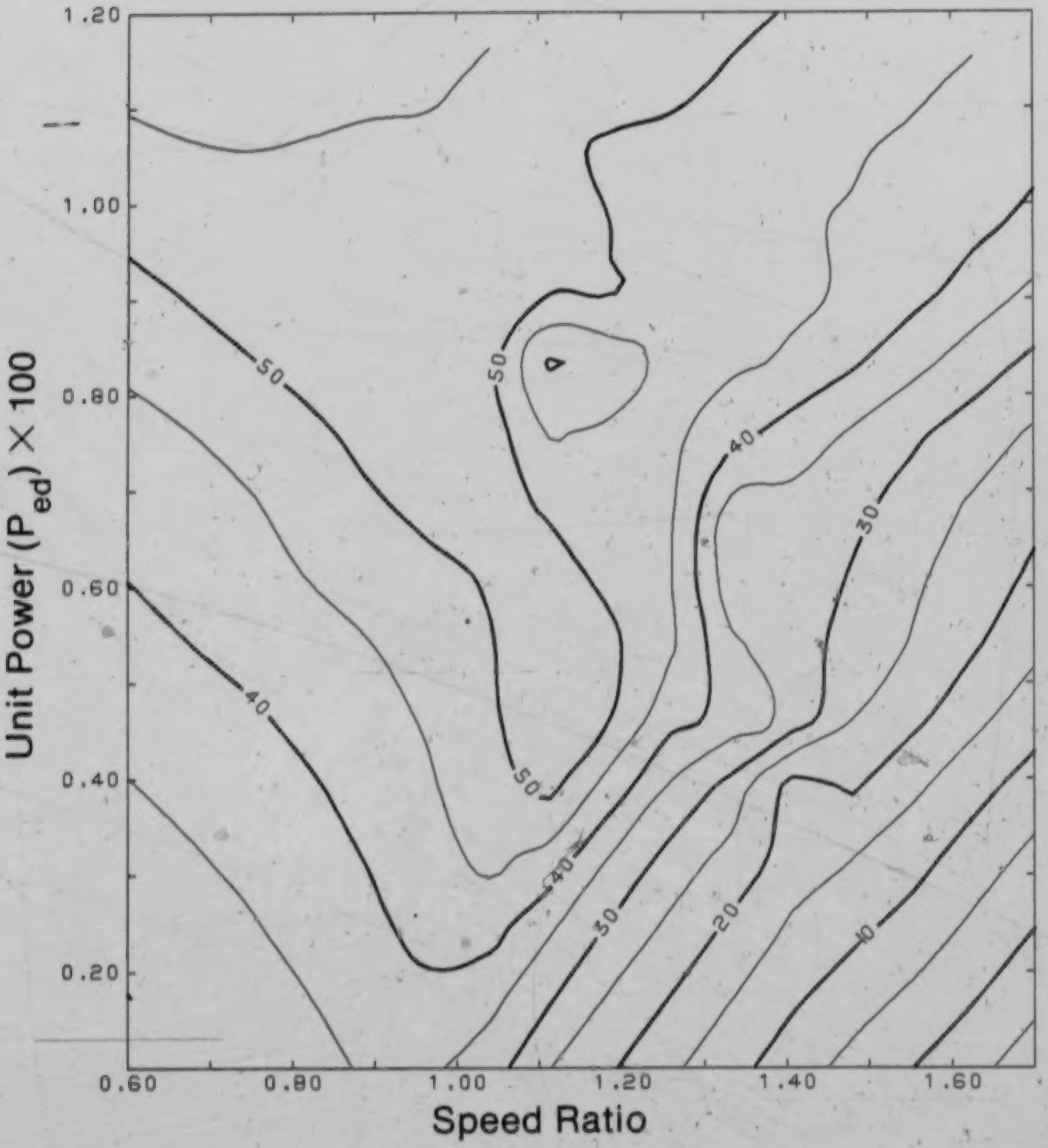

Figure 5.10 Hill curve for manufactured turbine under influence of a four-jet configuration

experiment. This was expected as the decreased jet diameter of the four-jet configuration over the two-jet configuations allows for higher flow rates before flooding begins to reduce efficiency.

Efficiency curves for the handcast turbine, Figures 5.11 and 5.12, are much more similar to each other than Figures 5.9 and 5.10 are to each other. A rapidly decreasing efficiency for the four jet system (Figure 5.12) over the two-jet-no-interference system (Figure 5.11) with increased speed ratio is the only major difference between figures. The handcast turbine was also tested within its operational limits as indicated by the closed contour for maximum efficiency for both the two-jet and four-jet configurations. In addition the four-jet system suffered a slight decrease in efficiency, as indicated by the smaller area. The reasons as discussed in section 5.2.2 would appear to be caused by the greater effect that misaligned buckets and rough bucket surfaces have on the smaller jet diameters of the four-jet configurations over the two-jet configuration.

These efficiency curves indicate that the manufactured turbine is slightly more efficient over a wider range of water flows than the handcast turbine. Since efficiency curves could only be developed for the high friction condition which reduced system sensitivity to changes in efficiency, more experimentation is required to determine the characteristics of each turbine efficiency curve for a low friction system. As the runaway speed for the

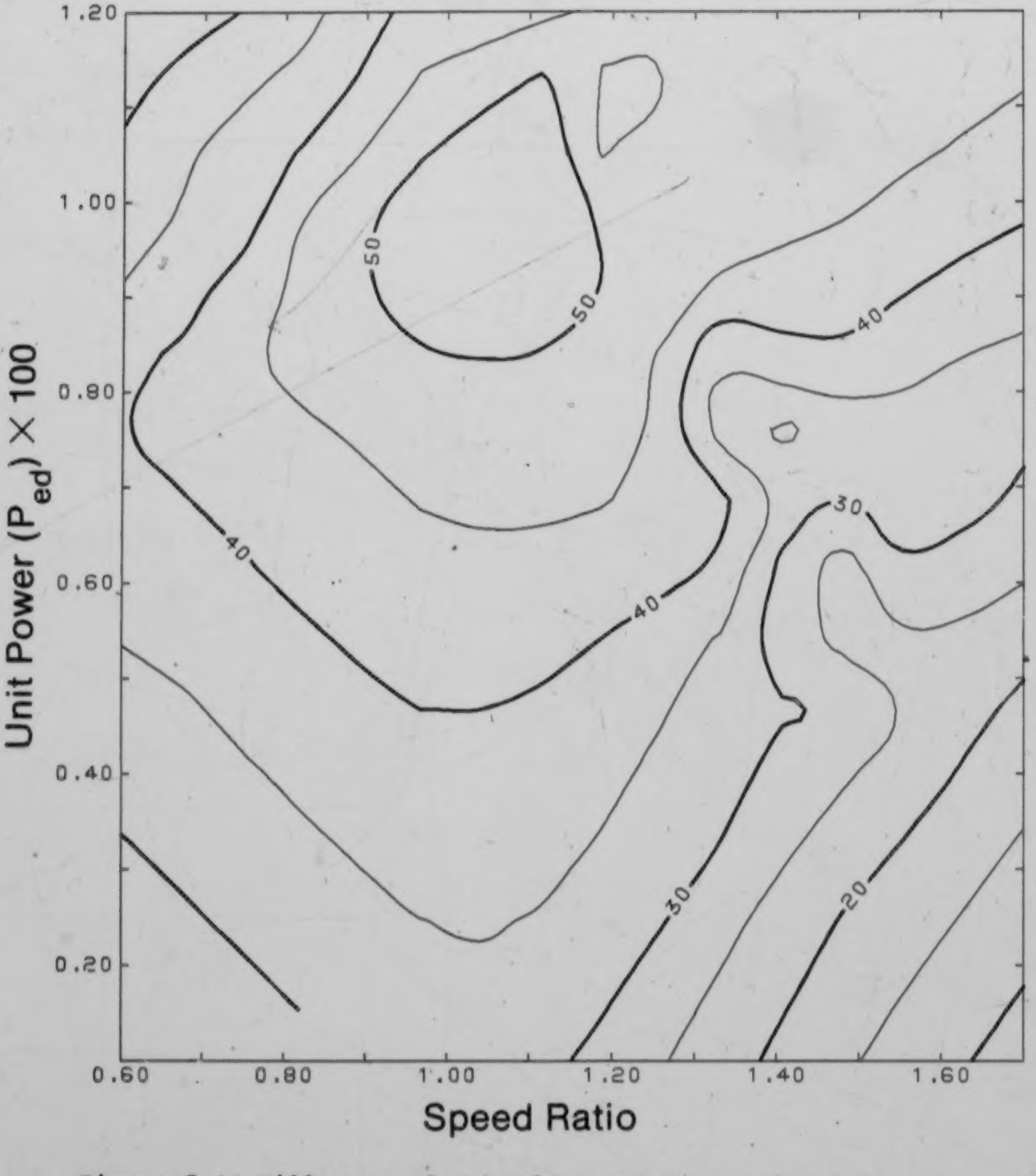

Figure 5.11 Hill curve for handcast turbine under influence of a two-jet-no-interference configuration

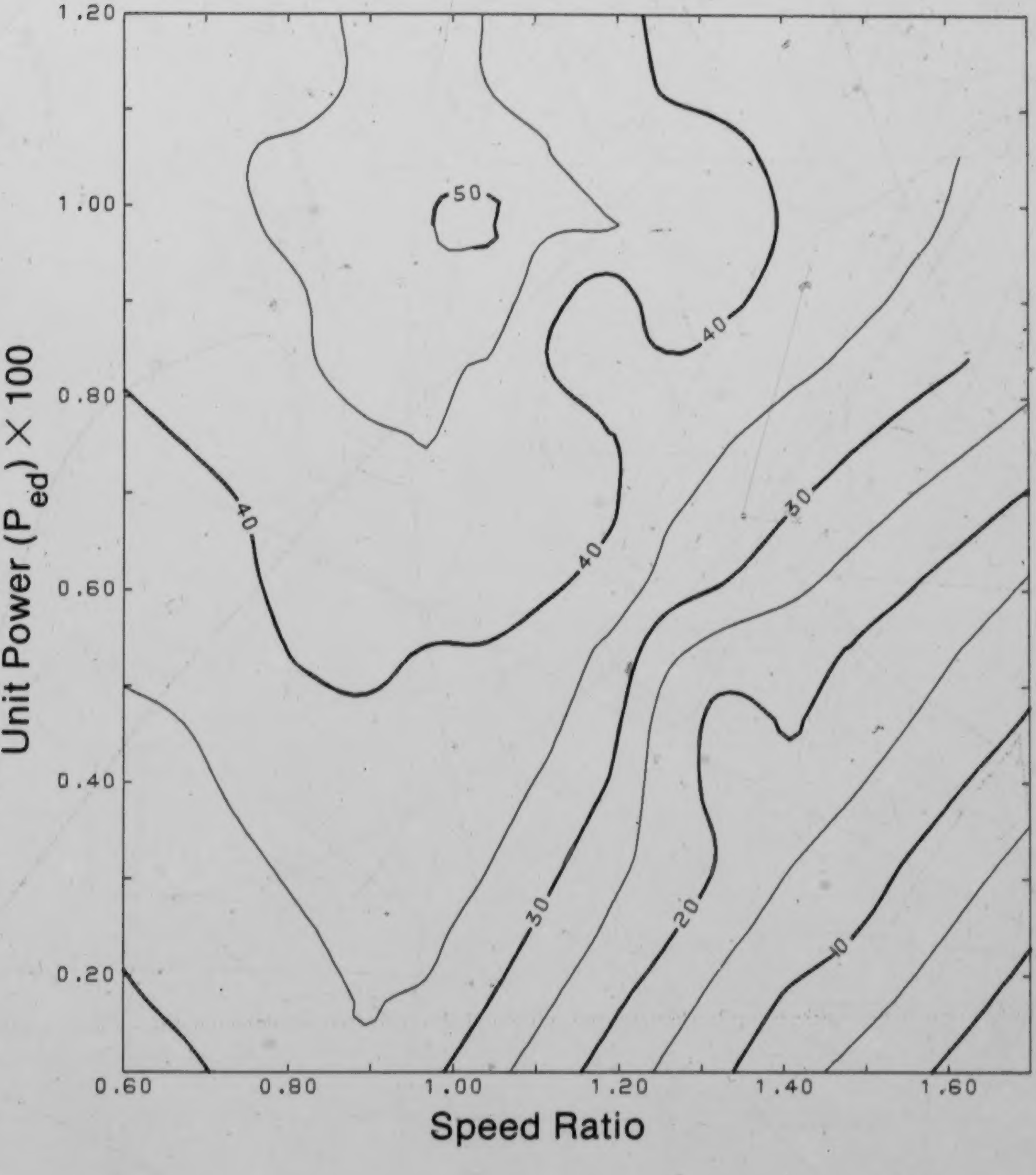

Figure 5.12 Hill curve for handcast turbine under influence of a four-jet confguration

two-jet-no-interference configuration of both turbines are similar, hydraulic efficiencies will most likely increase by the same proportion.

5.4 Voltage at Runaway Speed

A 25 percent reduction in runaway speed in the low friction system does not compare with the speed reductions observed in the field. Although the micro hydroelectric system in El Dormilon, Colombia, was not monitored directly for rotational speed, voltage was monitored. As voltage is directly proportional to rotational speed, a rough comparison can be made between the El Dormilon system and the micro hydroelectric system built by the author.

A voltmeter monitored the voltage characteristic of output power produced by the author`s micro hydroelectric system under conditions of high friction. When the voltage at normal speed was 110 volts for the four-jet configuration, runaway speed voltage often reached 150 volts. With a load of 60 watts, a maximum voltage of 130 volts was produced by the four-jet system operating in Colombia. This implies that methods other than those normally used to operate Pelton turbines were used by the four-jet micro hydroelectric system in Colombia which allowed it to reduce runaway speed more than the system tested at the University of Alberta.

Further experimentation is required to determine whether increasing the pitch radius of a given turbine reduces runaway speed. This could be accomplished by placing the lower edge of the water jet on the lower lip of the bucket. Wastewater volume increases when the perpendicular distance of the water jet to the hub increases. Wastewater segments could force more water from the adjacent jet from striking the turbine by pushing the adjacent water jet away from the lip of the bucket. The lower portion of the adjacent water jet would completely bypass the turbine and runaway speed would be reduced as a result of less water striking the turbine.

6. CONCLUSIONS

The following conclusions were drawn after careful consideration of the experimental design and data analysis methods.

Of the three parameters tested, water jet configuration had the greatest impact on speed control. Water jet configuration accounted for over ninety percent of the variation between runaway speeds within the same orifice series and turbine type. As the number of water jets and interference points increased, the runaway speed decreased. Effective speed control was achieved with only minor losses of hydraulic efficiency using multiple jet micro hydroelectric systems.

Of the five water jet configurations tested, the four-jet configuration achieved maximum speed control. Under conditions of low friction, runaway speed reductions of up to 27 percent were achieved with the four-jet system. The four-jet system was more effective then the other multiple jet configurations at reducing runaway speed because more interference points were available to prevent water from striking the turbine.

For the purposes of this experiment, the use of a pulley and belt system to transfer power to the alternator did not affect the influence of jet configuration or bucket design on speed control. Hence, the results obtained are valid for low friction systems as well. However, the use of a pulley and belt system to transfer power to the alternator was not practical. The power losses incurred reduced the hydraulic efficiency of the system to just over fifty percent. Better efficiencies would result if, whenever possible, the Pelton turbine were mounted directly onto the shaft of the alternator.

Experimental results confirm that speed reduction is the result of two factors, wastewater segments passing through the turbine and water prevented from striking the turbine because of collision with these wastewater segments at each interference point. The wastewater segment prevents a segment of water 0.66 the size of the wastewater segment from striking the turbine. To further reduce runaway speed and improve speed control further experimentation is required to increase the amount of water missing the turbine after the point of maximum power.

The effect of turbine design on speed control largely depends on flow conditions. The effect of surface friction between the water jet and bucket was a prominent factor in reducing hydraulic efficiency during low flow tests. During low flow rate tests turbine design accounted for fifty percent of the variation amongst runaway speeds. To a much lesser degree the number of buckets was more important during medium flow conditions while the shape of each bucket was more critical during high flow rate conditions. Except for a slight three percent loss of hydraulic efficiency the $US 100.00 handcast turbine reduced runaway speed as well as the much more expensive $US 500.00 manufactured turbine. This helps make the handcast Pelton turbine suitable for use in developing countries.

The CSMP model developed here can predict power output and runaway speed for Pelton turbines operated under normal conditions. The model cannot predict power output and runaway speed for Pelton turbines which are dynamically unbalanced or have misaligned buckets, buckets with surface imperfections, or excessive flow rates that result in flooding. The model predicted runaway speeds for the no interference jet configurations and was inconsistant for jet configurations which involved interference.

7. REFERENCES

Arnold, J.E.M., and J. Jongma. 1978. Fuelwood and charcoal in developing countries. Unasylva. 29(118): 2-9.

Baumister, T. and L.S. Marks. 1967. Standard handbook for mechanical engineers, 7th edition. McGraw-Hill Book Company. New York, NY.

Bhatia, R. 1982. Energy and development: demand, constraints and policy options. *In* H. Neu and D. Bain (editors), National Energy Planning and Management in Developing Countries. D. Reidel Publishing Company. Dordrecht. Holland.

Brater, E.F. 1959. Hydraulics. *In* L.C.Urquhart (editor), Civil Engineering Handbook. 4th edition. McGraw-Hill Book Company. New York, NY.

Burch, D. 1982. Appropriate technology for the third world; why the will is lacking. Ecologist. 12(2): 52-66.

Canadian Hunger Foundation. 1976. A handbook on appropriate technology. Ottawa, Ontario.

Cockran, G.W. and G.M. Cox. 1957. Experimental designs, 2nd edition. John Wiley and Sons, Inc. New York, NY.

Cox, D.R. 1958. Planning of experiments. John Wiley and Sons, Inc. New York, NY.

Daugherty, R.L. 1920. Hydraulic turbines. McGraw-Hill Book Company. New York, NY.

Davies, O.L. (editor). 1967. The design and analysis of industrial experiments, 2nd edition. Oliver and Boyd. London. England.

Dilip, L.B., B.Y. Murthy, K. Subir. 1972. A method of reducing the runaway speed of pelton turbine. *In* Proceedings of the Fourth Conference on Fluid Machinery. Budapest, Hungery.

Eckholm, E.P. 1975. The energy crisis: firewood. Worldwatch Paper 1. Worldwatch Institute. Washington, DC.

Forest, R.S., W. Edwardson, S. Vogal, and G. Yaciuk. 1982. Food systems. International Development Research Centre (IDRC). Ottawa, Ontario.

Fritz, J.J. 1984. Small and mini hydropower systems. McGraw-Hill. New York, NY.

Gaviria, D.L. 1977. Diseno y construccion de una turbina pelton con regulador mecanico de velocidad. Unpublished

Thesis. Department of Mechanical Engineering. Universidad de los Andes. Bogata, Colombia.

Genes, R.N. 1978. Control mechanico de velocidad para turbinas pelton. Unpublished Thesis. Department of Mechanical Engineering. Universidad de los Andes. Bogata, Colombia.

Hansen, V.E., O.W. Israelsen, G.E. Stringham. 1980. Irrigation principles and practices, 4th edition. John Wiley and Sons, Inc. New York, NY.

Harrison, P. 1980. Appropriate technology: how can it reach the villages. New Sci. Vol. 88: 521-523.

Hays, D. 1977. Energy for development:third world options. Worldwatch. Paper 15. Washington, DC.

Koester, F. 1911. Hydroelectric developments and engineering. D. Van Nostrand Company. New York, NY.

Lawand, T.A. 1981. Renewable energy applications in agricultural processes. Brace Research Institute. Macdonald College of McGill University. Montreal, Que.

Lobo Guerrero, J. and Burton, J.D. 1980. Hydraulic governor for small pelton turbines. Appropriate Technology. Vol.

6, No. 4.

Makhijani, A. 1975. Energy and agriculture in the third world. Ballinger Publishing Company. Cambridge, Mass.

Martin, G. 1981. Farm scale hydro-electric power. The Energy Journal. November:4-8.

Mnzava, E.M. 1981. Village industries vs. savanna forests. Unasylva, 33(131):24-29.

Molnar, A. 1980. The implications of women's role in food preparation in rural homes in Nepal. *In* R.S. Ganapathy (editor), Agriculture, Rural Energy and Development. Proceeding of the 1980 Symposium of the International Association for the Advancement of Appropriate Technology for Developing Countries. The University of Michigan. Ann Arbor, Michigan.

Nelson, S.B. 1976. Water engineering. *In* F.S. Merritt (editor), Standard Handbook for Civil Engineers. 2nd edition. McGraw-Hill Book Company. New York, NY.

Nie, N.H., C.H.Hull, J.G.Jenkins, K.Steinbrenner and D.H.Bent. 1975. SPSS Statistical package for the social sciences, 2nd edition. McGraw-Hill Book Company. New York, NY.

Reddy, P.P. 1966. Method of reducing the runaway speed of pelton turbine. M.Tech. Dissertation. Department of Mechanical Engineering. Indian Institute of Technology. Bombay, India.

Sampson, R.J. 1975. Surface II graphics system. Kansas Geological Survey. Kansas City, Kansas.

Schumacher, E.F. 1974. Small is beautiful: a study of economics as if people mattered. Blond and Briggs. London.

Shaner, W.W., P.F. Philip, and W.R. Schmehl. 1982. Farming systems research and development. Westview Press. Boulder, Colorado.

Shirgur, L.A. 1968. Runaway speed reduction methods for hydraulic turbines. M.Tech. Dissertation. Department of Mechanical Engineering. Indian Institute of Technology. Bombay, India.

Sokal, R.R. and F.J. Rohlf. 1969. Biometry. W.H.Freeman and Company. San Franciso, CA.

Steel, R.G.D. and J.H.Torrie. 1980. Principles and proceedures of statistics A biometrical approach. McGraw-Hill Book Company. New York, NY.

Stevens, R.D. 1977. Tradition and dynamics in small farm agriculture. The Iowa State University Press. Ames, Iowa.

Stout, B.A. 1979. Energy for world agriculture. FAO of the United Nations. Rome.

Siwatibau, S. 1981. Rural energy in Fiji: a survey of domestic rural energy use and potential. International Development Research Centre. Ottawa, Ontario.

Speckhart, F.H. and W.L. Green. 1976. A guide to using CSMP-the continuous modeling program. Prentice-Hall Inc. Englewood Cliffs, N.J.

Szekely, F. 1983. Energy alternatives in latin america. Tycooly International Publishing Ltd. Dublin, Ireland.

Tinker, I. 1980. Issues of women, energy and appropriate technologies in developing countries. *In* R.S. Ganapathy (editor), Agriculture, Rural Energy and Development. Proceedings of the 1980 Symposium of the International Association for the Advancement of Appropriate Technology for Developing Countries. University of Michigan, Ann Arbor, Michigan.

Todaro, M.P. 1977. Economic development in the third world. 2nd edition. Longman Inc.. New York, NY.

Toro, J.R. 1980. Investigacion de un governador de velocidad por reflujo para turbinas pelton. Unpublished Thesis. Department of Mechanical Engineering. Universidad de los Andes. Bogata, Colombia.

United Nations. 1983. World statistics in brief, 7th edition. United Nations Publications. New York, N.Y.

Warnick, C.C. 1984. Hydropower engineering. Prentice-Hall Inc.. New York, NY.

Wood's, T.B. 1981. Mechanical power transmission equipment, general catalog. T.B. Wood's Sons Company. Chambersburg, Pennsyvania.

World Bank. 1975. Rural electrification. Washington, DC.

8. APPENDICES

Appendix A.1 Computer Model of Micro Hydroelectric System

A.1 CSMP MODEL TO DETERMINE THEORECTICAL POWER

```
$RUN *CSMPTRAN PAR=Q

*   RUN IDENTIFIER
*      E3J150

INITIAL
       CONSTANT PD=.1016,TD=.13464,B=16,...
                G=9.806,PHI=3.14159,LMDA=165,...
                H=50.0000,...
                O=0.012255,...
                Q=0.0024600,...
                NJ=1,...
                NC=0
              R=4011
*    PARAMETER R=(1700,1900,2100,2300,2500,2700,2900,3100)
*     WHERE
*        PD=PITCH DIAMETER IN METERS
*        TD=TURBINE DIAMETER IN METERS
*        B =NUMBER OF BUCKETS
*        D =WATERJET DIAMETER IN METERS
*        H =HEAD IN METERS
*        G =GRAVITY CONSTANT
*        R =RPM
*        Q =FLOW PER WATERJET IN CUBIC METERS
*        NJ=NUMBER OF JETS OPERATING
*        NC=NUMBER OF JET INTERFERENCE CONTACT POINTS

       THETA=360/B
*         THETA IS THE ANGLE BETWEEN THE BUCKETS

       Y=PHI*THETA/180
*         "Y" IS THIS SAME ANGLE BUT EXPRESSED IN RADIANS
```

```
      D=O*.816
*        D IS THE ORIFICE DIAMETER TIMES THE RESTRICTION FACTOR
*        AS DETERMINED BY EXPERIMENT

      A=((D/2)**2)*PHI
*       "A" IS THE AREA OF THE ORIFICE IN METERS SQUARED

      VJ=(Q/NJ)/A
*       VJ IS THE VELOCITY OF THE WATER JET AT THE ORIFICE
*       IN METERS PER SECOND

      W=2*PHI*R/60
*       "W" OR OMEGA IS THE ANGULAR VELOCITY OF THE TURBINE
*        EXPRESSED IN RADIANS PER SECOND

      XO=PD/2
*       XO IS THE DISTANCE FROM THE CENTER OF THE TURBINE
*       TO THE CENTER OF THE JET EXPRESSED IN METERS
*       THIS ALSO IS THE "MOMENT ARM" USED IN SUBSEQUENT
*       CALCULATIONS.

      FC=XO+D/2
      IC=XO-D/2
*       FC=FINAL CONDITIONS FOR INTEGRATION
*       IC=INITIAL CONDITIONS FOR INTEGRATION

      RO=TD/2
*       RO IS THE RADIUS OF THE TURBINE EXPRESSED IN METERS

      LMDAR=LMDA*PHI/180
*       LMDAR=LMDA EXPRESSED IN RADIANS

* CALCULATE POWER ABSORBED BY WINDAGE AND BEARING FRICTION
      PMW=20.2603*EXP(.00133*R)
      PMO=-31.86+0.06554*R
*       PMW=POWER ABSORBED WITH ALTERNATOR "SYSTEMFRIC"
*         PMO=POWER ABSORBED WITHOUT ALTERNATOR "TURBINFRIC"


DYNAMIC
  NOSORT

       J=(D/2)**2-(TIME-XO)**2
       IF(J.LE.0)J=0
*        HERE I WANT TO INSURE THAT WHEN TIME IS LESS
*        THEN THE DISTANCE FROM THE CENTER TO THE INSIDE
*        EDGE OF THE WATERJET IT WILL SET J TO 0 INSURING
*        THAT THE VOLUME OF WATER PASSING ALSO EQUALS 0

       N=2*SQRT(J)
       K=2*SQRT(RO**2-TIME**2)
       L=2*ARCOS(TIME/RO)-Y
       M=VJ/W
*        THE VARIABLES N,K,L,M ARE USED TO SIMPLIFY SETTING
*        UP THE INTEGRAL EQUATION

       DV=N*(K-M*L)
*        THIS IS THE FORMULA TO BE INTEGRATED CSMP STYLE

       Z=W*TIME
       IF(Z.GE.VJ)DV=N*K
       IF(DV.LE.0)DV=0
*        SINCE I WANT TO ONLY MEASURE THE POSITIVE VOLUME
*        OF WATER PASSING THE TURBINE I SET THE NEG. TO 0

       V=INTGRL(0,DV)
*        "V" IS THE VOLUME OF WATER PASSING THE TURBINE ON
*         A PER BUCKET BASIS

       VOL=(B*V*R)/60
*         VOL IS THE VOLUME OF WATER PASSING THE TURBINE
*        EXPRESSED IN CUBIC METERS


TERMINAL
 TITLE     VOLUME OF WATER PASSING TURBINE
   TIMER  FINTIM=0.086, PRDEL=.001
   METHOD RKS
*    REQUEST FOR THE COMPUTER TO USE THE RUNGE-KUTTA METHOD

   RELERR V=5.0E-11
   ABSERR V=5.0E-11
*    DEFINES THE RELATIVE AND ABSOLUTE ERROR FOR THE INTEGRATOR

   FINISH TIME=FC
   PRINT K,L,M,N,DV,V,VOL

    P=(Q-(VOL*(NJ+NC)))*1000*(VJ-XO*W)*(1-COS(LMDAR))*XO*W
*          ESTIMATES THE POWER PRODUCED BY THE TURBINE (Watts)

    PWM=P-PMW
    POM=P-PMO
*     THE DIFFERENCE ESTIMATES THE AMOUNT OF POWER  AVAILABLE
*     TO THE ALTERNATOR

   101 FORMAT(2E20.4)
       WRITE(6,101) VJ,R,P,VOL
       WRITE(6,101) PMW,PWM,PMO,POM
END
STOP
ENDJOB
$run *fortg scards=-csmp#7
$run *csmpexec+-load#+*csmplib t=3 6=-g
```

A.2 Data Acquisition Computer Programs

A.2.1 CALIBRATION PROGRAM FOR THE VALIDYNE PRESSURE TRANSDUCER

```
10 PRINT "CALIBRATION RUN FOR VALIDYNE-START?"
20 GETCHAR(F$) \ IF F$="" THEN 20
30 IF F$="Y" THEN 50
40 IF F$="N" THEN 640
50 DISPLAYCLEAR
60 REM CREAT FILE TO HOLD DATA
70 REM IDENTIFY FILE BY CURRENT DATE
80 PRINT "TYPE TODAY'S DATE PROCEEDED BY INITAL OF RUN (EG. VM12 =MAY12)"
90 LINPUT U$
100 OPEN U$ FOR OUTPUT AS FILE #1
110 PRINT #1
120 REM CREATE ARRAYS FOR DATA
130 DIM U1(10)
140 DIM V1(10)
150 DIM W1(10)
160 DIM X1(10)
161 DIM Y1(10)
170 REM ZERO ALL VARIABLES
180 T1=0 \ T2=0 \ T3=0 \ T4=0 \ T5=0
190 A1=0 \ A2=0 \ A=0 \ B=0 \ M=0 \ N=0
200 P=0 \ P1=0
201 T6=0 \ T7=0 \ S=0 \ R=0
210 REM START DATA COLLECTION
220 FOR J=1 TO 10
230 PRINT "READY TO READ VOLTAGE, TYPE S TO START"
240 GETCHAR(V$) \ IF V$="" THEN 240
250 IF V$="S" THEN 260
260 REM ZERO P AND P1 AS THEY ARE USED IN AVERAGING LOOP
270 P=0 \ P1=0
280 FOR I=1 TO 50
290 AIN(,P,1,1/50,2,1)
300 REM ACCUMULATE READING TO REDUCE ERROR FROM FLUCTUATION
310 P1=P+P1
```

```
320 NEXT I
330 REM AVERAGE READINGS
340 U1(J)=P1/50
350 PRINT "VOLTAGE="U1(J)
360 PRINT "TYPE IN PRESSURE IN METERS HEAD"
370 INPUT D
371 IF D=99 THEN 640
380 V1(J)=D
390 PRINT "METERS:"V1(J)
400 W1(J)=U1(J)*V1(J)
410 X1(J)=U1(J)*U1(J)
411 Y1(J)=V1(J)*V1(J)
420 PRINT #1,U1(J),V1(J)
430 T1=U1(J)+T1
440 T2=V1(J)+T2
450 T3=W1(J)+T3
460 T4=X1(J)+T4
461 T6=Y1(J)+T6
462 T7=T2*T2
470 NEXT J
480 REM CALCULATIONS FOR LINEAR REGRESSION
490 T5=T1*T1
500 PRINT T1,T2,T3,T4,T5
510 M=(10*T3)-(T1*T2)
520 N=(10*T4)-T5
521 S=(10*T6)-T7
522 R=M/SQR(N*S)
530 B=M/N
540 A1=T1/10 \ A2=T2/10
550 A=A2-(B*A1)
555 PRINT #1,A,B
560 PRINT "THE LINEAR REGRESSION COEFFS.,A AND B, ARE:"A,B
561 PRINT "REGRESSION COEFFICIENT R:"R
570 PRINT "ARE THE RESULTS OF THIS RUN TO BE SAVED? Y OR N"
580 GETCHAR(A$)
590 IF A$="" THEN 580
```

```
600 IF A$="Y" THEN 630
610 IF A$="N" THEN 620
620 GO TO 170
630 CLOSE
640 END
```

A.2.2 CALIBRATION PROGRAM FOR LVDT

```
10 PRINT "CALIBRATION RUN FOR LVDT ON WEIR-START?"
20 GETCHAR(F$) \ IF F$="" THEN 20
30 IF F$="Y" THEN 50
40 IF F$="N" THEN 650
50 DISPLAYCLEAR
60 REM CREAT FILE TO HOLD DATA
70 REM IDENTIFY FILE BY CURRENT DATE
80 PRINT "TYPE TODAY'S DATE PROCEEDED BY INITAL OF RUN (EG. VM12 =MAY12)"
90 LINPUT U$
100 OPEN U$ FOR OUTPUT AS FILE #1
110 PRINT #1
120 REM CREATE ARRAYS FOR DATA
130 DIM U1(10)
140 DIM V1(10)
150 DIM W1(10)
160 DIM X1(10)
161 DIM Y1(10)
170 REM ZERO ALL VARIABLES
180 T1=0 \ T2=0 \ T3=0 \ T4=0 \ T5=0
190 A1=0 \ A2=0 \ A=0 \ B=0 \ M=0 \ N=0
200 L=0 \ L1=0
201 T6=0 \ T7=0 \ P=0 \ R=0
203 Q=0
210 REM START DATA COLLECTION
220 FOR J=1 TO 10
230 PRINT "READY TO READ VOLTAGE, TYPE S TO START"
240 GETCHAR(V$) \ IF V$="" THEN 240
250 IF V$="S" THEN 260
260 REM ZERO READING L AND L1
270 L=0 \ L1=0
280 FOR I=1 TO 50
290 AIN(,L,1,1/50,3,1)
300 REM ACCUMULATE READING TO REDUCE ERROR FROM FLUCTUATION
```

```
310 L1=L1+L
320 NEXT I
330 REM AVERAGE READINGS
340 U1(J)=L1/50
350 PRINT "VOLTAGE="U1(J)
360 PRINT "TYPE IN WATER ELEVATION IN CM."
370 INPUT D
371 IF D=99 THEN 650
380 V1(J)=D
390 PRINT "WATER ELEV.:"V1(J)
400 W1(J)=U1(J)*V1(J)
410 X1(J)=U1(J)*U1(J)
411 Y1(J)=V1(J)*V1(J)
420 PRINT #1,U1(J),V1(J)
430 T1=U1(J)+T1
440 T2=V1(J)+T2
450 T3=W1(J)+T3
460 T4=X1(J)+T4
461 T6=Y1(J)+T6
470 NEXT J
480 REM CALCULATIONS FOR LINEAR REGRESSION
490 T5=T1*T1
491 T7=T2*T2
500 PRINT T1,T2,T3,T4,T5
510 M=(10*T3)-(T1*T2)
520 N=(10*T4)-T5
521 P=(10*T6)-T7
530 B=M/N
531 Q=SQR(N*P)
532 R=M/Q
540 A1=T1/10 \ A2=T2/10
550 A=A2-(B*A1)
560 PRINT "THE LINEAR REGRESSION COEFFS., [illegible] AND B, ARE:"A,B
561 PRINT "REGRESSION COEFFICIENT R="R
570 PRINT #1,A,B
580 PRINT "ARE THE RESULTS OF THIS RUN TO BE SAVED? Y OR N OR E (ESCAPE)"
```

```
590 GETCHAR(A$)
600 IF A$="" THEN 590
610 IF A$="Y" THEN 640
620 IF A$="N" THEN 630
621 IF A$="E" THEN 650
630 GO TO 170
640 CLOSE
650 END
```

A.2.3 CALIBRATION PROGRAM FOR THE HALL EFFECT SENSOR

```
10 PRINT "CALIBRATION RUN FOR HALL EFFECT MONITOR-START?"
20 GETCHAR(F$) \ IF F$="" THEN 20
30 IF F$="Y" THEN 50
40 IF F$="N" THEN 640
50 DISPLAYCLEAR
60 REM CREAT FILE TO HOLD DATA
70 REM IDENTIFY FILE BY CURRENT DATE
80 PRINT "TYPE TODAY'S DATE PROCEEDED BY INITAL OF RUN (EG. VM12 =MAY12)"
90 LINPUT U$
100 OPEN U$ FOR OUTPUT AS FILE #1
110 PRINT #1
120 REM CREATE ARRAYS FOR DATA
130 DIM U1(10)
140 DIM V1(10)
150 DIM W1(10)
160 DIM X1(10)
161 DIM Y1(10)
170 REM ZERO ALL VARIABLES
180 T1=0 \ T2=0 \ T3=0 \ T4=0 \ T5=0
190 A1=0 \ A2=0 \ A=0 \ B=0 \ M=0 \ N=0
200 H=0 \ H1=0
201 T6=0 \ T7=0 \ S=0 \ R=0
210 REM START DATA COLLECTION
220 FOR J=1 TO 10
230 PRINT "READY TO READ VOLTAGE, TYPE S TO START"
240 GETCHAR(V$) \ IF V$="" THEN 240
250 IF V$="S" THEN 260
260 REM ZERO H & H1
270 H=0 \ H1=0
280 FOR I=1 TO 50
290 AIN(,H,1,1/50,1,1)
300 REM ACCUMULATE READING TO REDUCE ERROR FROM FLUCTUATION
310 H1=H1+H
```

```
320 NEXT I
330 REM AVERAGE READINGS
340 U1(J)=H1/50
350 PRINT "VOLTAGE="U1(J)
360 PRINT "TYPE IN SPEED IN RPM"
370 INPUT D
371 IF D=99 THEN 640
380 V1(J)=D
390 PRINT "SPEED:"V1(J)
400 W1(J)=U1(J)*V1(J)
410 X1(J)=U1(J)*U1(J)
411 Y1(J)=V1(J)*V1(J)
420 PRINT #1,U1(J),V1(J)
430 T1=U1(J)+T1
440 T2=V1(J)+T2
450 T3=W1(J)+T3
460 T4=X1(J)+T4
461 T6=Y1(J)+T6
462 T7=T2*T2
470 NEXT J
480 REM CALCULATIONS FOR LINEAR REGRESSION
490 T5=T1*T1
500 PRINT T1,T2,T3,T4,T5
510 M=(10*T3)-(T1*T2)
520 N=(10*T4)-T5
521 S=(10*T6)-T7
522 R=M/SQR(N*S)
530 B=M/N
540 A1=T1/10 \ A2=T2/10
550 A=A2-(B*A1)
555 PRINT #1,A,B
560 PRINT "THE LINEAR REGRESSION COEFFS.,A AND B, ARE:"A,B
561 PRINT "REGRESSION COEFICIENT R:"R
570 PRINT "ARE THE RESULTS OF THIS RUN TO BE SAVED? Y OR N"
580 GETCHAR(A$)
590 IF A$="" THEN 580
```

```
600 IF A$="Y" THEN 630
610 IF A$="N" THEN 620
620 GO TO 170
630 CLOSE
640 END
```

A.2.4 MINC PROGRAM FOR DATA ACQUISITION

```
10 PRINT "START NEW RUN ?"
20 CHAR(F$) \ IF F$="" THEN 20
30 IF F$="Y" THEN 50
40 IF F$="N" THEN 2740
50 CLEAR
60 REM
70 H=0 \ H1=0 \ H2=0 \ H3=0
80 V=0 \ V1=0 \ V2=0 \ V3=0
90 L=0 \ L1=0 \ L2=0 \ L3=0 \ L4=0
100 C=0 \ C1=0 \ C2=0
110 H5=0 \ H6=0
120 F5=0 \ F6=0
130 Q3=0 \ V5=0 \ V6=0 \ V7=0
135 J5=0 \ J1=0
140 REM
150 REM GEN HAL VARIABLES
160 A1=-57.2262
170 B1=1039.1
180 REM PRESSURE VARIABLES
190 A2=-1.3546
200 B2=13.8497
210 REM LDT VS VARIABLES
220 A3=23.3963
230 B3=-3.5584
240 REM WINDAGE AND FRICTION CONSTANTS
250 A4=35.9856
260 B4=1.11000E-03
270 REM GRAVITY (M/S^2)
280 G=9.806
290 REM PITCH RADIUS IN METERS
300 P4=.0508
310 REM GENERATOR RESISTANCE IN OHMS
320 R=.5
```

```
330 REM INTERNAL AREA OF 1 1/2 IN. PIPE
340 P=13.134
350 REM
360 FOR Z=1 TO 100
370 AIN(,H,,1/50,1)
380 AIN(,V,,1/50,2)
390 AIN(,L,,1/50,3)
400 H1=H1+H
410 V1=V1+V
420 L1=L1+L
430 NEXT Z
440 H2=H1/100
450 V2=V1/100
460 L2=L1/100
470 REM TURBINE RPM
480 PRINT "RPM VOLTAGE=";H2
490 H3=A1+B1*H2
500 PRINT "TURBINE RPM=";H3
510 REM  HEAD(M)
520 PRINT "PRESSURE VOLTAGE=";V2
530 V3=A2+B2*V2
540 PRINT "HEAD (M)=";V3
550 REM  FLOW
560 PRINT "WEIR VOLTAGE=";L2
570 L3=A3+B3*L2
580 L4=.0138*L3^2.5
590 PRINT "FLOW OVER WEIR (L/S)=";L4
600 REM USE BERNOULLI'S EQUATION TO FIND TOTAL HEAD(M)
610 PRINT "ENTER NUMBER OF JETS"
620 INPUT K
630 Q3=L4/K
640 V5=10*Q3/P
650 V6=(V5^2)/(G*2)
660 REM TOTAL HEAD(M)
670 V7=V6+V3
680 PRINT "TOTAL HEAD (M)=";V7
```

```
690 PRINT "TYPE: C TO CONTINUE W/ RUN OR A TO ADJUST OR E TO END"
700 CHAR(V$)
710 IF V$="" THEN 700
720 IF V$="C" THEN 750
730 IF V$="A" THEN 60
740 IF V$="E" THEN 2870
750 REM CONSTRUCT OUTPUT IDENTIFIER
760 REM   THIS SYSTEM HELPS ME IDENTIFY THE DIFFERENT RUNS
770 REM   AND NOT CONFUSE THEM
780 REM INPUT ORIFICE SIZE AND NUMBER OF JETS
790 REM
800 PRINT "ORIFICE SIZE IN MM"
810 INPUT O
820 PRINT "NUMBER OF JETS STRIKING PELTON"
830 INPUT N
840 REM
850 REM THE IDENTIFIER IS IN THE FORM J#O#H#
860 REM
870 PRINT "ENTER IDENTIFIER FOR THIS RUN IN THE FOLLOWING FORM"
880 PRINT "TURBINE(E,C),ORIFICE SERIES(1,2,3,4,5),J,#OF JETS,HEAD(M)"
890 LINPUT U$
900 OPEN U$ FOR OUTPUT AS FILE #1
910 PRINT #1
920 REM
930 REM CREATE ARRAYS TO HOLD DATA OUTPUT
940 REM
950 DIM R2(11)
960 DIM P1(11)
970 DIM P2(11)
980 DIM H3(11)
990 DIM E2(11)
1000 DIM H2(11)
1010 DIM V2(11)
1020 DIM L2(11)
1030 DIM P(11)
1040 DIM Q(11)
```

```
1050 DIM E(11)
1060 DIM S(11)
1070 DIM P3(11)
1080 REM   FOR A GIVEN HEAD THE LOAD WILL VARY 11 TIMES
1090 REM
1100 FOR I=1 TO 11
1110 REM
1120 REM READ GEN. RPM TO HELP SPACE DATA
1130 PRINT "ADJUST LOAD-HIT ANY KEY WHEN READY"
1140 PRINT "HIT 'H' FOR PRESSURE HEAD CHECK"
1150 CHAR(Y$) \ IF Y$="" THEN 1150
1160 IF Y$="H" THEN 2750
1170 H1=0
1180 FOR Q=1 TO 100
1190 AIN(,H,,1/50,1)
1200 H1=H1+H
1210 NEXT Q
1220 H2=H1/100
1230 PRINT "RPM VOLTAGE=";H2
1240 REM
1250 H3=A1+B1*H2
1260 PRINT "RPM=";H3
1270 REM
1280 REM IF RPM IS OK CONTINUE
1290 REM
1295 PRINT "DATA POINT";I
1300 PRINT "HIT Y TO START OR N TO ADJUST LOAD OR E TO END RUN"
1310 CHAR(Z$) \ IF Z$="" THEN 1310
1320 IF Z$="N" THEN 1170
1330 IF Z$="E" THEN 2870
1340 REM
1350 REM ZERO ALL VARIABLES EXCEPT N AND O
1360 H=0 \ H1=0 \ H2=0 \ H3=0
1370 V=0 \ V1=0 \ V2=0 \ V3=0
1380 L=0 \ L1=0 \ L2=0 \ L3=0 \ L4=0
1390 V5=0
```

```
1400 J1=0
1410 D2=0 \ K1=0
1420 K2=0 \ K3=0
1430 X=0 \ B=0
1440 REM
1450 REM START LOOP TO COLLECT DATA
1460 REM
1470 FOR J=1 TO 100
1480 REM
1490 REM VARIABLE COLLECTION SEQUENCE;LOAD CELL,HAL EFFECT,
1500 REM VALIDYNE,LDT.READ FROM EACH ONCE EVERY SECOND
1510 REM
1520 AIN(,H,,1/50,1)
1530 AIN(,V,,1/50,2)
1540 AIN(,L,,1/50,3)
1550 REM
1560 REM ACCUMULATE READINGS TO REDUCE FLUCTUATION ERROR
1570 REM
1580 H1=H1+H
1590 V1=V1+V
1600 L1=L1+L
1610 NEXT J
1620 REM AVERAGE INSTRUMENT VOLTAGE
1630 REM
1640 H2=H1/100
1650 V2=V1/100
1660 L2=L1/100
1670 H2(I)=H2
1680 V2(I)=V2
1690 L2(I)=L2
1700 REM
1710 REM TRANSLATE VOLTAGES TO USEFUL DATA
1720 REM TURBINE RPM
1730 H3=A1+B1*H2
1740 H3(I)=H3
1750 REM ANGULAR VELOCITY OF TURBINE
```

```
1760 W=PI*H3/30
1770 REM ACTUAL POWER PRODUCED
1780 PRINT "INPUT POWER PRODUCED IN WATTS"
1790 INPUT X
1800 P1(I)=X
1810 PRINT "INPUT VOLTAGE"
1820 INPUT B
1830 REM PRESSURE HEAD (M)
1840 V3=A2+B2*V2
1850 REM    L4 IS FLOW OVER WEIR IN L/S
1860 L3=A3+B3*L2
1870 L4=.0138*L3^2.5
1880 REM
1890 REM CALCULATE VELOCITY OF WATER JET
1900 REM DETERMINE ACTUAL WATERJET DIA.(MM)
1910 D2=O*.816
1920 REM   A=AREA OF THE ORIFICE IN CM^2
1930 A=(PI*(D2^2))/400
1940 F2=L4/N
1950 REM TOTAL HEAD FROM BERNOULLI'S EQUATION
1960 REM VELOCITY HEAD (V5)
1970 V5=((10*F2/P)^2)/(2*G)
1980 REM TOTAL HEAD H1
1990 V8=V5+V3
2000 REM J2=VELOCITY OF WATER M/S
2010 J1=F2*10/A
2020 REM
2030 REM CALCULATE VELOCITY OF BUCKETS
2040 REM
2050 B6=P4*W
2060 REM
2070 REM CALCULATE RELATIVE VELOCITY
2080 REM
2090 R2(I)=J1-B6
2110 REM  1.939=(1-COS(160))WHERE160ISTHEANGLEOFWATERRETURN
2120 P2(I)=L4*R2(I)*W*P4*1.939
```

```
2130 REM VALUES FOR HILL CURVES
2140 REM TO COMPARE TURBINES USE UNIVERSAL UNIT VALUES
2150 REM UNIVERSAL UNIT SPEED
2160 S(I)=W*2*P4/SQR(V8)
2170 REM UNIVERSAL UNIT DISCHARGE
2180 Q(I)=L4/(((2*P4)^2)*SQR(V8))
2190 REM UNIVERSAL UNIT POWER
2200 P(I)=P1(I)/(((2*P4)^2)*V8^1.5)
2210 REM THEORETICAL POWER "QH"
2220 P3=L4*V8*G
2240 E(I)=100*X/P3
2250 REM CALCULATE LOSSES
2260 REM LOSSES DUE TO BEARING AND WINDAGE FRICTION
2270 K1=A4*EXP(B4*H3)
2280 REM INTENAL GENERATOR LOSSES(WINDINGS)
2290 K2=((X/B)^2)*R
2300 REM ACTUAL POWER FROM TURBINE
2310 P3(I)=P1(I)+K1+K2
2320 REM EFFICIENCY OF THE TURBINE
2330 E2(I)=(P3(I)/P3)*100
2340 REM
2350 REM CALCULATE ORIFICE CONSTANT
2360 C1=F2*10/((((O/200)^2)*PI)*SQR(2*G*V8))
2370 C2=C1+C2
2380 H5=V8+H5
2390 F5=L4+F5
2400 J5=J1+J5
2410 REM S=UUSPEED, P=UUPOWER, Q=UUDISCHARGE, E=ACT.EFF.,E2=NO FRIC EFF.
2420 REM P1=ACT.POWER, P2=PREDIC.POWER, P3= NO FRIC. POWER, H3=RPM
2430 REM INSTRUMENT VOLTAGES H2=RPM,V2=PRESS.,L2=WEIR, J1=JET VEL.
2440 REM
2450 REM STORE DATA INTO ARRAYS
2460 PRINT #1
2470 PRINT #1,S(I),P(I),Q(I),E(I),E2(I)
2480 PRINT #1,P1(I),P2(I),P3(I),R2(I),H3(I)
2490 PRINT #1,H2(I),V2(I),L2(I)
```

```
2500 NEXT I
2510 C=C2/11 \ H6=H5/11 \ F6=F5/11
2520 J6=J5/11
2530 REM C=ORIFICE COEFF. H6=TOTAL HEAD F6=TOTAL FLOW(L/S)J6=JETVEL.
2540 PRINT #1,C,H6,F6,J6,P3
2550 PRINT #1,U$
2560 REM
2570 REM A GRAPH OF RPM VS. POWER WILL INDICATE BEST SPEED OF OPERATION
2580 REM
2590 CLEAR
2600 MODE("LONG")
2610 GRAPH("LINES,POINTS,SHADE",,S(0),E(0))
2620 LABEL("BOLD","UNIVERSAL UNIT SPEED","% EFFICIENCY")
2630 POINT(X1,Y1)
2640 PRINT X1,Y1
2650 PRINT "ARE THE RESULTS TO BE SAVED?"
2660 CHAR(H$) \ IF H$="" THEN 2660
2670 IF H$="Y" THEN 2700
2680 IF H$="N" THEN 1100
2690 GO TO 10
2700 CLOSE #1
2710 PRINT "START ANOTHER RUN?"
2720 CHAR(T$) \ IF T$="" THEN 2720
2730 IF T$="Y" THEN 50
2740 IF T$="N" THEN 2870
2750 V=0 \ V1=0
2760 FOR K=1 TO 50
2770 AIN(,V,,1/50,2)
2780 V1=V1+V
2790 NEXT K
2800 V2=V1/50
2810 V3=A2+B2*V2
2820 PRINT "PRESSURE HEAD (M)=";V3
2830 PRINT "TYPE A TO READJUST OR C TO CONTINUE WITH RUN"
2840 CHAR(R$) \ IF R$="" THEN 2840
2850 IF R$="A" THEN 2750
```

```
2860 IF R$="C" THEN 1170
2870 CLEAR
2880 END
```

A.3 Circuit For Hall Effect Sensor

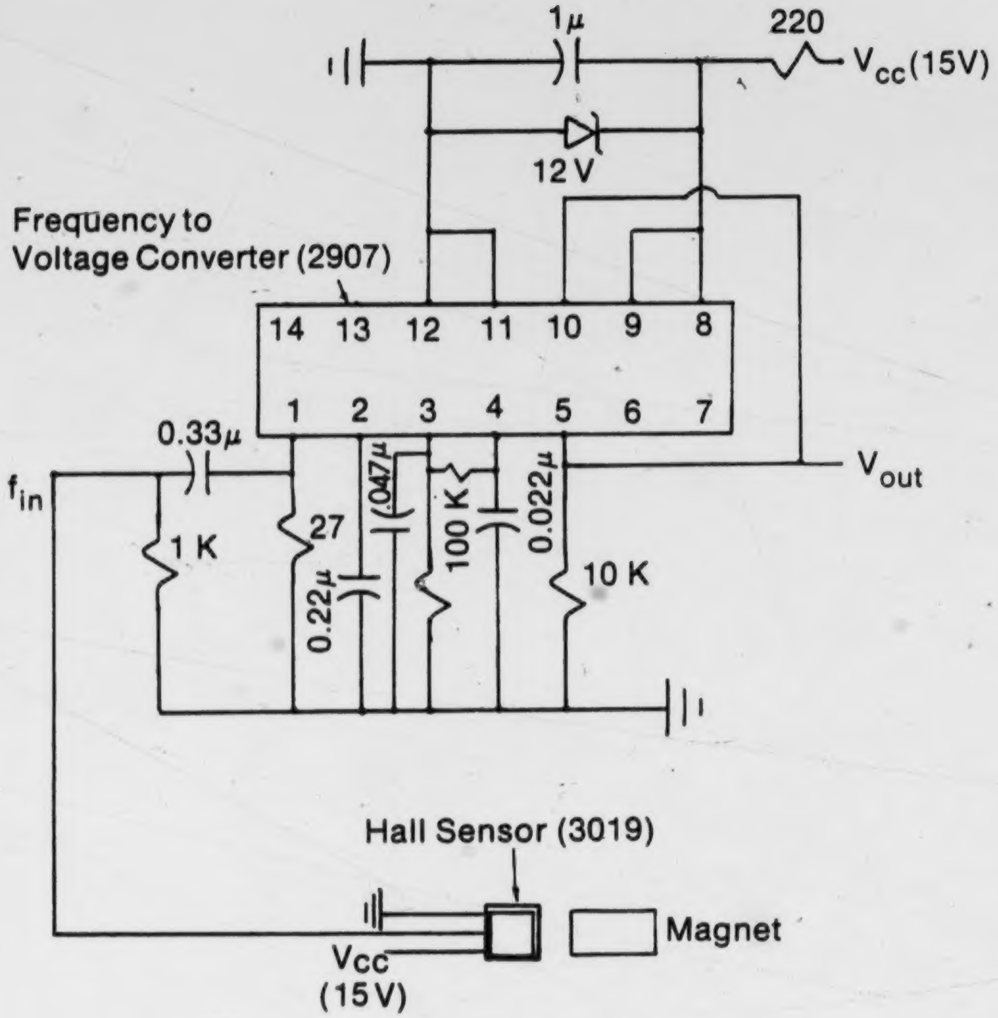
1μ
220
V_{cc}(15V)
12 V
Frequency to Voltage Converter (2907)
14 13 12 11 10 9 8
1 2 3 4 5 6 7
0.33μ
f_{in}
V_{out}
1 K
27
.047μ
100 K
0.022μ
0.22μ
10 K
Hall Sensor (3019)
Magnet
Vcc (15 V)

A.4 Data Summary Tables

Together, the ten data summary tables contain all the data collected from the three instruments as well as the runaway speeds predicted by the CSMP model. For each table, the title reflects the turbine and orifice series used for all the runs represented on the table. The columns are laid out in the following order: The jet configuration numbers (Column 1) correspond to the configurations presented in Figure 3.2 where 1 to 5 match Figures a to e respectively. The second column records the total flow rate in ℓ/s as determined by the weir. Two patterns are seen in the flow rate data. When compared amongst tables, flow rates increase by approximately one liter per second for each series number. The average flow rate for series 1 nozzle was 3.44 ℓ/s and increased to 8.07 ℓ/s for the series 5 nozzles, an increase of 23 percent per series.

Within each table and within each configuration set, the flow rate increases as hydraulic head increases. As mentioned in section 3.3, jet configuration comparisons are valid when power inputs to the turbine are the same for different jet configurations under the same hydraulic head. The differences in flow rate The percent differences in flow rate from the two-jet-no-interference configuration (jet configuration 2) from the other jet configurations are recorded in column 3. All flow rates at the same head were compared to their counterpart in jet configuration 2. The following example calculation shows how the numbers were calculated for column 3. The flow rate for the three-jet configuration (jet configuration 4) at 40 meters head differs from the flow rate for the two-jet-no-interference configuration at 40 meters head (Table A.4.1) by 0.63 percent calculated using the data in column 2 as follows ((3.21-3.19)/3.19)(100)=0.63%. Within a series and hydraulic head, the flow rate may vary by as much as 11 percent. This makes the comparison of runaway speeds difficult.

Column 4 lists the average hydraulic head obtained throughout the run. Hydraulic heads need to be constant for accurate determination of the effect of jet configuration on runaway speed. Column 5 compares the variance amongst similar heads using the same procedure outlined for flow rate. Since the experiment offered more control over head than flow rate, variances amongst head values were seldom greater than 0.50 percent. The theoretical runaway speeds (columns 6 and 7) were calculated using the CSMP model at exactly the same hydraulic head and flow rates determined in the experiment. This allowed the comparison of runaway speeds, which indicated how well the CSMP model predicted runaway speed.

Several generalities can be made about the runaway speeds presented in Tables A.4.1 - A.4.10:

1) Runaway speed increases as hydraulic head increases.

2) Runaway speed for the low friction system is always higher than for the high friction system.
3) The two jet no interference configuration generates the fastest runaway speeds.
4) A reduction in runaway speeds occurs with the introduction of jet interference.
5) The four jet configuration does reduce the runaway speed the most.

Further discussion and more precise conclusions regarding the generalities mentioned here are found in section 5.2.

TABLE A.4.1 SUMMARY DATA FOR MANUFACTURED TURBINE AND SERIES 1 ORIFICES

					Theoretical runaway speed		Actual runaway speed	
Jet Configuration	Flow Rate ℓ/s	% Diff.	Total Head m	% Diff.	High fric. System rpm	Low fric. System rpm	High fric. System rpm	Low fric. System rpm
1	2.80	1.82	30.57	1.75	2385	2929	2815	3247
1	3.02	0.73	34.91	-0.39	2597	3200	2900	3491
1	3.24	1.57	39.91	-0.17	2773	3466	3077	3763
1	3.41	-0.47	44.76	-0.28	2908	3664	3262	3970
1	3.59	-0.13	50.06	-0.19	3024	3883	3418	4208
2	2.75	0.00	30.04	0.00	2470	3053	2632	3150
2	3.00	0.00	35.04	0.00	2700	3376	2847	3410
2	3.19	0.00	39.98	0.00	2853	3625	3035	3653
2	3.43	0.00	44.[illegible]8	0.00	3045	3925	3220	3875
2	3.63	0.00	50.16	0.00	3179	4168	3364	4077
3	2.74	-0.25	30.05	0.02	2452	2865	2494	2972
3	2.96	-1.34	34.96	-0.23	2625	3130	2715	3256
3	3.15	-1.10	39.98	0.00	2808	3351	2900	3470
3	3.35	-2.22	45.01	0.28	2971	3581	3050	3720
3	3.52	-3.11	50.10	-0.11	3099	3830	3216	3880
4	2.76	0.58	30.07	0.08	2430	2795	2475	2914
4	2.99	-0.23	34.69	-1.00	2625	3053	2660	3174
4	3.21	0.63	39.86	-0.29	2821	3300	2863	3404
4	3.41	-0.53	44.86	-0.07	2974	3500	3026	3634
4	3.60	-0.83	49.90	-0.50	3115	3715	3185	3833
5	2.89	5.24	30.38	1.13	2519	2844	2443	2870
5	3.11	3.77	34.80	-0.72	2710	3070	2620	3140
5	3.36	5.24	39.60	-0.95	2911	3332	2818	3340
5	3.57	4.20	44.84	-0.10	3077	3558	2995	3570
5	3.73	2.75	49.76	-0.80	3204	3727	3150	3768

TABLE A.4.2 SUMMARY DATA FOR MANUFACTURED TURBINE AND SERIES 2 ORIFICES

					Theoretical runaway speed		Actual runaway speed	
Jet Configuration	Flow Rate ℓ/s	% Diff.	Total Head m	% Diff.	High fric. System rpm	Low fric. System rpm	High fric. System rpm	Low fric. System rpm
1	3.75	9.14	29.96	0.22	2681	3247	2747	3262
1	4.03	9.59	34.83	-0.13	2865	3529	2970	3517
1	4.33	14.03	40.07	0.79	3042	3798	3170	3785
1	4.73	16.00	45.03	-0.01	3268	4180	3370	----
1	4.95	6.77	49.71	-0.70	3395	4370	3530	4209
1	3.44	-8.4	29.90	0.00	2498	3000	2693	3210
2	3.68	0.00	34.87	0.00	2667	3243	2920	3445
2	3.79	0.00	39.76	0.00	2752	3360	3110	3740
2	4.08	0.00	45.07	0.00	2950	3643	3315	3975
2	4.64	0.00	50.06	0.00	3268	4176	3515	4215
3	3.46	0.64	30.02	0.41	2484	2830	2572	3094
3	3.72	1.09	34.92	0.13	2675	3070	2800	3368
3	3.99	5.22	39.88	0.32	2851	3325	2972	3571
3	4.24	3.90	44.98	-0.20	3014	3544	3134	3800
3	4.63	-0.17	49.96	-0.20	3240	3876	3375	4083
4	3.53	0.27	29.96	0.20	2490	2809	2450	2980
4	3.81	3.48	34.91	0.09	2696	3049	2656	3260
4	4.08	7.49	39.86	0.26	2880	3275	2840	3482
4	4.35	6.64	45.04	0.07	3042	3523	3015	3725
4	4.68	0.97	50.15	0.19	3236	3798	3287	3984
5	3.62	5.21	29.93	0.13	2540	2809	2450	----
5	3.90	5.92	34.97	0.27	2742	3050	2670	3160
5	4.17	9.91	39.84	2.87	2929	3268	2850	3380
5	4.44	8.67	44.91	-0.34	3100	3494	3010	3600
5	4.83	4.16	49.85	-0.42	3325	3820	3055	----

TABLE A.4.3 SUMMARY DATA FOR HANDCAST TURBINE AND SERIES 3 ORIFICES

Jet Configuration	Flow Rate ℓ/s	% Diff.	Total Head m	% Diff.	Theoretical runaway speed High Fric. System rpm	Theoretical runaway speed Low Fric. System rpm	Actual runaway speed High Fric. System rpm	Actual runaway speed Low Fric. System rpm
1	4.91	-11.50	30.22	-0.63	2898	3482	2860	3295
1	5.29	-11.40	35.08	-0.06	3087	3783	3085	3570
1	5.66	-11.00	39.80	0.87	3241	3989	3260	3820
1	5.92	-9.80	45.11	-0.16	3396	4247	3450	4012
1	6.21	-8.60	50.06	0.12	3590	4500	3615	4250
2	4.41	0.00	30.03	0.00	2730	3271	2800	3300
2	4.75	0.00	35.06	0.00	2923	3460	3022	3507
2	5.10	0.00	40.15	0.00	3108	3817	3214	3750
2	5.39	0.00	45.04	0.00	3259	4041	3413	3970
2	5.72	0.00	50.12	0.00	3413	4316	3600	4220
3	4.46	-1.10	29.94	0.30	2717	3065	2634	3138
3	4.82	-1.50	35.07	0.03	2915	3336	2843	3384
3	5.12	-0.40	40.00	0.37	3087	3559	3050	3632
3	5.46	-1.30	45.02	0.04	3250	3800	3214	3873
3	5.75	-0.50	49.93	0.38	3400	4015	3426	4087
4	4.50	-2.00	30.10	-0.23	2803	3180	2540	3100
4	4.81	-1.30	34.93	0.37	2992	3405	2745	3330
4	5.13	-0.60	39.86	0.72	3173	3645	2934	3585
4	5.46	-1.30	45.01	0.31	3344	3886	3097	3800
4	5.49	4.00	49.95	0.34	3362	3903	3340	4054
5	4.88	-10.70	30.07	-0.13	2855	3143	2484	2945
5	5.27	-10.50	35.06	0.00	3066	3403	2680	3180
5	5.57	-9.20	40.04	0.27	3206	3600	2863	3424
5	5.82	-8.00	45.09	-0.11	3344	3770	3040	3650
5	6.02	-5.20	50.06	0.12	3439	3900	3180	3800

TABLE A.4.4 SUMMARY DATA FOR MANUFACTURED TURBINE AND SERIES 4 ORIFICES

Jet Configuration	Flow Rate ℓ/s	% Diff.	Total Head m	% Diff.	Theoretical runaway speed		Actual runaway speed	
					High fric. System rpm	Low fric. System rpm	High fric. System rpm	Low fric. System rpm
1	6.00	4.36	30.04	0.44	2942	3471	2905	3232
1	6.48	4.6	35.07	0.12	3146	3777	3135	3530
1	6.91	4.15	40.11	0.24	3315	4032	3330	----
1	7.31	3.54	45.34	0.58	3474	4268	3550	4000
1	7.54	3.12	48.48	-2.60	3566	4420	3633	----
2	5.75	0.00	29.90	0.00	2891	3394	2920	3313
2	6.20	0.00	35.02	0.00	3082	3668	3165	3580
2	6.63	0.00	40.02	0.00	3267	3968	3357	3825
2	7.06	0.00	45.08	0.00	3439	4220	3555	4040
2	7.31	0.00	49.78	0.00	3547	4388	3710	----
3	5.70	-0.85	30.02	0.37	2808	3120	2717	3167
3	6.19	-0.05	34.94	0.23	3031	3414	2931	3428
3	6.59	-0.68	40.04	0.04	3197	3643	3120	3657
3	6.99	-0.91	45.01	-0.15	3369	3872	3295	3877
3	7.33	0.30	49.96	0.36	3512	4067	3444	----
4	5.51	-4.12	30.06	0.53	2745	3018	2526	3060
4	5.95	-3.95	34.93	0.26	2955	3273	2750	3306
4	6.37	-3.99	40.07	0.14	3140	3516	2940	3572
4	6.75	-4.39	45.07	0.01	3305	3726	3110	3753
4	7.13	-2.52	50.02	0.49	3465	3942	3265	4125
5	5.64	-1.98	30.04	0.44	2732	2955	2450	2994
5	6.09	-1.77	34.98	-0.13	2942	3197	2650	3228
5	6.52	-1.70	40.08	0.16	3133	3438	2800	3468
5	6.85	-2.95	45.03	-0.10	3270	3614	2995	3656
5	7.20	-1.55	29.81	0.07	3417	3808	3135	----

TABLE A.4.5 SUMMARY DATA FOR MANUFACTURED TURBINE AND SERIES 5 ORIFICES

Jet Configuration	Flow Rate ℓ/s	% Diff.	Total Head m	% Diff.	Theoretical runaway speed High fric. System rpm	Theoretical runaway speed Low fric. System rpm	Actual runaway speed High fric. System rpm	Actual runaway speed Low fric. System rpm
1	7.48	7.79	30.17	0.19	3107	3643	2952	3270
1	8.05	7.61	35.06	-0.11	3299	3930	3180	3497
1	8.64	8.16	40.19	0.19	3502	4235	3380	----
1	9.06	7.22	44.22	-1.56	3636	4452	3525	----
1	0.00	0.00	00.00	0.00	----	----	----	----
2	6.94	0.00	30.11	0.00	2955	3439	2985	3323
2	7.48	0.00	35.09	0.00	3152	3713	3215	3580
2	7.99	0.00	40.12	0.00	3330	4134	3430	3763
2	8.45	0.00	44.92	0.00	3496	4223	3615	----
2	8.82	0.00	29.05	0.00	3620	4417	3740	4205
3	6.96	0.29	30.09	0.07	2890	3190	2800	3205
3	7.50	0.29	34.94	0.45	3090	3445	3010	3446
3	8.01	0.27	40.00	-0.30	3273	3688	3200	3650
3	8.50	0.63	44.73	-0.43	3450	3926	3370	----
3	8.90	0.94	49.43	0.77	3592	4108	3528	4125
4	6.73	-2.58	30.10	0.04	2750	2980	2700	3153
4	7.29	-2.53	34.90	0.56	2955	3225	2915	3420
4	7.84	-1.88	40.20	0.21	3146	3477	3132	3660
4	8.28	-1.95	44.96	0.09	3310	3680	3295	----
4	8.68	-1.57	49.80	1.54	3452	3847	3455	4110
5	6.76	-2.69	30.09	0.06	2799	2996	2425	2980
5	7.29	-2.57	35.05	0.13	3006	3248	2622	3235
5	7.76	-2.90	40.00	0.30	3178	3458	2800	3454
5	8.23	-2.51	45.13	0.48	3353	3675	2965	----
5	8.62	-2.21	49.81	1.55	3496	3853	3120	3965

TABLE A.4.6 SUMMARY DATA FOR HANDCAST TURBINE AND SERIES 1 ORIFICES

					Theoretical runaway speed		Actual runaway speed	
Jet Configuration	Flow Rate ℓ/s	% Diff.	Total Head m	% Diff.	High fric. System rpm	Low fric. System rpm	High fric. System rpm	Low Fric. System rpm
1	3.33	2.30	29.89	-0.56	2861	3731	2650	3221
1	3.56	2.71	35.03	0.08	3029	4006	2870	3590
1	3.74	1.99	39.95	-0.07	3143	4194	3030	3830
1	3.93	2.16	44.94	-0.28	3269	4441	3250	4093
1	4.12	2.56	49.92	-0.48	3390	4641	3390	4330
2	3.26	0.00	30.06	0.00	2931	3841	2630	3245
2	3.47	0.00	35.00	0.00	3080	4100	2840	3505
2	3.67	0.00	39.98	0.00	3222	4343	3015	3770
2	3.85	0.00	45.06	0.00	3331	4555	3225	4033
2	4.02	0.00	50.17	0.00	3441	4759	3362	4250
3	3.22	-1.20	29.88	-0.58	2887	3568	2465	3032
3	3.45	-0.61	34.93	-0.19	3057	3832	2690	3275
3	3.64	-0.65	40.00	0.06	3193	4061	2970	3500
3	3.82	-0.83	45.07	0.02	3304	4249	3026	3750
3	4.01	-0.30	50.00	0.33	3423	4478	3200	3965
4	3.21	-1.41	29.98	-0.25	2837	3465	2375	2980
4	3.43	-1.18	35.08	0.24	3025	3692	2585	3250
4	3.65	-0.54	40.10	0.31	3182	3943	2775	3495
4	3.79	-1.53	45.05	0.03	3269	4108	2984	3725
4	3.98	-1.00	50.16	0.01	3394	4320	3084	3900
5	3.33	2.27	30.02	-0.11	2932	3453	2435	2857
5	3.55	2.48	35.02	0.07	3087	3692	2626	3115
5	3.76	2.51	40.05	0.19	3220	3924	2830	3350
5	3.96	2.86	45.03	-0.07	3350	4125	3000	3560
5	4.16	3.36	50.16	0.01	3474	4346	3159	3777

TABLE A.4.7 SUMMARY DATA FOR HANDCAST TURBINE AND SERIES 2 ORIFICES

					Theoretical runaway speed		Actual runaway speed	
Jet Configuration	Flow Rate ℓ/s	% Diff.	Total Head m	% Diff.	High fric. System rpm	Low fric. System rpm	High fric. System rpm	Low fric. System rpm
1	3.92	6.52	30.01	-0.68	2819	3552	2760	3309
1	4.17	4.25	35.01	0.08	2985	3802	2961	3593
1	4.46	4.94	39.96	-0.25	3148	4060	3153	3855
1	4.83	5.92	45.09	-0.09	3350	4431	3303	4074
1	4.96	4.20	49.96	0.10	3423	4534	3465	4320
2	3.68	0.00	30.22	0.00	2717	3371	2782	3320
2	4.00	0.00	34.98	0.00	2933	3690	2916	3545
2	4.25	0.00	40.06	0.00	3087	3948	3115	3800
2	4.56	0.00	45.13	0.00	3260	4241	3286	4045
2	4.76	0.00	49.91	0.00	3372	4448	3434	4240
3	3.72	1.09	30.13	-0.30	2717	3212	2455	3025
3	3.99	-0.25	35.08	0.03	2872	3458	2660	3260
3	4.26	0.24	40.11	0.12	3010	3699	2850	3500
3	4.47	-1.97	44.97	-0.35	3113	3888	2990	3700
3	4.68	-1.68	49.45	-0.92	3217	4086	3165	3950
4	3.78	2.72	30.21	-0.03	2717	3156	2500	3160
4	4.00	0.00	35.00	0.06	2846	3363	2703	3436
4	4.32	1.65	40.00	-0.15	3010	3643	2883	3662
4	4.56	0.00	45.16	0.22	3173	3858	3040	3905
4	4.74	0.42	49.17	-1.48	3217	4017	3175	4076
5	3.82	3.80	30.06	-0.53	2756	3115	2390	2885
5	4.08	2.00	35.06	0.23	2932	3340	2585	3130
5	4.35	2.35	40.14	0.20	3094	3580	2775	3350
5	4.57	0.22	44.92	-0.46	3228	3770	2930	3555
5	4.77	0.21	49.68	-0.46	3347	3945	3069	3745

TABLE A.4.8 SUMMARY DATA FOR HANDCAST TURBINE AND SERIES 3 ORIFICES

Jet Configuration	Flow Rate ℓ/s	% Diff.	Total Head m	% Diff.	Theoretical runaway speed High fric. System rpm	Theoretical runaway speed Low fric. System rpm	Actual runaway speed High fric. System rpm	Actual runaway speed Low fric. System rpm
1	4.90	-9.38	30.09	-0.43	2933	3617	2867	3383
1	5.27	-8.44	35.08	0.20	3122	3897	3068	3667
1	5.62	-8.70	40.09	0.12	3290	4190	3286	3924
1	5.94	-8.79	44.92	0.58	3436	4431	3448	4180
1	6.25	-9.84	50.02	-0.60	3583	4680	3627	4405
2	4.48	0.00	29.96	0.00	2827	3436	2856	3360
2	4.86	0.00	35.15	0.00	3022	3763	3063	3660
2	5.17	0.00	40.14	0.00	3190	4013	3276	3930
2	5.46	0.00	45.18	0.00	3338	4247	3470	4175
2	5.69	0.00	49.72	0.00	3463	4434	3615	4363
3	4.39	2.01	29.85	0.37	2726	3163	2586	3150
3	4.77	1.85	35.06	0.26	2953	3446	2800	3460
3	5.06	2.13	40.03	0.27	3103	3665	2983	3681
3	5.36	1.83	45.05	0.29	3258	3884	3167	3955
3	5.68	0.18	49.91	-0.38	3442	4132	3295	4143
4	4.33	3.35	29.95	0.03	2781	3178	2580	3183
4	4.69	3.50	35.05	0.28	2987	3459	2787	3465
4	5.01	3.09	40.00	0.35	3155	3700	2980	3715
4	5.30	2.93	45.02	0.35	3311	3919	3130	3960
4	5.56	2.28	49.60	0.24	3440	4122	3288	4180
5	4.70	-4.91	30.03	-0.23	2827	3150	2384	2926
5	5.08	-4.53	35.05	0.28	3034	3410	2653	3200
5	5.42	-4.84	40.15	0.03	3214	3664	2845	3413
5	5.70	-4.40	44.94	0.53	3354	3857	3000	3630
5	6.02	-5.80	50.01	0.58	3516	4075	3169	3850

TABLE A.4.9 SUMMARY DATA FOR HANDCAST TURBINE AND SERIES 4 ORIFICES

Jet Configuration	Flow Rate ℓ/s	% Diff.	Total Head m	% Diff.	Theoretical runaway speed: High fric. System rpm	Theoretical runaway speed: Low fric. System rpm	Actual runaway speed: High fric. System rpm	Actual runaway speed: Low fric. System rpm
1	6.28	-10.17	30.01	0.46	3108	3790	2940	3019
1	6.77	-11.53	34.93	0.17	3305	4090	3155	----
1	7.17	-11.16	39.87	0.02	3464	4361	3330	----
1	7.57	-10.35	44.98	0.16	3618	4614	3518	----
1	7.79	-8.80	48.46	3.02	3687	4743	3650	3930
2	5.07	0.00	30.15	0.00	2932	3490	2990	----
2	6.07	0.00	34.99	0.00	3086	3756	3240	----
2	6.45	0.00	39.88	0.00	3241	4000	3440	----
2	6.86	0.00	45.05	0.00	3412	4260	3630	----
2	7.16	0.00	49.97	0.00	3537	4451	3790	4295
3	5.69	0.18	30.14	0.03	2872	3249	2680	3320
3	6.15	-1.32	35.09	-0.29	3078	3545	2895	----
3	6.62	-2.64	40.38	-1.25	3275	3816	3080	----
3	7.01	-2.19	45.01	0.09	3438	4048	3263	----
3	7.36	-2.79	49.77	0.40	3584	4262	3400	4268
4	5.56	2.46	29.92	0.76	2846	3180	2500	3460
4	6.02	0.82	34.92	0.20	3060	3464	2715	----
4	6.41	0.62	40.00	-0.28	3232	3696	2900	----
4	6.77	1.31	44.97	0.18	3378	3915	3045	4240
4	7.13	0.42	50.14	-0.34	3541	4116	3230	----
5	5.70	0.00	30.06	0.30	2840	3118	2525	3375
5	6.14	-1.15	34.94	0.14	3052	3375	2731	----
5	6.55	-1.55	39.95	-0.17	3220	3607	2910	----
5	6.96	-1.46	45.06	-0.02	3404	3843	3089	----
5	7.26	-1.40	29.89	-0.16	3530	4016	3240	4328

TABLE A.4.10 SUMMARY DATA FOR HANDCAST TURBINE AND SERIES 5 ORIFICES

					Theoretical runaway speed		Actual runaway speed	
Jet Configuration	Flow Rate ℓ/s	% Diff.	Total Head m	% Diff.	High fric. System rpm	Low fric. System rpm	High fric. System rpm	Low fric. System rpm
1	7.80	-6.99	30.04	-0.03	3266	3970	2955	----
1	8.41	-7.55	35.06	-0.26	3481	4279	3195	----
1	8.93	-8.77	39.77	0.82	3644	4571	3375	----
1	9.36	-6.12	44.19	1.73	3781	4777	3517	----
1	0.00	0.00	0.00	0.00	----	----	----	----
2	7.29	0.00	30.03	0.00	3146	3773	3000	----
2	7.82	0.00	34.97	0.00	3335	4047	3265	----
2	8.21	0.00	40.10	0.00	3472	4262	3480	----
2	8.82	0.00	44.97	0.00	----	----	3660	----
2	9.21	0.00	50.18	0.00	3678	4605	3800	4360
3	7.18	1.51	30.02	0.03	----	----	2700	3290
3	7.73	1.15	35.06	0.00	----	----	2905	----
3	8.24	-0.36	40.07	0.07	----	----	3080	----
3	8.62	2.27	44.90	0.16	----	----	3280	----
3	8.86	3.80	47.52	5.31	----	----	3320	4146
4	6.99	4.12	30.09	-2.00	2923	3224	2668	----
4	7.55	3.45	35.01	-0.11	3129	3490	2880	----
4	8.09	1.46	40.08	0.05	3318	3756	3060	----
4	8.57	2.83	45.04	-0.15	3498	3988	3200	----
4	9.00	2.28	49.92	0.52	3644	4189	3400	4300
5	7.05	3.29	30.03	0.00	3000	3277	2465	3034
5	7.59	2.94	35.07	-0.29	3133	3537	2675	----
5	8.10	1.34	40.03	0.17	3396	3784	2850	----
5	8.57	2.83	45.10	-0.29	3565	4002	3015	----
5	9.00	2.28	50.22	-0.08	3720	4213	3185	3970

A.5 Statistical Programs

A.5.1 SPSSX PROGRAM FOR T-TESTS

```
$R *SPSSX SPRINT=-OUT
TITLE            ANALYSIS OF VARIANCE
FILE HANDLE      REGDAT/NAME='MTJ5'
DATA LIST     FILE=REGDAT/TURBO,JET,HEAD,FLOWRATE,HEADEX,RUN1 TO RUN4
                (F1,F4,F4,F7.2,F8.2,4F7)
LIST
VALUE LABELS
  JET
   1 '1JET'
   2 '2JET (NO INTERFER.)'
   3 '2JET'
   4 '3JET'
   5 '4JET'
VALUE LABELS
  TURBO
   1 'HANDCAST'
   2 'MANUFACTURED'
COMPUTE THEORY=(RUN1+RUN2)/2
COMPUTE EXPER=(RUN3+RUN4)/2
T-TEST PAIRS=THEORY,EXPER
T-TEST PAIRS=RUN1,RUN3
T-TEST PAIRS=RUN2,RUN4
FINISH
$ENDFILE
```

A.5.2 SPSSX PROGRAM FOR ANALYSIS OF VARIANCE AND MCA

```
$R *SPSSX SPRINT=-OUT
TITLE           ANALYSIS OF VARIANCE
FILE HANDLE     REGDAT/NAME='MAT4'
DATA LIST    FILE=REGDAT/TURBO,JET,HEAD,FLOWRATE,HEADEX,
              RUN1 TO RUN4,AREA (F1,F4,F4,F7.2,F8.2,5F7)
LIST
VALUE LABELS
  JET
   1 '1 JET'
   2 '2 JET(NO INTERFER)'
   3 '2 JET'
   4 '3 JET'
   5 '4 JET'
VALUE LABELS
  HEAD
   1 '30 M'
   2 '35 M'
   3 '40 M'
   4 '45 M'
   5 '50 M'
VALUE LABELS
  TURBO
   1 'HANDCAST'
   2 'MANUFAC'
COMPUTE NRMLSP=FLOWRATE*109833/AREA
COMPUTE URUN3=RUN3/NRMLSP
COMPUTE URUN4=RUN4/NRMLSP
LIST
ANOVA           URUN3 BY TURBO(1,2) JET(1,5) HEAD(1,5)/
STATISTICS      ALL
OPTION          4
ANOVA           URUN4 BY TURBO(1,2) JET(1,5) HEAD(1,5)/
STATISTICS      ALL
```

A.6 Multiple Classification Analysis (MCA) Summary Tables

TABLE A.6.1 SUMMARY OF MCA TABLES ON TURBINE INFLUENCE ON RUNAWAY SPEED

		Orifice Series Number									
	Turbine Type	1		2		3		4		5	
		F Value	Change θn	F Value	Change θn	F Value	Change θn	F Value	Change θn	F Value	Change θn
Run3	Handcast	44.0	-0.11	20.7	-0.06	3.4	0.10	0.0	0.0	10.0	-0.03
	Manufactured		0.11		0.06		-0.01		0.0		0.031
	% of variation	67.0		28.0		0.36		0.0		10.2	
Run4	Handcast	26.8	-0.11	8.6	-0.04	6.7	0.03	9.9	0.06	3.4	-0.02
	Manufactured		0.11		0.04		-0.03		-0.03		0.01
	% of variation	49.0		13.0		9.6		26.0		1.4	

TABLE A.6.2 PERCENT REDUCTION OF RUNAWAY SPEED WITH RESPECT TO NORMAL SPEED

MCA TABLE SUMMARY OF JET CONFIGURATION EFFECT

Run Number	Jet Configuration	Orifice Series Number 1	2	3	4	5	Mean
3	1	0.0	10.0	7.1	14.3	16.4	12.0†
3	2 N	15.8	0.0	0.0	0.0	0.0	0.0†
3	2	25.4	18.6	15.7	22.0	19.2	20.2
3	3	28.6	22.8	25.7	32.5	15.1	24.9
3	4	34.9	34.3	37.1	35.1	39.7	36.2
% of total variation		29	58	96	94	88	
4	1	0.0	7.6	5.9	11.0	13.5	9.5†
4	2 N	12.1	0.0	0.0	0.0	1.0	0.2†
4	2	21.2	12.4	7.9	8.0	7.3	11.4
4	3	22.2	11.4	12.9	8.0	0.0	10.9
4	4	31.3	25.7	27.7	18.0	17.7	26.2
% of total variation		46	69	85	55	85	

† excluding series 1 results

TABLE A.6.3 SUMMARY OF MCA TABLES ON EFFECT OF HEAD

		Orifice Series Number (% reduction in speed ratio)				
Run	Head	1	2	3	4	5
3	%Var	0.16	2.25	0.36	0.09	0.16
3	30	3.90	3.30	3.40	0.00	1.60
3	35	3.90	0.00	1.70	0.00	0.00
3	40	2.0	0.00	1.70	0.00	1.60
3	45	0.00	5.00	1.70	0.00	1.60
3	50	2.00	8.30	0.00	0.00	3.30
4	%Var	2.00	2.25	2.56	0.49	4.80
4	30	5.90	5.20	5.40	2.20	3.30
4	35	3.60	3.10	4.30	1.10	3.30
4	40	2.40	0.00	3.20	1.10	4.40
4	45	0.00	3.10	2.20	0.00	0.00
4	50	0.00	4.20	0.00	1.10	0.00